



저작자표시-비영리-변경금지 2.0 대한민국

이용자는 아래의 조건을 따르는 경우에 한하여 자유롭게

- 이 저작물을 복제, 배포, 전송, 전시, 공연 및 방송할 수 있습니다.

다음과 같은 조건을 따라야 합니다:



저작자표시. 귀하는 원저작자를 표시하여야 합니다.



비영리. 귀하는 이 저작물을 영리 목적으로 이용할 수 없습니다.



변경금지. 귀하는 이 저작물을 개작, 변형 또는 가공할 수 없습니다.

- 귀하는, 이 저작물의 재이용이나 배포의 경우, 이 저작물에 적용된 이용허락조건을 명확하게 나타내어야 합니다.
- 저작권자로부터 별도의 허가를 받으면 이러한 조건들은 적용되지 않습니다.

저작권법에 따른 이용자의 권리는 위의 내용에 의하여 영향을 받지 않습니다.

이것은 [이용허락규약\(Legal Code\)](#)을 이해하기 쉽게 요약한 것입니다.

[Disclaimer](#)

지리학석사 학위논문

**A Diatom-Based Reconstruction of
the Paleoenvironmental Changes
during the Last Deglaciation
in Jeju Island, Korea**

구조분석을 통한 마지막 해빙기 동안의
제주도 하논 마르형 호수 고환경 복원

2015년 8월

서울대학교 대학원

지리학과

한 지 우

A Diatom-Based Reconstruction of the Paleoenvironmental Changes during the Last Deglaciation in Jeju Island, Korea

지도교수 박 정 재

이 논문을 지리학석사 학위논문으로 제출함
2015년 4월

서울대학교 대학원
지리학과
한지우

한지우의 지리학석사 학위논문을 인준함
2015년 6월

위 원 장 _____ (인)

부위원장 _____ (인)

위 원 _____ (인)

Abstract

A Diatom-Based Reconstruction of the Paleoenvironmental Changes during the Last Deglaciation in Jeju Island, Korea

Jiwoo Han

Department of Geography

The Graduate School

Seoul National University

Reconstructing the paleoclimate/paleoenvironment has become more important as the prediction of future climate change becomes a more pressing issue. Future climate change can be predicted by reconstructing the paleoclimate of the past, as it reoccurs in a repeated cyclical fashion. In particular, the last deglaciation is the focus of much research these days because it consists of various climate shifts which may be similar to the future climate change triggered by global warming.

Hanon maar paleolake, in the southern part of Jeju Island, is located in a geographically significant place that can provide the missing link to the paleoenvironment between Japan and China because the southern part of Jeju Island is influenced by the East Asia monsoon and the Kuroshio Current. However, only the morphology and terrestrial environment of Hanon maar has been researched so far, so it is necessary to investigate Hanon maar paleoenvironment using another type of proxy data to observe it from a different angle. Because Hanon maar had been a paleolake until 500 years ago, diatom analysis is an appropriate methodology to reconstruct the paleoenvironment around Hanon paleolake; it provides information on

lacustrine environmental changes.

The aquatic environment during the last deglaciation of Hanon maar paleolake in Jeju Island, Korea, has been reconstructed through diatom analysis. Diatom analysis is a methodology investigating diatom microfossils in sediments, which are phytoplankton with silicic valves. Diatoms are a good indicator of environmental changes; they provide various environmental information such as salinity, water depth, acidification, trophic status, water temperature, and so on. Among them, water depth, trophic status, saprobity, water temperature and the acidification of Hanon paleolake during the last deglaciation has been reconstructed in detail based on the information derived from diatom analysis.

The sediment core(HN-1) had been extracted and analyzed using diatom analysis. This study covers from 90 to 250cm in the 10 meter long core, which includes the last deglaciation(ca. 15,500 – 8,000 cal. yr BP). After identifying diatoms by microscope analysis, diatom diagrams were constructed. The zones in the diagram were determined based on constrained incremental sum of squares cluster analysis, and climate events during the last deglaciation in Hanon paleolake have been zoned: Oldest Dryas for 15,440 – 14,670 cal. yr BP, the beginning of Bølling-Allerød for 14,670 – 14,180 cal. yr BP, ongoing Bølling-Allerød for 14,180 cal. yr BP – 12,810 cal. yr BP, Younger Dryas for 12,810 – 12,150 cal. yr BP, Preboreal for 12,150 – 10,440 cal. yr BP, and Boreal for 10,440 – 7,980 cal. yr BP. The time table of the climate shifts in Hanon maar which is reconstructed in this study corresponds with other studies of Hanon maar paleoclimate.

The result of the diatom diagram was schematized to reconstruct the water depth, trophic status, saprobity, water temperature and acidification of the paleolake based on changes in the diatom assemblage and limnological processes. The reconstructed aquatic environment has also been drawn in the

graph which outlined relative phase-dependent environment changes in the Hanon paleolake. Afterwards, the reconstructed environment based on the diatom diagram has been verified by the results of PCA and P:B ratio. The components of Axis 1, 2 and 3 and the value of P:B ratio were made into several graphs, and they were compared to each other. Based on the meaning of each value such as trophic status, water depth and pH, the verification made the previously reconstructed lacustrine environment revised. Overall, Hanon maar paleoenvironment during the last deglaciation has changed as follows: cold and dry for the Oldest Dryas, increasing temperatures and moisture for the Bølling-Allerød, cold and wet-dry for the Younger Dryas, an increase in temperatures and temporarily drier for the Preboreal, and warm and dry/wet for the Boreal.

This was the first time a paleoenvironment of Korean freshwater zone was constructed using diatom analysis; therefore, this study itself is meaningful. Furthermore, this study reconstructed trophic status, water depth, saprobity, water temperature and acidification of Hanon paleolake by diatom analysis. In conclusion, it was possible to reconstruct the paleo-lacustrine environment of Hanon maar paleolake during the last deglaciation using diatom analysis, and it provided a new proxy data for the paleoenvironment/paleoclimate during the last deglaciation on the Korean Peninsula.

Keyword : diatom analysis, Jeju Island, Hanon maar paleolake, reconstruction of paleoenvironment, paleoclimate, the last deglaciation

Student Number : 2013-20114

Table of Contents

Abstract	i
Table of Contents	iv
List of Figures.....	vii
List of Tables	ix
Chapter 1. Introduction	1
1.1. Study Backgrounds	1
1.2. Regional and Temporal Settings: Hanon Paleo-Maar Lake in Jeju Island	3
1.3. Research Purpose and Structure.....	7
Chapter 2. Literature Review	10
2.1. Studies on Hanon Paleo-Maar Lake	10
2.2. Introduction to Diatoms	14
2.3. Studies on Diatom Analysis for Reconstruction of Paleoenvironment in Korea and Abroad	15
Chapter 3. Methodology.....	18
3.1. Preparation of Diatom Slides.....	18
3.2. Microscope Examination	20
3.3. Diatom Diagram and Diatom Concentration	21
3.4. Principal Component Analysis	25
3.5. The Ratio of Planktonic to Benthic Diatom Species	26
Chapter 4. Research Results and Analysis.....	28
4.1. Principal Component Analysis	28
4.2. Diatom Flora in the Diagram	40

4.1.1. Zone 1: 15,440 cal. yr BP – 14,670 cal. yr BP (Oldest Dryas)	43
4.1.2. Zone 2-a: 14,670 cal. yr BP – 14,180 cal. yr BP (The beginning of Bølling-Allerød)	43
4.1.3. Zone 2-b: 14,180 cal. yr BP – 12,810 cal. yr BP (Bølling-Allerød)	44
4.1.4. Zone 3: 12,810 cal. yr BP – 12,150 cal. yr BP (Younger Dryas)	44
4.1.5. Zone 4: 12,150 cal. yr BP – 10,440 cal. yr BP (Pre-Boreal: the beginning of Holocene)	45
4.1.6. Zone 5: 10,440 cal. yr BP – 7,980 cal. yr BP (Boreal)	45
4.3. The Ratio of Planktonic to Benthic Diatom Species	46
Chapter 5. Discussion	51
5.1. Reconstructing the Paleoenvironment of Hanon Maar based on the Diatom Diagram and Schematization	52
5.1.1. Reconstructing the Paleoenvironment of Hanon Maar through schematization of each zone based on Diatom Diagram	52
5.1.2. Summary of the Paleoenvironment of Hanon Maar based on the Schematization	63
5.2. Verification of the Reconstructed Paleoenvironment of Hanon Maar Based on Axis 1, 2, 3, and the Values of P:B Ratio	65
5.3. Comparison and Analysis between Diatom Analysis and Other Multi-Proxy Data from Another Research on the Paleoenvironment of Hanon Maar	74

Chapter 6. Conclusions	81
Bibliography	84
APPENDIX	94
Appendix I. A diagram including all diatom species.....	94
Appendix II. A count sheet of 17 major diatom species	96
Appendix III. The component scores of Axis 1, 2, 3 and 4 by depth	105
Appendix IV. The component scores of major species at Axis 1, 2, 3 and 4 from PCA	108
Appendix V. Images of diatom species in Hanon maar paleolake	109
국 문 초 록	112

List of Figures

Figure 1. Map of Hanon maar and coring site(yellow arrow)	4
Figure 2. Climate data of Seogwipo City, Jeju Island (1981-2010).....	5
Figure 3. Research flow chart	9
Figure 4. The time table of climate events in Hanon maar paleolake (Chung, 2007; Park et al., 2014a; Park et al., 2014b).....	12
Figure 5. The morphology of a diatom	14
Figure 6. PCA graphs with major diatom taxa (A) excluding "spp." and (B) including "spp."	28
Figure 7. Principal component analysis of the HN-1 diatom data	32
Figure 8. Diagram for examination of Axis 1, 2 and 3	34
Figure 9. The graphs of component scores on the PCA Axis 1, 2, 3....	36
Figure 10. The graph of component scores on the PCA Axis 1	37
Figure 11. The graph of component scores on the PCA Axis 2	38
Figure 12. The graph of component scores on the PCA Axis 3	39
Figure 13. Diatom diagram including "spp."	42
Figure 14. The respective changes of planktonic and benthic species.	49
Figure 15. P:B ratio.....	50
Figure 16. Diatom diagram excluding "spp."	54
Figure 17. Schematization of diatom assemblage changes – zone 1 ..	57
Figure 18. Schematization of diatom assemblage changes – zone 2-a	57
Figure 19. Schematization of diatom assemblage changes – zone 2-b	59
Figure 20. Schematization of diatom assemblage changes – zone 3 ..	59
Figure 21. Schematization of diatom assemblage changes – zone 4 ..	61
Figure 22. Schematization of diatom assemblage changes – zone 5 ..	62
Figure 23. Schematization of relative phase-dependent reconstruction of aquatic environmental changes	64
Figure 24. P:B ratio and the component scores of Axis 2	67
Figure 25. The component scores of Axis 1 and 2	70
Figure 26. The component scores of Axis 1 and 3	71

Figure 27. The component scores of Axis 2 and 3	72
Figure 28. The revised version of the paleoenvironment in Hanon	73
Figure 29. Climate shifts in Hanon maar by adding the one reconstructed by diatom proxy data of this study	75
Figure 30. Diagram for comparisons between the changes of <i>Botryococcus</i> & <i>Celtis</i> and <i>D. confervacea</i> & PC 1, 2, 3 ..	77

List of Tables

Table 1. Eigenvalues and variance explained by PCA of the diatom species from core HN-1	29
Table 2. Saprobity index – the classes of water quality (Kelly et al., 2005).....	55
Table 3. Habitat environments of major diatom species in Hanon	56
Table 4. Table of relative phase-dependent reconstruction of the aquatic environmental changes in Hanon maar paleolake.....	63

Chapter 1. Introduction

1.1. Study Backgrounds

Global warming is a very familiar and even a clichéd topic these days. However, it poses an important question called ‘abrupt climate change’ impact that could possibly happen in the future. The hygienic, economic and cultural impact cannot be imagined easily in the aftermath of climate change triggered by global warming. However, the matter of whether climate change can be predicted is important because it is directly related to our lives rather than those reasons. Because climate is repetitive according to the Milankovitch Theory (Roberts, 1998), building a predictive model based on fluctuations of past climate is a good way to prepare for climate shifts in the future.

There are several ways to build a predictive model for future climate; however, analyzing proxy data is the most common way. Proxy data is a substitute literally for real climatic/environmental data; therefore, it cannot show us the exact same environment at that time due to limitations in the data. For example, the figures of dinosaurs people think could be wrong because they are restored from their proxy data; fossilized bones, imprints, et cetera (Conway et al., 2012). Therefore, researchers should use and gather as much proxy data as possible to minimize errors that may occur. A predictive model for future climate cannot be made without proxy data. Models are reconstructions of climate shifts that have happened in the past. Therefore, proxy data is necessary to build predictive models of the future climate.

Diatoms are cosmopolitan primary producers. They are everywhere that contains moisture and water; therefore, it is one of the easiest ways to obtain climate data among many other proxy data (Round et al., 1990). That is, diatom is one of the crucial proxy data to reconstruct paleoenvironment. Through diatom analysis, aquatic environment can be reconstructed according to the habitats of each diatom species such as water depth, temperature, pH, salinity, and so on (Mackay et al., 2005). The aquatic environment is always related to the atmosphere and/or other environmental factors (Meyers et al., 1993; Kuwae et al., 2002; Wang et al., 2012). In summation, diatoms offer valuable information for paleoenvironmental reconstructions (Wang et al., 2012; Chen et al., 2014; Katsuki et al., 2003; Ribeiro and Senna, 2010).

Jeju Island is located in a critical area affected by the East Asia monsoon and the Kuroshio Current. Also, Hanon maar lies between Japan and China, so the data from Hanon maar can bridge the gap between those two countries and play a key role for reconstructing East Asia climate (Chung, 2007; Park, 2015). Therefore, it is necessary to compile environmental and climatic data for reconstruction of paleoenvironment around Jeju Island. Above all, Hanon maar paleolake is a good place to study paleoenvironment because it contains over 10m long sediment under the ground that shows good preservation (Park et al., 2014a; Park et al., 2014b). However, Hanon paleolake has not been studied enough in spite of this in the field of paleoclimatology; what has been done only focuses on the terrestrial environment and climate (Chung, 2007; Park et al., 2014a; Park et al., 2014b) even though the place was a paleolake until around 500 years ago (Bowers et al., 2014). Consequently, reconstructing the paleoenvironment in Hanon maar using diatom analysis is necessary to

observe it within the paleolake, which is close to what really happened.

1.2. Regional and Temporal Settings: Hanon Paleo-Maar Lake in Jeju Island

Hanon paleo-maar Lake, which is located in 400m from the coast of southern part of Jeju Island, is the only maar lake on the Korean Peninsula (Bowers et al., 2014; Choi et al., 2006; Chung, 2007; Park et al., 2014a; Park et al., 2014b). It is located at 33°14'N, 126°32'E and is 53m above sea level. Hanon maar was formed during the late Pleistocene, ca. 50,000 yr BP. The diameter is about 1km for the crater and 850m for the crater lake, and the floor area is about 216,000m² (Bowers et al., 2014). The depth of water is estimated about 5m for average and 13m for maximum depth according to Choi et al. (2006).

Hanon maar paleolake is a critical place to reconstruct paleoclimate and paleoenvironment in East Asia, not only because of its location, but also because of the particular physical environment. According to Yoon et al. (2006c) and Lee et al. (2008), Hanon crater lake developed in the summit of Hanon maar as a closed aquatic environment, which has low inflow and outflow (low energy environment). Therefore, the characteristics of the sediment in Hanon paleolake are mainly influenced by its own ecology and climate, so the sediment reflects the changes in the biological, geological and morphological environment within the lake. Thus, the sediments of Hanon paleolake are very important as an indicator of the paleoenvironment considering its location and topography. Especially,

diatoms living in the lake will be a good reference for reconstructing paleoenvironment.

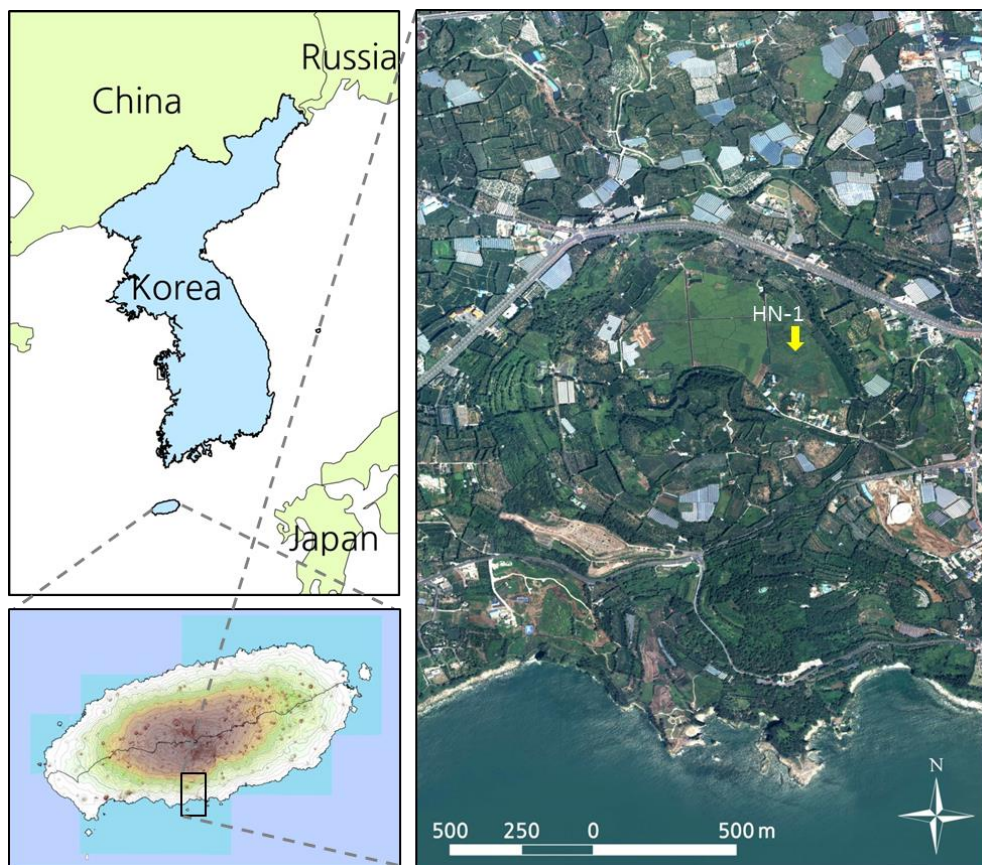


Figure 1. Map of Hanon maar and coring site(yellow arrow)

The physical environment of Jeju Island where Hanon maar lies is a crucial place to observe the paleoclimate and paleoenvironment around East Asia because Jeju Island is affected by two important environmental factors concerning the environment of East Asia. First, the Kuroshio Current flows south of Jeju Island. It is a warm current starting from the east side of Taiwan and transfers heat energy from the tropics; therefore,

the current definitely has an influence on the climate and ecology of Jeju Island, especially the southern part (Park, 2015; Chung, 2007).

The second factor is the East Asian monsoon(EAM). Hanon maar paleolake is located in the EAM belt, and the climate of Jeju Island is normally hot and humid in summer and cold and dry in winter (Anonymous, 2010). However, the characteristics of climate around Hanon maar during winter are lessened than in other parts of the Korean Peninsula and the northern part of Jeju Island due to the warm Kuroshio Current. According to the data from Domestic Climate Data at Korea Meteorological Administration, the lowest mean monthly temperature is 6.8°C in January, the highest mean monthly temperature is 27.1°C in August, and the mean rainfall is 1,923mm in southern Jeju Island (Anonymous, 2010). It rains mainly between July and August (Figure 2).

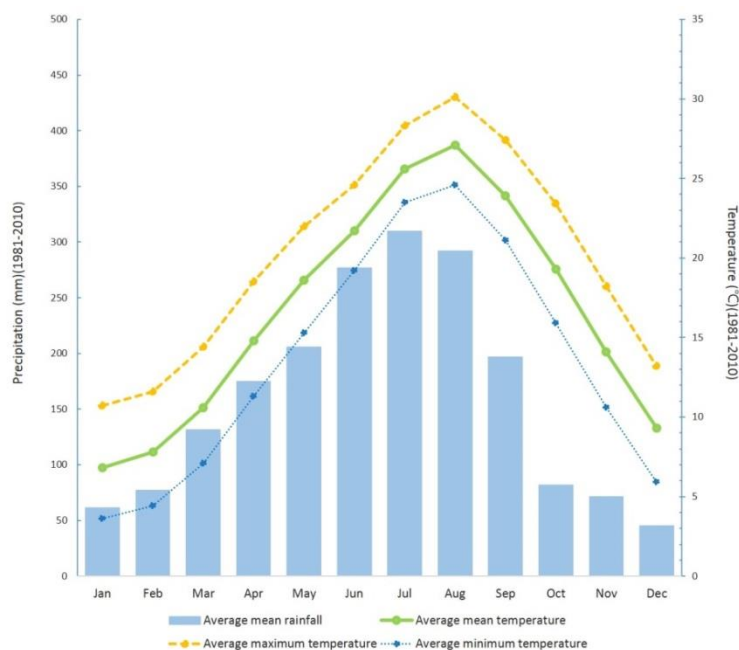


Figure 2. Climate data of Seogwipo City, Jeju Island (1981-2010)

Accordingly, Hanon maar is a transitional zone between climate signals of North Atlantic(EAM – terrestrial deposits) and western North Pacific(Kuroshio Current – pelagic deposits) (Park and Park, 2015). Therefore, it is possible to say that Hanon paleolake shows the climate fluctuations around East Asia. Researchers in China and Japan have actively studied paleoclimate and paleoenvironment changes in East Asia, and Hanon maar paleolake is a central place to connect studies from China and Japan. In other words, in the context of that Hanon maar is located in a transitional zone between terrestrial and marine environment and there is not enough data since the last glacial period, Hanon maar has an important meaning in the matter of climate change in East Asia (Park, 2015).

The coring site of HN-1¹ for this study is pointed in Figure 1. The core was taken using a hydraulic piston corer in November, 2012. Its total length is about 10m, and each is sampled by 1cm thickness. For this study, samples between 250 and 90cm were analyzed every 2cm, which covers from 15,500 to 8,000 cal. yr BP. Samples from the core were stored in refrigerator before using, so the samples for this study were in wet condition, not dry.

Reconstructing the environment during the last deglaciation is one of the main goals in this study. Because the last deglaciation is a transition period which consists of centennial- to millennial-scale climate changes, it is necessary to observe exactly how climate had shifted to improve the predictability of future climate change (Park, 2015). During the period being studied, the Bølling-Allerød(BA), Younger Dryas(YD), Preboreal, 8.2ka event and Holocene Climate Optimum(HCO) for centennial-scale

¹ The same core(HN-1) had been used for this study with Park et al., 2014a and 2014b.

occurred. In the northern hemisphere, the BA, Preboreal and HCO were warm periods(interglacial and interstadial), while the Younger Dryas and the 8.2ka events were cold periods(stadial). The cause of both stadial events has not been revealed clearly, yet. However, it has become common knowledge that the YD and the 8.2ka happened because freshwater from melted glacier flowed into the oceans and cut the thermohaline circulation, which is called Atlantic Meridional Overturning Circulation nowadays (Park, 2015). Researchers are very interested in both climate events because there is a possibility that the abrupt decline in temperature could happen again in the future due to global warming; glacier melting will cause unpredictable environmental changes as global warming proceeds continuously or even is accelerated in the future. That is, the unpredictable environmental change can be predicted through studying in climate change during the YD and the 8.2ka event. Therefore, researching in the last deglaciation is important for our future. In particular, the transition between BA and YD was the period when climate had been changed abruptly, so it is necessary to be reconstructed in detail; this is why the last deglaciation has been chosen for this study.

1.3. Research Purpose and Structure

In this study, the paleoenvironment during the last deglaciation(ca. 15,500 - 8,000 cal. yr BP) in Hanon maar will be reconstructed by using diatom analysis. Through diatom analysis, the paleoenvironment in Hanon maar can be reconstructed in different aspects showing the environmental

changes within the lake. It is possible because diatoms live in the lake, so they can reflect environmental changes of the paleolake much more sensitively and closely as the climate change around Hanon maar. Furthermore, the reconstructed environment during the last deglaciation will provide proxy data that would be useful for predicting future climate change on the Korean Peninsula. This study could be helpful to bridge the gap between China and Japan which has been missed out frequently so that the change of paleoenvironment in East Asia can be reconstructed.

To sum up, the purposes of this research are to:

1. Reconstructing the paleoenvironment in Hanon maar during the last deglaciation using diatom analysis, which indicates various environmental changes in the paleolake.
2. Providing another proxy data for the reconstruction of paleoenvironment on the Korean Peninsula during the last deglaciation.

The literature review related to this study is explained in Chapter 2, including the introduction of diatoms. The methodology, diatom analysis, is introduced in Chapter 3: how to prepare diatom microscope slides, how to count diatoms for microscope analysis, how to draw diatom diagram, and applications of PCA and P:B ratio. In Chapter 4, the results of diatom diagram, PCA and P:B ratio are described. In Chapter 5, the results from the previous chapter are interpreted, and the verification of the previous interpretation of this study and comparison study to other proxy data of other studies are discussed.

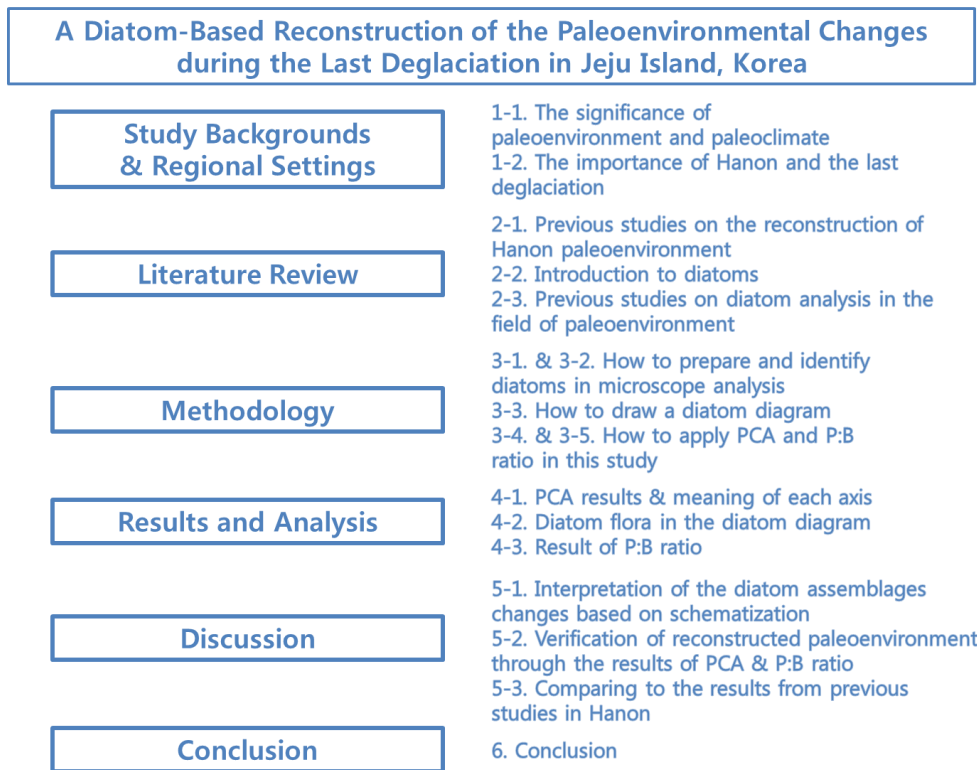


Figure 3. Research flow chart

Chapter 2. Literature Review

2.1. Studies on Hanon Paleo-Maar Lake

Hanon maar is a significant place for reconstructing the paleoenvironment of the Korean Peninsula and even East Asia due to some reasons explained in Chapter 1.2. There are several studies dealing with Hanon maar paleolake² in various fields.

First, there have been done several studies to reconstruct paleoclimate of Hanon. Among of them, Chung (2007) and Park et al. (2014a; 2014b) especially used microfossil analysis – pollen – in the sediment of Hanon for reconstructing. Chung (2007) analyzed the pollen record of Hanon maar, which was taken at the center of the lake, and showed how it provided a vegetation history of Jeju Island during the last deglaciation. Three zones were established: zone 1(21,800-14,400 cal. yr BP) dominated by *Artemisia* and *Gramineae* shows much a colder and drier climate than the present one on Jeju Island, which means the period is related to the Last Glacial Maximum(LGM). Zone 2(14,400-11,800 cal. yr BP) shows a sudden increased in *Polypodiaceae* ferns and an abrupt decline in herbaceous taxa indicates the transitional period from glacial to interglacial while suggesting warmer climate than before. Zone 3(11,800-9,900 cal. yr BP) showing the retreat of grassland vegetation and further expansion of temperate deciduous broadleaved forests displays similar climate, warm and humid, to the modern climate in Jeju Island. He asserts that it is related to stronger influence of the East Asian summer monsoon.

² “Hanon maar paleolake” is a correct term; however, it is going to be written in mostly “Hanon” after then for the simplicity.

Park et al. (2014a; 2014b) also studied the area of Hanon maar lake using pollen analysis and many geochemical proxies such as magnetic susceptibility, grain size, $\delta^{13}\text{C}$, $\delta^{15}\text{N}$, total organic carbon, carbon-nitrogen ratio, algae, etc. Park et al. (2014a; 2014b) recovered an approximately 10m-long core, and they published two papers covering different time scopes – the one between 32.5 and 6.9k cal. yr BP and another one focusing on the last deglaciation. In particular, Park et al. (2014b) divided into 6 zones to reconstruct the climate change and its effects on the vegetation around Hanon in the past. It contends that there were Oldest Dryas(15,450-14,650 cal. yr BP), Bølling-Allerød(14,650-12,900 cal. yr BP), Younger Dryas(12,900-11,900 cal. yr BP), Pre-Boreal(11,900-10,300 cal. yr BP), Boreal(10,300-7,800 cal. yr BP), and Holocene Climate Optimum(7,800-7,300 cal. yr BP) occurred during this time frame. The paper interpreted proxy data conjunctly so that they could reconstruct environmental change, particularly in vegetation and climate, accurately and with high-resolution. The Younger Dryas on the Korean Peninsula is detected for the first time in this paper. The timelines for Park et al. (2014a) and Park et al. (2014b) are slightly different because the samples were analyzed at 8cm intervals in Park et al. (2014a) – pre LGM(32,500-25,200 cal a BP³), the earlier part of LGM(25,200-21,500 cal a BP), the later part of LGM(21,500-17,600 cal a BP), early deglacial period(17,600-14,700 cal a BP), late deglacial period(14,700-10,700 cal a BP), and early Holocene(10,700-6,900 cal a BP). This paper focuses much on the climate changes in orbital- and millennial-scale.

³ All dates in Park et al. (2014a) is written in cal a BP which is calibrated with the intcal09 data set (Park et al., 2014a; Reimer et al., 2009).

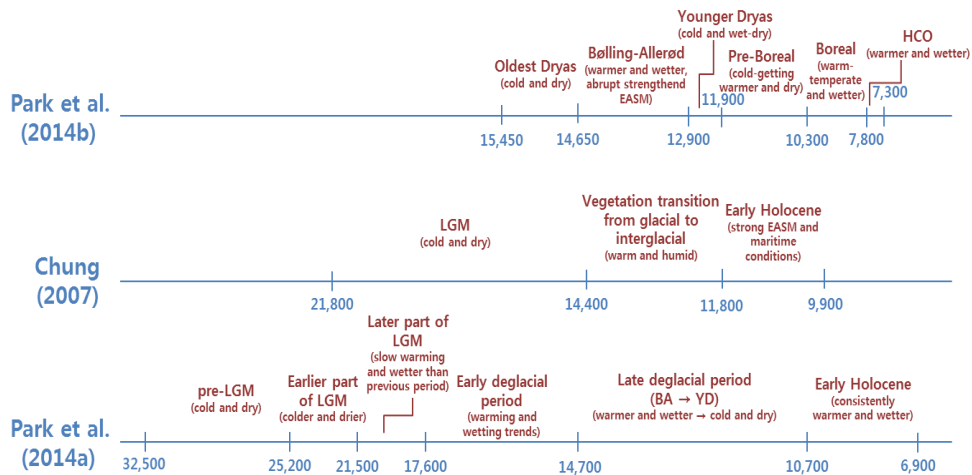


Figure 4. The time table of climate events in Hanon maar paleolake (Chung, 2007; Park et al., 2014a; Park et al., 2014b)

Those results from both Chung (2007) and Park et al. (2014a; 2014b) were slightly different because the intervals of analyzed samples were different for each study; Chung (2007) did 10cm interval, Park et al. (2014a) did 8cm interval, and Park et al. (2014b) did 2cm interval. Therefore, the distinction in resolution delineates slightly different stories in each scale. Timeline of Hanon maar lake from the three studies have been schematized in Figure 4. Yoon et al. (2006a; 2006b; 2006c) and Lee et al. (2008) also reconstructed the paleoclimate and paleoenvironment of Hanon and Jeju Island using by sedimentological analyses.

Second, some researchers tried to reconstruct the geomorphology of Hanon such as Yoon et al. (2006a) and Choi et al. (2006). Yoon et al. (2006a) recovered the morphology and geological process in Hanon crater using resistivity survey and boring. Choi et al. (2006) reconstructed the volcanic lake in Hanon crater by applying the spatial statistical techniques based on the depth information from the seismic survey and known data. Overall, there were some attempts to recover Hanon morphology. Third,

Lee and Ahn (2005) did a simple fundamental study in flora and fauna of Hanon to reconstruct what it looked like before people converted it to farmland.

In conclusion, considering the value of Hanon in an aspect of reconstructing paleoenvironment and paleoclimate, there have been fewer researches done until now than expected. Although there are some studies have been carried out to reconstruct paleoclimate using pollen analyses and geochemical analyses (Park et al, 2014a; Park et al., 2014b; Chung, 2007; Lee et al., 2008; Bowers et al., 2014), it is not still enough for Hanon reconstruction. It is necessary to have much closer look of the real past environment around Hanon.

Because Hanon was a (maar) lake, the proper way of reconstructing paleo-environment would be reconstructing the “lake” environment of Hanon in the past; Hanon was a lake basically, so reconstructing aquatic environment of the past would be a key to investigate paleoenvironment and paleoclimate around Hanon. Diatoms live in a lake, and thus they show the status of lake at that time closely. However, there is no research using diatom analysis that has been done around Hanon. This is why diatom analysis should be performed in this area. Without reconstructing lacustrine environment in Hanon, the reconstructed paleoenvironment around Hanon would just show the half of what happened in the past actually. Therefore, diatom analysis is going to be carried out to reconstruct Hanon paleo-maar lacustrine environment in the past, where is a significant place to study for paleoenvironment reconstruction in East Asia.

2.2. Introduction to Diatoms

The first observation of diatom was recorded in 1703 by an English gentleman. The recorded diatom adhered to the roots of the Lemna, which are pond-weed herbs (Round et al., 1990). After then, studies on diatoms have begun and being done actively until now.

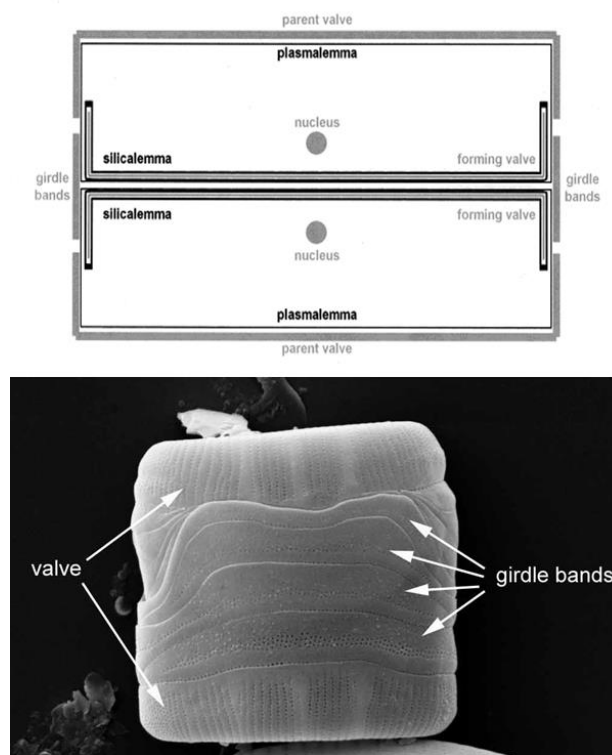


Figure 5. The morphology of a diatom – two valves(epitheca and hypotheca) are tied up together by girdle bands (Kelly et al., 2005)

Diatoms are unicellular algae and phytoplankton. The name diatom comes from Greek, which means “cut into two.” It is because a diatom consists of two valves with girdle bands (Figure 5). When a diatom dies,

their silicic valves become separated and deposited on the floor, and those valves are counted by diatomists. As diatoms are phytoplankton aforementioned, most of them are photosynthetic, so their habitats are usually in/on sunlit places. They occur in environment containing water/moisture such as streams, lakes, oceans, and even in wetlands. That is, diatoms are in everywhere. Also, diatoms are primary producers – they play an important role in nutrient supply along with bacteria and other kinds of plankton (Sigman and Hain, 2012) in aquatic environment.

Diatoms are ecological indicators because each diatom species lives differently, conditions by conditions such as pH, salinity, water temperature, water depth, trophic level, thermal stratification, and so on. For these reasons, they are being used as an indicator of pollution these days. What is better, their frustules(valves) are made from silica, SiO_2 . It is because silica is insoluble, they are fossilized when they die and sink into the sediment. Also, their complexly shaped valves seem different according to each species. Therefore, diatoms can be used as a proxy data to unearth the paleoenvironment. In other words, diatoms can be good indicators of past environment (Mackay et al., 2005).

2.3. Studies on Diatom Analysis for Reconstruction of Paleoenvironment in Korea and Abroad

There have been a lot of works related to diatom analysis. Due to its useful roles as proxy data, diatom analysis is a popular method in many other countries, especially in United Kingdom, Germany, and Japan.

Diatom analysts can be divided into two groups largely: people who classify diatoms taxonomically and people who analyze the change of diatom assemblages to reconstruct an environment of the past or present. In the latter case, it is necessary to have adequate information to interpret diatoms in the environment; which environment (pH, salinity, temperature, organic pollution, etc) is the best for which diatom species. Chapter 2.3. mainly focuses on studies on diatom analysis for reconstructing the paleoenvironment – the latter usage.

There are many paleoclimate/paleoenvironment studies applying diatom analysis in Japan. Japanese diatomists have worked on reconstructing the paleoenvironment using diatoms such as in Lake Biwa and Suigetsu (Meyers et al., 1993; Kuwae et al., 2002; Kosseler et al., 2011). Beyond reconstruction of lacustrine environmental changes in the past, many diatom researchers study on various topics using diatom analysis such as reconstructing productivity changes in the ocean and lagoon (Katsuki et al., 2003; Katsuki et al., 2012). Also, there have been many studies on paleoclimate and paleoenvironment using diatoms rousing in China. Especially, many paleoclimate studies have been performed in the Long Gang Volcanic Field (LGVF) region recently – Lake Xiaolongwan, Sihailongwan, and Erlongwan – in Jilin Province, northeast China (Wang et al., 2012).

In contrast with the situation in other countries in the world, especially comparing to Japan and China, studies on diatom analysis in Korea are very calm. Most diatom analyses in South Korea have been carried out in coastal regions or ocean – brackish water and seawater. There are a few of researchers performing in lagoon and/or ocean: Go et al. (2013) in Hwajinpo on the eastern coast of Korea, Bak et al. (2006; 2009;

2010) in Seokrim-dong in Seosan City and Uleung Basin in East Sea, and Yoon et al. (2004) in the eastern part of Jeju Island, etc. Research performed in coastal regions is generally to determine sea level fluctuation in the past.

Reconstructing sea level changes is important; however, reconstructing inland paleoenvironmental change is also important, because the environments of brackish and salt water contain different stories from that of freshwater. That is, investigating freshwater diatoms in the past would let us see things that cannot be seen in lagoons or oceans such as how strong wind blew or how much it rained or how strong sunlight was, etc. Therefore, to reconstruct regions in freshwater environments is to reconstruct the major part of the past environment on the Korean Peninsula. Even though there are some studies which have done in freshwater regions in Korea, the past environment has not been studied. Instead, it was done to investigate the habitats of diatoms and the present environment to observe how much the place is polluted. Although it seems that using diatom analysis in the field of paleoenvironment reconstruction is not popular yet, collecting and recording diatoms in Korea have been more actively pursued recently⁴. There may be some ongoing studies that are reconstructing the paleoenvironment right now, but more are needed. Because diatom analysis is a good indicator of ecological and environmental change, it is a good tool to reconstruct paleoenvironment. There ought to be more studies on this field on the Korean Peninsula.

⁴ By leading of National Institute of Biological Resources, Korean diatoms in streams, lakes, and oceans are collected and recorded. The project has started since 2010s. They published illustrated books of diatoms and provide the information on their website.

Chapter 3. Methodology

3.1. Preparation of Diatom Slides

For diatom analysis, sample preparation is needed in some ways to remove materials such as calcareous and organic matters and to improve visibility of diatoms under the microscope. According to Round et al. (1990), “there is no universally best method and every diatomist has some preferred recipe.” There are various methods for diatom preparation, and the method can be modified properly depends on soil condition in each environment. In this study, a modified version of Katsuki et al. (2003) was chosen for sample preparation. The samples are dried at room temperature⁵ and treated as below:

- a. About 0.1g of sample is treated by H₂O₂ to remove organic matter and distilled water in a 100mL beaker⁶.
- b. The sample is boiled for 1-2 hours at 120°C until the foam is gone.
- c. A minute amount of sodium hexametaphosphate(SHMP) is mixed and left for 15-30 minutes.
- d. The pH of the solution is checked, and the surface solution is thrown away when pH is less than 7 (In case the pH shows more than 7, mix it with distilled water and check the pH. Repeat the same step until it shows less than 7).

⁵ Samples for diatom analysis should be dried naturally because silicic valves are easily broken by heat.

⁶ The sediments in Hanon barely contain calcareous matters, so using hydrochloride (HCl) could be omitted for this experiment.

- e. The beaker is filled with distilled water to the top and left for 5 hours.
- f. The pH is checked again, which shows less than 7, and then its surface solution thrown away.
- g. The beaker is filled with distilled water until the water level is at 25mL and shaken thoroughly.
- h. The sample is taken by using micropipette (Make sure the sample is shaken thoroughly and taken from the middle of the beaker). The amount of sample can be decided according to each sample's abundance of diatoms.
- i. The sample is put on a heated cover slide with low temperature.
- j. When the sample is dried, minute mountmedia (i.e. Naphrax) is put to mount samples on the cover slide.
- k. The mountmedia is melted at 120°C until its bubbles are gone.
- l. The cover slide is put onto a microscope slide.

In step g, each 25mL water volume of beakers should be measured by cylinder accurately. The values are used to calculate diatom concentration afterward. Three samples at 100, 164, 250cm had insufficient amount. The remained samples of 100 and 250 were almost half of normal, so a lesser amount of distilled water was used in step g. In the similar way, only 1/10 amount remained for sample 164, so the sample was treated by less H₂O₂ and distilled water in step a and g.

3.2. Microscope Examination

Among of 10m core of HN-1 from Hanon in Jeju Island, sediment from 90cm to 250cm has been examined for this study. Samples for diatom analysis are taken every 2cm interval, and the thickness of each sample is 1cm; 81 slides have been examined. Diatoms in the slides are counted on an optical microscope, Leica ICC50 microscope, at a magnification of $\times 1000$ with an oil immersion objective (index of refraction = 1.515). Because Leica ICC50 has a built-in HD digital camera, pictures of diatoms are taken for reference in order to prevent/reduce mistakes and errors for the first 1,500 valves. The identification of diatoms are referred to the taxonomy studies and illustrated books such as Algal Flora of Korea series (Joh, 2010; Joh et al., 2010; Joh, 2011; Lee, 2011; Joh, 2012), Freshwater Algae of North America (Stoermer et al., 2003; Kingston, 2003; Kociolek and Spaulding, 2003a; Kociolek and Spaulding, 2003b; Lowe, 2003), The Diatoms (Round et al., 1990), Bacillariophyceae 1, 2 (Krammer and Lange-Bertalot, 1986; Krammer and Lange-Bertalot, 1988), and Bibliotheca Diatomologica (Krammer and Lange-Bertalot, 1985; Lange-Bertalot and Krammer, 1987; Lange-Bertalot and Krammer, 1989). Moreover, several websites containing illustrated guides are very helpful in identifying diatoms: Common Freshwater Diatoms of Britain and Ireland (Kelly et al., 2005), Diatoms of the United States (Spaulding et al., 2010), and Diatoms of the Southern California Bight (Kociolek, 2012). The classification system of diatom species in Hanon paleolake is based on Round et al. (1990).

Microscopic analysis in this study has been performed in species level. About 350 valves are counted for each slide on average.

Unidentifiable diatoms are not counted; for example, there were a few very small and/or broken diatoms to identify with 1000× magnification. Some broken diatoms which cannot be counted fully as one diatom species are not counted, either; centric diatoms without central area and/or remained less than 1/3 and pennate diatoms without raphe and/or both apex and/or remained less than a half are not counted. Those which are unable to be identified into species level are counted as genus level, and they are written in “xxx spp.”; that is, “xxx spp.” does not mean that it is a sum of the genus. The pictures of major diatom species from Hanon are in Appendix V.

3.3. Diatom Diagram and Diatom Concentration

All prepared diatoms are counted by light microscopic examination as aforementioned – 350 diatom valves roughly for each sample. Tilia version 1.7.16 (Grimm, 1992) is used to construct stratigraphic diatom diagram with zonation based on constrained incremental sum of squares cluster analysis, CONISS in Tilia software: the zones are given numbers for identification such as zone 1, 2-a, 2-b, 3, 4 and 5. Totally, six zones including subzones are decided at depths of 120, 136, 156, 220 and 236cm (Grimm, 1987). The zonation has been determined in consideration of the principles of CONISS and the pattern of change in diatom assemblages (Figure 10 and 12). Several clusters can be divided and merged into slightly differently according to the dendrogram; however, six zones at these depths are established finally by considering the main changes of the diatom assemblages. Even though CONISS is a quantitative way to define zones, it

is not always right (Bennett, 1996); clusters can be divided into several zones by cutting the dedrogram at various units of height(total sum of squares), so zones can be splitted and merged in various ways. Therefore, it is better to ponder the zonation based on CONISS while considering the changes in major diatom assemblages.

The data acquired from counting diatom valves is necessary to be converted into relative abundance with an equation below in order to draw a diatom diagram (Boden, 1991):

Relative abundance of a particular species in depth XX

$$= \frac{\text{number of a particular species counted in depth XX}}{\text{total number of diatom valves counted in depth XX}} \times 100$$

The data with absolute values of counted diatom valves is not appropriate to compare the changes in each diatom assemblage because the valves in each depth are not counted in the exact same amount. Therefore, converting absolute values into relative values is required for accurate analysis. Finally, a diatom diagram can be constructed after the calculation and zonation. The diatom diagram shows the sum of each species through the depths, and it represents which species are dominant/rare, increase/decrease, appear/disappear, and so forth. Relevant species are arranged side by side in the diagram for prehension (Figure 13 and 16).

Hanon radiocarbon dates were not obtained individually in this study because the AMS radiocarbon dates were already measured and the age-depth model were already created by Park et al. (2014b), which used the exact same core(HN-1). They did not use the median ages. They took the

minimum or maximum two-sigma ages to smoothen the interpolating curve (Park et al., 2014b). For more detailed information about the radiocarbon dating, refer to the Park et al. (2014a; 2014b).

Next, diatom concentration is calculated and described. Calculating diatom concentration is a way to estimate the actually existed number of population of diatom valves from the number of observed(counted) diatom valves (Moos et al., 2009; Boden, 1991; Scherer, 1994; Bak et al., 2001; Bak et al., 2002; Bak et al., 2010). The equation to calculate diatom concentration is as follow:

$$\begin{aligned}
 & \text{Diatom valves per 1g of dry sediment} \left[\frac{\text{valves}}{1g} \right] = \\
 & \text{counted diatom valves} [\text{valves}] \times \frac{\text{cover slide glass area} [\text{mm}^2]}{\text{counted area} [\text{mm}^2]} \times \\
 & \frac{\text{beaker water volume} [\text{mL}]}{\text{pipet water volume} [\mu\text{L}]} \times 1000 [\text{mL} \rightarrow \mu\text{L}] \times \frac{1}{\text{dry sediment volume} [\text{g}]} \\
 & \text{Dry sediment}^7 \text{ volume} [\text{g}] \\
 & = \text{wet sediment volume} [\text{g}] \times (1 - \text{water content rate})
 \end{aligned}$$

This equation is modified from the calculation method of Katsuki et al. (2003) based on the author's advice. The graph of diatom concentration is inserted in the diatom diagram of Figure 13 and 16 to make it easy to compare the changes in diatom assemblage. The diatom concentration is also called "absolute number of diatom valves," and its unit is [valves/1g of dry sediment].

⁷ Sediments for diatom analysis should be dried at room temperature because diatom valves, which consist of silica, are vulnerable to heat. The sediments for this study were stored in refrigerator, so they were in wet condition when they were prepared as sediment samples for diatom analysis.

There are some factors which control the abundance of diatom such as diatom productivity, microbial decomposition, dilution by clastic sedimentation, dissolution of diatom valves, etc., and diatom concentration is ultimately related to the autochthonous water column productivity and paleoclimatic changes (Kuwae et al., 2002). There have been several studies in the relationship between diatom concentration and environmental conditions: Meyers et al. (1993) maintains that diatom productivity increases as regional precipitation, soil erosion and rock weathering increase, and coarser detrital sediment particles are usually delivered with washed out nutrients during wetter intervals by runoff. Xiao et al. (1997) asserts that the values of higher biogenic silica flux signify warmer and wetter paleoclimatic conditions as well. That is, water temperature is closely associated with diatom productivity, which is driven by air temperature. Kuwae et al. (2002) also suggests that the nutrients washed into the lake result in enhanced diatom productivity, and more nutrient input into the lake happens during a warm period with greater levels of precipitation. Therefore, diatom concentration is certainly influenced by lake productivity(trophic status of the lake) and paleoclimate(water temperature in lake), which can be connected to the paleoclimate and paleoenvironment around the lake. The interpretation of diatom concentration is going to be explained in Chapter 5.

3.4. Principal Component Analysis (PCA)

In the field of community ecology, data are aligned and organized using ordination methods to find a relationship of species, sites and environmental variables. There are two ways of ordination methods whether or not it contains environmental variables – ordination analysis and canonical ordination analysis (Ko et al., 2015). Ordination analysis is used to investigate the relation between species and its appearance by deriving indirect environmental factors from species and appearance data which do not have environmental information. This is called indirect ordination analysis, and it includes Principal Component Analysis(PCA), Correspondence Analysis(CA), and so on (Ko et al., 2015).

PCA converts high-dimensional data into low-dimensional data(dimension reduction) using orthogonal transformation to extract several principal components (Janžekovič and Novak, 2012). Principal components are the major components that can explain all the variables in the data, and each component is represented as uncorrelated axes by orthogonal transformation (Janžekovič and Novak, 2012). That is, PCA interprets and summarizes the major patterns of variation within the data (Väliiranta and Weckstrom, 2007); therefore, it is helpful to focus on the main characteristics of the phenomenon (Janžekovič and Novak, 2012). Even though PCA can indicate environmental niche due to its process, it cannot cover all dimensions of an environmental niche (Janžekovič and Novak, 2012).

PCA is carried out to see the tendency of diatom assemblages in this study. PCA graphs will be shown in Figure 7, and the graphs drawn by

component scores of Axis 1, 2 and 3 will be shown in Figure 9 – 12 in Chapter 4 and 5. Those are graphed by selecting species with greater than 5% frequency in at least one depth(sample) using CANOCO 5.0.2.0 (ter Braak and Šmilauer, 2012). The variable loadings of major species are going to be interpreted to find out what each axis stands for in Chapter 4.1. It is because the component scores reflect how significant a species is at delineating the variation within an assemblage (Allen et al., 2005). Accordingly, it is necessary to construe what each axis means. The analyses of the axes are going to be explained in Chapter 4.1 and the comparisons of trend of respective axes will be discussed in Chapter 5.2. The component scores of the major species are recorded in Appendix IV.

3.5. The Ratio of Planktonic to Benthic Diatom Species (P:B ratio)

A graph describing P:B ratio has been constructed as well (Figure 15). P:B ratio is a ratio of planktonic to benthic diatom species. Planktonic species are free floating species(not attached to a plant or rock or bed); therefore, they cannot usually thrive in shallow water comparing to benthic species. Actually, there are various conditions that planktonic diatoms can prosper besides water depth; for example, long ice-free season is more favorable to planktonic species than benthic species because ice melts from the littoral area(shallow water area) to the middle of the water(deep water area), so an ice-cover season is unfavorable to planktonic diatoms (Wang et al., 2012). However, the temperature in Seogwipo where Hanon is located

does not fall less than 0°C (Figure 2), and thus ice-free/ice-cover season is not going to be considered significantly in this study. Therefore, the P:B ratio is likely to be related to the water depth of Hanon paleolake; the graph will be helpful to see the change of water depth according to the change in ratio between planktonic and benthic diatom species. The ratio of planktonic to benthic diatom species is calculated as below (Wang et al., 2013):

$$P:B \text{ ratio} = \frac{\sum \text{planktonic taxa}}{\sum (\text{planktonic} + \text{benthic taxa})}$$

A. ambigua, *D. stelligera*, and *D. pseudostelligera* are chosen for planktonic species. *F. capucina* var. *mesolepta* and *Staurosirella pinnata* are tychoplanktons; however, they are basically benthic species, so these species were not counted for planktonic taxa in the calculation for the P:B ratio. The result of P:B ratio is going to be show and explained in Chapter 4.3, and it will be discussed in detail with the result of PCA in Chapter 5.2.

Chapter 4. Research Results and Analysis

4.1. Principal Component Analysis (PCA)

Principal component analysis is carried out to condense all the data into two-dimensional presentation to show its major representative features by projection as explained previously (Janžekovič and Novak, 2012). Above all, PCAs have been tried twice to see which one would be appropriate for analysis: one excluding “spp.” counting and the other one including “spp.” counting. The “spp.” counting in here means counted diatoms in genus level that were unable to be identified in species level; however, it does not mean that it is the sum of the genus level. The reason why this step is needed is to notice which one would be better to interpret; which one is easy to observe the meaning of principal components.

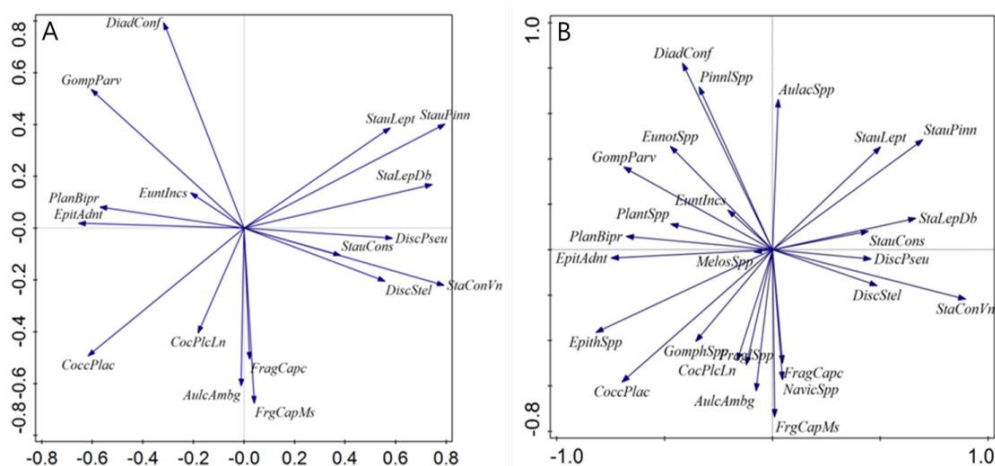


Figure 6. PCA graphs with major diatom taxa (A) excluding “spp.” and (B) including “spp.”

For principal component analyses, 17 and 26 diatom species are selected respectively in Figure 6: Figure 6-A excluding “spp.” shows the distribution of 17 species⁸ while Figure 6-B shows the arrangement of 26 diatom species including “spp.”⁹ Each axis in both graphs represents the same thing because both graphs are drawn from the same data. Thus, it is good to interpret only one of the graphs. Consequently, the graph excluding “spp.” is selected because it is plain enough to interpret the meaning of axes indicating information of environment/habitat/distribution in species level. Therefore, the simple version graph is better for interpretation – easy to find the tendency of the distribution of species.

From now on, the analysis on the results of PCA excluding “spp.” is going to be explained. The eigenvalues are essential to judge how many axes it should be considered for interpretation. As a result, four axes are chosen by referring to scree plot, and the eigenvalues are below (Table 1):

Axes (PCA)	Axis 1	Axis 2	Axis 3	Axis 4
Eigenvalues	0.2723	0.1694	0.1194	0.0964
Explained variation(cumulative) [%]	27.23	44.17	56.11	65.74

Table 1. Eigenvalues and variance explained by PCA of the diatom species from core HN-1

- ⁸ *Diadesmis Confervacea*, *Gomphonema parvulum*, *Eunotia incisa*, *Planothidium biporum*, *Epithemia adnata*, *Cocconeis placentula*, *Cocconeis placentula* var. *lineata*, *Aulacoseira ambigua*, *Fragilaria capucina*, *Fragilaria capucina* var. *mesolepta*, *Discostella stelligera*, *Staurosira construens* var. *venter*, *Staurosira construens*, *Discostella pseudostelligera*, *Staurosirella leptostauron* var. *dubia*, *Staurosirella leptostauron*, and *Staurosirella pinnata* (counterclockwise)
- ⁹ *Pinnularia* spp., *Diadesmis confervacea*, *Eunotia* spp., *Eunotia incisa*, *Gomphonema parvulum*, *Planothidium* spp., *Planothidium biporum*, *Epithemia adnata*, *Melosira* spp., *Epithemia* spp., *Cocconeis placentula*, *Gomphonema* spp., *Cocconeis placentula* var. *lineata*, *Fragilaria* spp., *Aulacoseira ambigua*, *Fragilaria capucina* var. *mesolepta*, *Navicula* spp., *Fragilaria capucina*, *Discostella stelligera*, *Staurosira construens* var. *venter*, *Discostella pseudostelligera*, *Staurosira construens*, *Staurosirella leptostauron* var. *dubia*, *Staurosirella pinnata*, *Staurosirella leptostauron*, and *Aulacoseira* spp (counterclockwise)

The eigenvalues are 27.23% for Axis 1, 16.94% for Axis 2, 11.94% for Axis 3 and 9.64% for Axis 4, and their cumulative explained variation is 65.74%. That is, the PCA explains 65.74% of the total variance within the first four axes, and the graphs of PCA are shown in Figure 7¹⁰. It is going to be explained about what these axes represent respectively.

The graph of Axis 1 and 2 (Figure 7), *S. construens* var. *venter* and *S. pinnata* show the highest positive values, 0.7914 and 0.7952, while *C. placentula* and *E. adnata* show the highest negative values, -0.6171 and -0.654, along Axis 1. Considering *S. construens* var. *venter* and *S. pinnata* prefer mesotrophic (Fluin et al., 2010; Joh et al., 2010) while *C. placentula* and *E. adnata* prefer eutrophic (Joh, 2012; Kelly et al., 2005; Round et al., 1990; Krammer and Lange-Bertalot, 1988), Axis 1 can be interpreted as a representative of the nutrient status in the lake.

In the same way, *D. confervacea* and *G. parvulum* show highly positive values of 0.794 and 0.5355, respectively, while *A. ambigua*, *F. capucina* var. *mesolepta* and *C. placentula* show highly negative values such as -0.6095, -0.6766 and -0.4939 along Axis 2, which is able to observe in the graph of Axis 2 and 3 in Figure 7. *D. confervacea* is a benthic species attached to plants (Jena et al., 2006; Torgan and Santos, 2008). On the other hand, *C. placentula* is also a benthic species but attached to rocks (Joh, 2012; Round et al., 1990; Kelly et al., 2005; Spaulding et al., 2010), *A. ambigua* is a planktonic species (Joh, 2010; Kelly et al., 2005; Spaulding et al., 2010), and *F. capucina* var. *mesolepta* is a tychoplanktonic (Stoermer et al., 1971). Therefore, Axis 2 seems to represent the water depth in Hanon.

¹⁰ In Figure 7, the axis having smaller number is always positioned on the horizontal line; for example, Axis 1 is at horizontal line in the graph of Axis 1 and 2.

E. incisa and *F. capucina* show the highest positive values such as 0.7277 and 0.5623, while *C. placentula* var. *lineata*, *E. adnata* and *P. biporomum* show the highest negative values of -0.5039, -0.4923 and -0.6173 along Axis 3, respectively (Figure 7 – Axis 1 and 3). *E. incisa* prefers an acidic condition (Ortiz-Lerin and Cambra, 2007; Fukumoto et al., 2012; Flower et al., 1997), while the three diatom species with the highest negative values are alkaliphilous (Barbiero, 2000; Metcalfe et al., 1991; Kelly et al., 2005; Spaulding et al., 2010). Therefore, Axis 3 seems to be related to the pH of the lake.

For Axis 4 (Figure 7 – Axis 2 and 4), *D. stelligera* and *D. pseudostelligera* show highly positive values of 0.6016 and 0.5853, while *S. construens* and *S. construens* var. *venter* show highly negative values of -0.7213 and -0.3978. However, the Axis 4 was difficult to interpret due to the lack of habitat information. *D. stelligera* and *D. pseudostelligera* have very low sinking velocity, so they can persist throughout summer thermal stratification (Wang et al. 2012). *S. construens* and *S. construens* var. *venter* can increase in abundance as opportunistic diatoms when macrophytes are plentiful (Fluin et al., 2010). These species are common species all year around, especially from spring to summer (Kelly et al., 2005; Wang et al., 2012). Likewise, the information about these four diatom species does not correlate well, so it is hard to analyze what Axis 4 reflects.

The interpretation of Axis 1, 2 and 3 is going to be examined briefly whether Axis 1, 2 and 3 indicates trophic status, water depth and pH. The principal components are compared to the change of several diatom assemblages. Several diatoms are plotted beside the diagrams of each axis (Figure 8), and the diatoms are compared to the axes based on the ecology of each diatom. In Figure 8, the diagrams of Axis 1, 2 and 3 are 10 times enlarged to clarify their changes so as to compare other variations precisely. Also, the grey shadings in the diagram mean that the graph is exaggerated by three times.

First, *C. placentula* is very widely distributed except oligotrophic environment. Therefore, its fluctuation must be inversely proportional to the trend of Axis 1, and it seems they are in inverse proportion to each other. That is, it is right that Axis 1 indicates trophic status. Second, Axis 2 is compared to *A. ambigua* and *D. confervacea*. Because *A. ambigua* is planktonic while *D. confervacea* is epilithic/epiphytic, Axis 2 must be proportional to *D. confervacea* and inversely proportional to *A. ambigua*, and so are they. Although it seems that the fluctuation of *A. ambigua* does not fit well to Axis 2, *D. confervacea* seems to match Axis 2 well. These differences may have been caused to various environmental factors such as temperature, pH, trophic status, etc. Thus, it is possible to say Axis 2 reflects water depth. Third, *E. incisa* and *S. pinnata* are compared to verify the interpretation of Axis 3 was right. Because *E. incisa* reflects acidification of lacustrine environment while *S. pinnata* is alkaliphilous, *E. incisa* must be proportional and *S. pinnata* must be inversely proportional to Axis 3. As a result, they are also harmonized with each other. In conclusion, the interpretations of Axis 1, 2 and 3 were right, and there would be no crucial problems/errors for further discussion.

Even though it was impossible to find out what Axis 4 means, it is still possible to reconstruct paleoenvironment of Hanon using Axis 1, 2 and 3 by having interpretations so far. Additional graphs drawn by components of the first three axes are going to be shown in the next pages (Figure 9 - 12). These graphs are going to be discussed in detail to verify the reconstructed paleoenvironment by diatom diagram in Chapter 5.2.

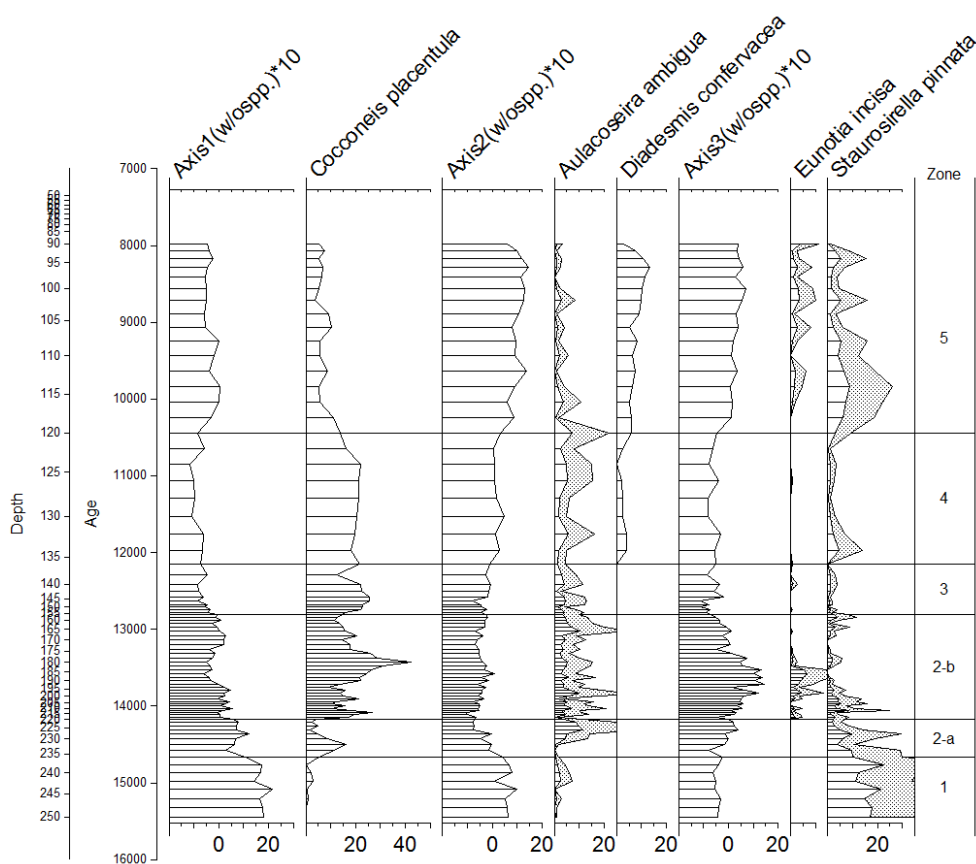


Figure 8. Diagram for examination of Axis 1, 2 and 3 by comparisons of several diatoms

Lastly, PCA graphs are used to rearrange the diatom species in diatom diagrams – gathering similar diatom assemblages together, so this

analysis was also helpful to start solving a diatom diagram. The component scores of the Axis 1, 2, 3 and 4 are described in Appendix III, and each species score at Axis 1, 2, 3 and 4 is also reported in Appendix IV.

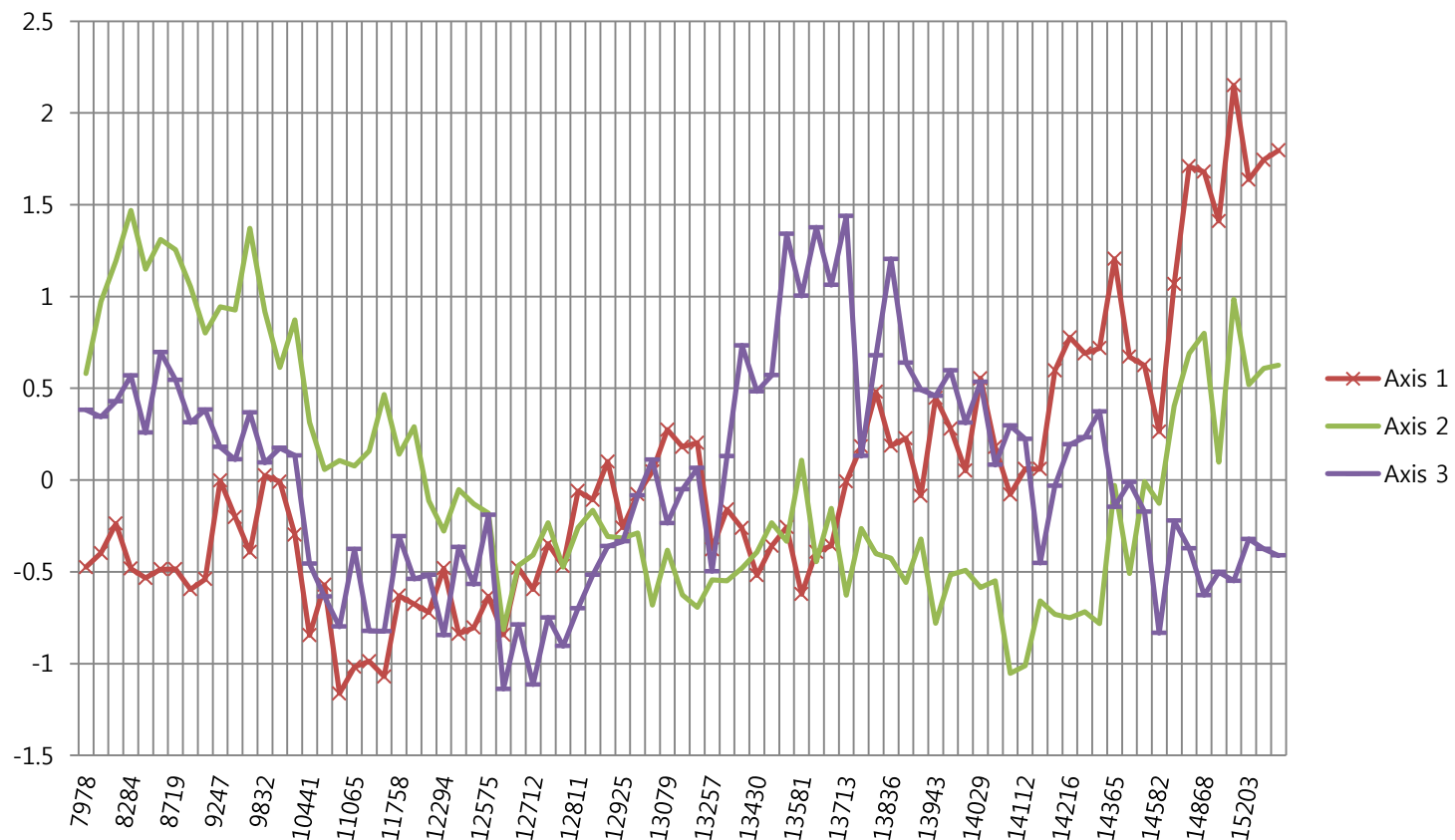


Figure 9. The graphs of component scores on the PCA Axis 1, 2 and 3

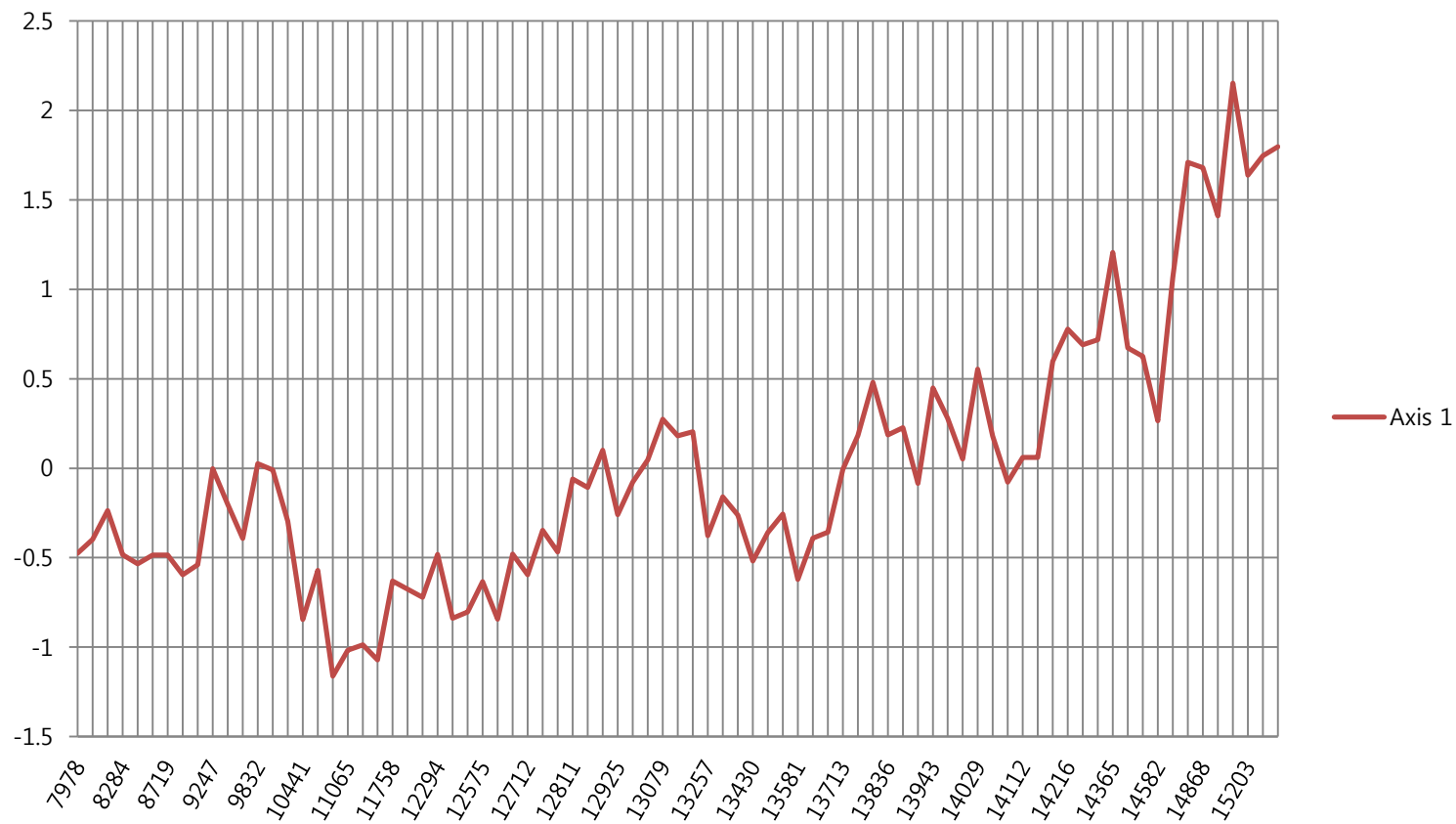


Figure 10. The graph of component scores on the PCA Axis 1

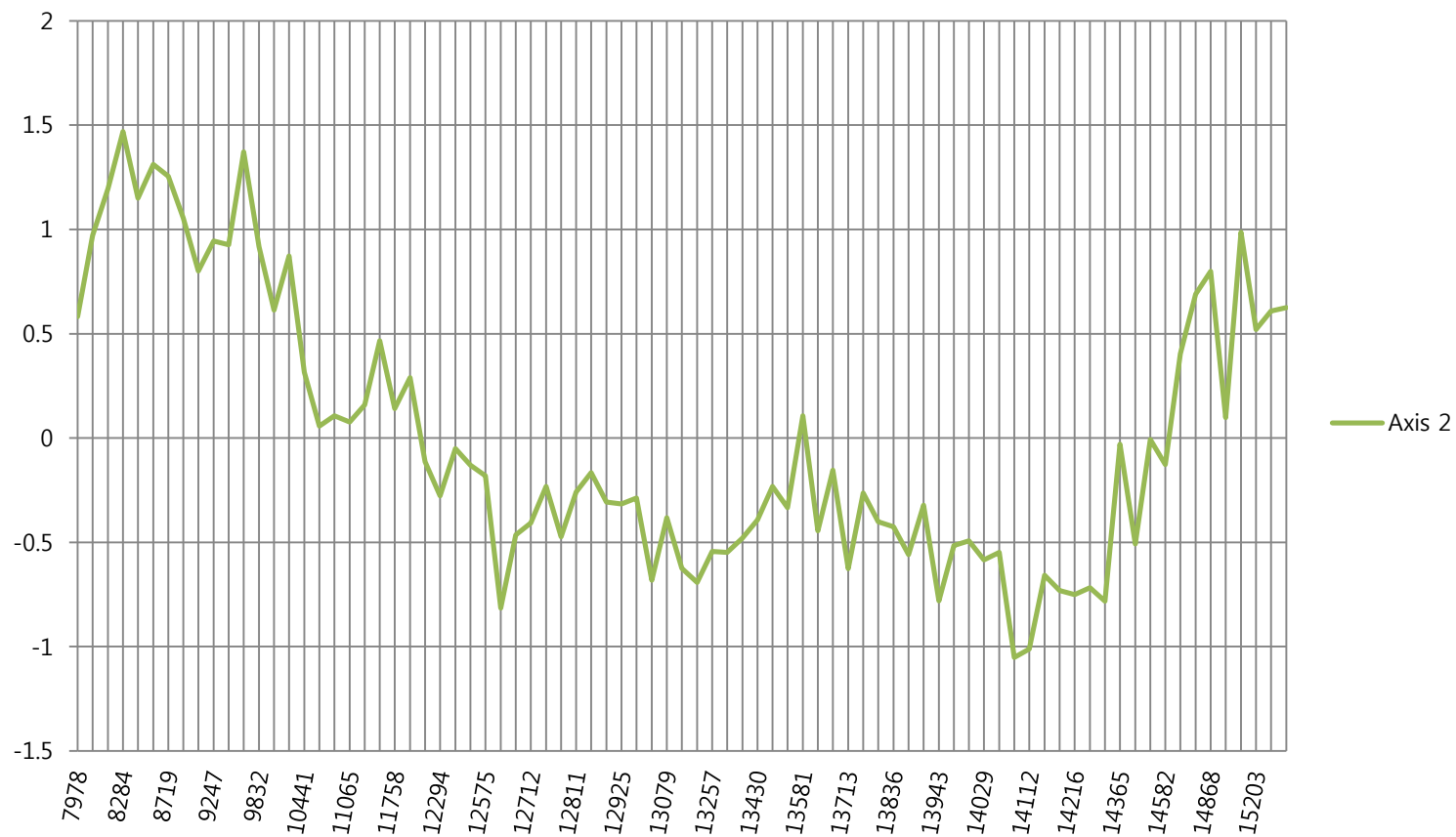


Figure 11. The graph of component scores on the PCA Axis 2

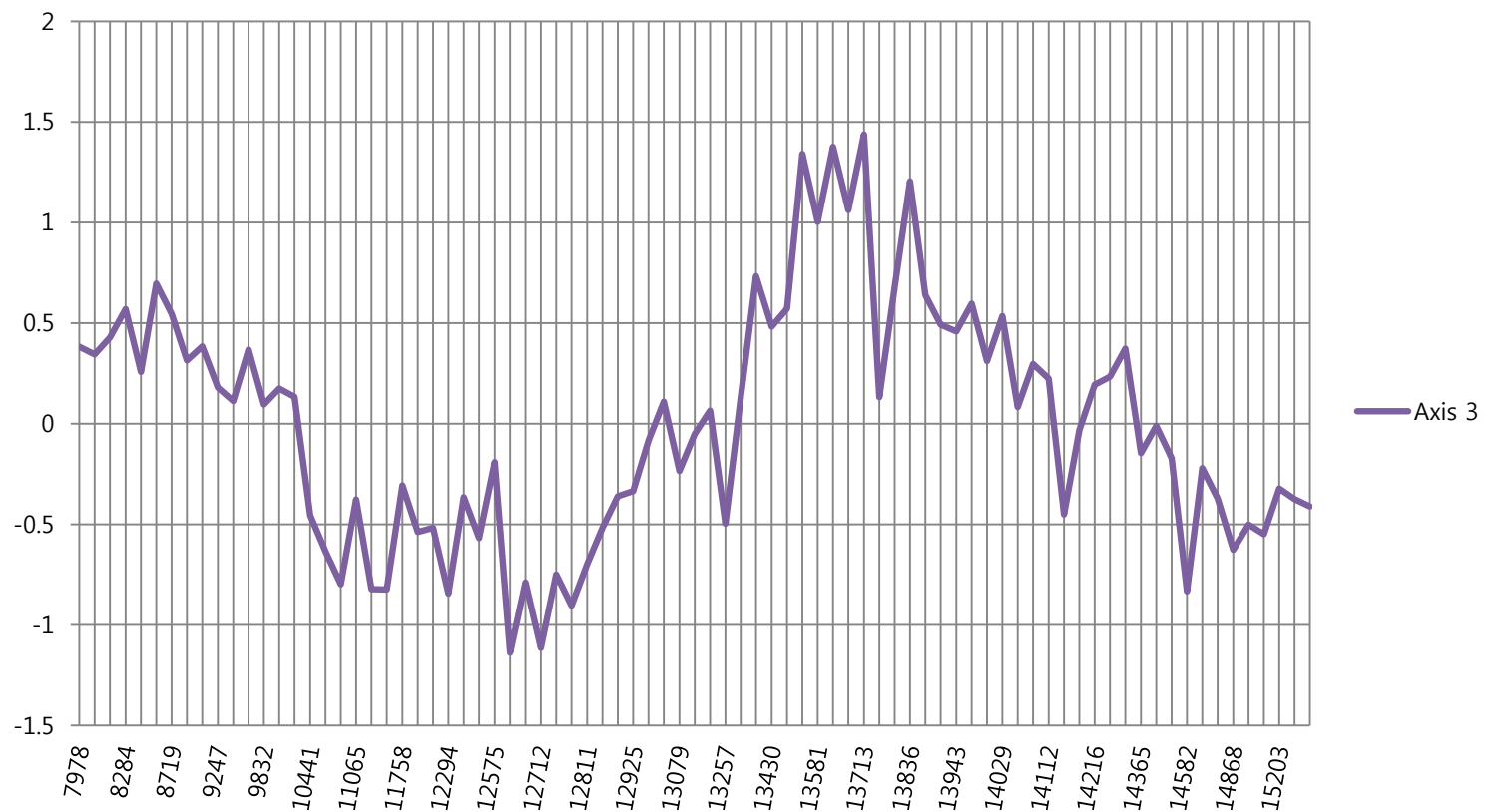


Figure 12. The graph of component scores on the PCA Axis 3

4.2. Diatom Flora in the Diagram

In this chapter, diatom flora in the diagram is going to be explained: which species are dominant/rare, increase/decrease and appear/disappear (Figure 10). As explained in Chapter 3.3, the diatom assemblages in the stratigraphic diatom diagram are totally divided into five large zones and two subzones with zonation based on constrained incremental sum of squares cluster analysis, CONISS in Tilia software (Grimm, 1987) (Figure 13 and 16). In the diagram, each diatom diagram is exaggerated by a factor of five with grey shadings, for a good grasp of each species' fluctuations. Original values are specified in black solid diagrams.

A total of 47 genera and 221 species have been identified in 81 samples with 2cm interval from Hanon paleo-maar lake sediment. Diatoms are present throughout the whole HN-1 core, and the composition of diatom species are getting very different from top to bottom in the core. As the depth is getting deeper, the sizes of diatoms are getting smaller and many broken valves found. Moreover, the diatom concentration at the bottom is very little degressively even though the concentration is not low. Also, genera *Karayevia* and *Cavinula* appear rarely in other depths, but are present in deeper parts of the core. On the other hand, the sizes of diatoms are getting larger and have distinguishable feature easy to identify as the depth is getting shallower. The degressive diatom concentration is high even though its tendency actually decreases as the depth gets shallower; it was hard to identify diatoms sometimes because they were overlapped too much due to its high concentration and density. It may be connected to the sedimentation rate in Hanon. In the upper depths, genera *Gomphonema*,

Epithemia, *Cocconeis* and *Diadesmis* appear frequently. The upper part of the core is made up of a wide variety of diatoms, and they are exhibited evenly in general. The greater part of the species from Hanon paleo-maar lake consist of freshwater and fresh brackish species.

For the diagram in Chapter 4.2, the 26 species are selected based on their relative abundance which is larger than 5% frequency in at least one sample. Also, the “spp.” is included for Figure 13 because it would be good to try to examine the whole change of diatom assemblages that were counted originally. It is difficult to figure out the paleoenvironmental changes in detail based on the habitat information in genus level because of its ambiguity; therefore, the new diatom diagram which does not contain “spp.” assemblages will be discussed and interpreted in Chapter 5. Despite of its difficulty, the diatom diagram including “spp.” is going to be explained from Chapter 4.1.1. to 4.1.6. for information for whom may be interested. As mentioned before, the order of arrangement of diatoms in the diagrams was referred to the result of PCA; PCA makes diatoms that have common environmental conditions gather. This makes it easy to understand the fluctuations in diatom assemblage over time and compare to the other changes of diatom assemblages changing in a similar or different way. The diagram showing the fluctuations of all species is in Appendix I.

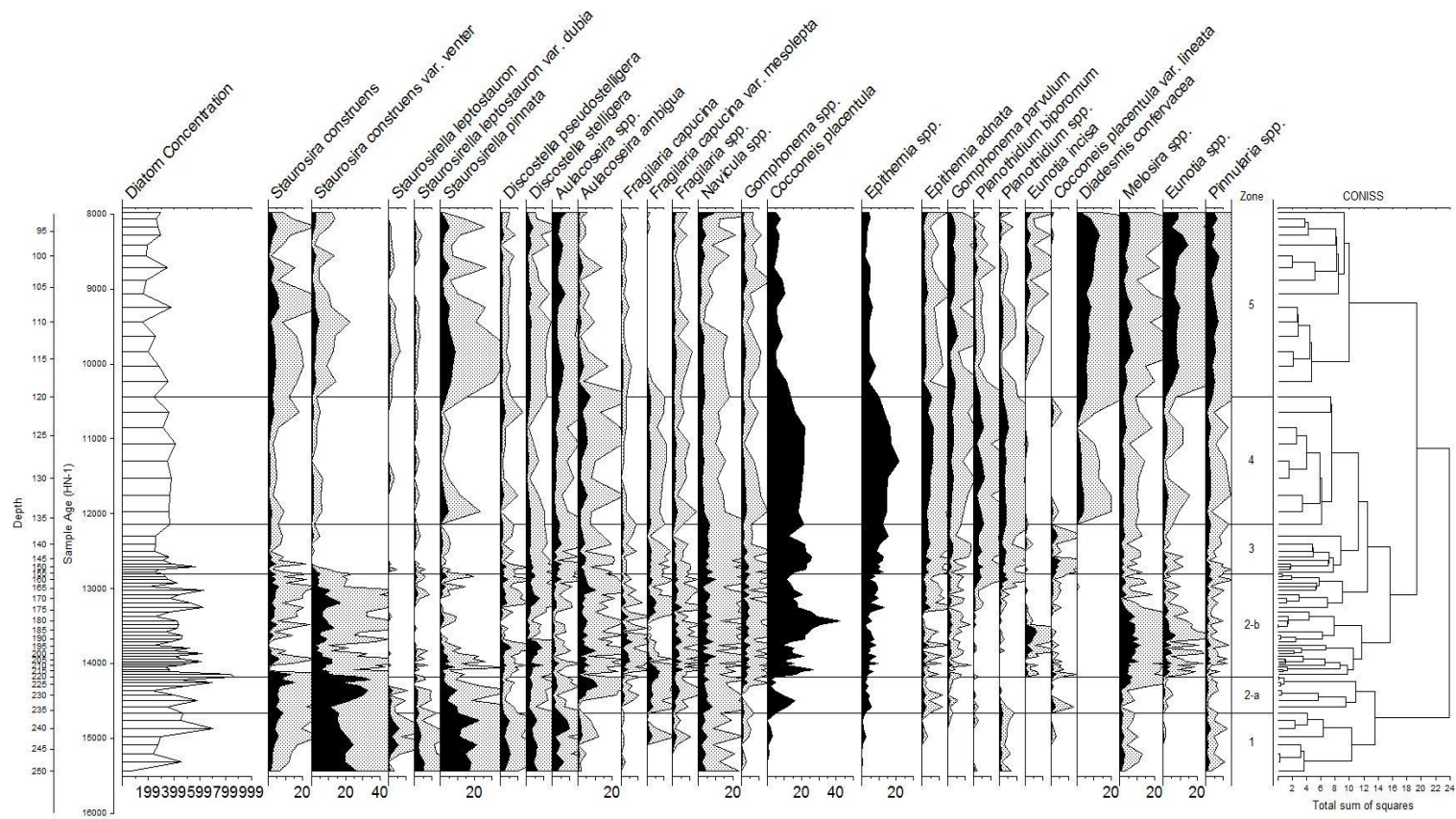


Figure 13. Diatom diagram including “spp.” – grey shading means that it is enlarged by five times

4.1.1. Zone 1: 15,440 cal. yr BP – 14,670 cal. yr BP (Oldest Dryas)

Zone 1 from 250cm to 236cm does contain diatoms, but quite a few diatoms in this zone are small and broken as mentioned before, so it is hard to identify them into species level. New species that do not appear in upper sediments are also observable. In particular, the sample at 250cm is very difficult to identify diatoms due to the degressive low diatom concentration comparing to other depths.

As it is detectable in Figure 13, there are two main dominant species; *Staurosira construens* var. *venter* and *Staurosirella pinnata*. They reach approximately 50% together. Besides, *Staurosira construens*, *Staurosirella leptostauron*, *Staurosirella leptostauron* var. *dubia*, *Discostella stelligera*, *Discostella pseudostelligera*, *Aulacoseira* spp., and *Navicula* spp. are common in zone 1. The other species rarely show up or have very low relative abundance whose power of explanation would be poor for representing the change of environment in the past around Hanon.

4.1.2. Zone 2-a: 14,670 cal. yr BP – 14,180 cal. yr BP (The beginning of Bølling-Allerød)

Zone 2 between 236 and 220cm still consists of small diatoms, however, it is much better to identify than zone 1. *Staurosira construens* var. *venter*, the predominant species in zone 1, is still abundant in zone 2-a. Also, *Staurosira construens*, *Aulacoseira ambigua*, and *Cocconeis placentula* are dominant with about 70% in total abundance in this zone.

Especially, *C. placentula* has begun to appear and increase abruptly, whereas *S. pinnata* decrease gradually.

4.1.3. Zone 2-b: 14,180 cal. yr BP – 12,810 cal. yr BP (Bølling-Allerød)

The prevailing species in zone 2-b between 220 and 156cm from the surface of the earth of the core sediment are *Cocconeis placentula* and *Eunotia incisa*. *C. placentula* shows the maximum relative abundance at ca. 13,500 cal. yr BP throughout the core, which almost reaches to 40% by itself. *E. incisa* is present newly and increase until the midst of zone 2-b mainly. It is also told that *Melosira* spp. is dominant, and *Staurosira construens* var. *venter* decreases notably. Also, *Aulacoseira ambigua* maintains its abundance while *Staurosirella pinnata* keeps decreasing. Also, *Eunotia* spp. just appears.

4.1.4. Zone 3: 12,810 cal. yr BP – 12,150 cal. yr BP (Younger Dryas)

First of all, *Cocconeis placentula* shows a declining trend, albeit in high relatively abundance. The prevalent species in zone 3 (156-136cm) are *Epithemia adnata*, *Planothidium biporum*, and *Cocconeis placentula* var. *lineata* by 15% of relative total abundance although their percentage is not that high. It is because the substantial shift in the diatom species is considered importantly. The actual dominant species with high abundances are *Epithemia* spp. and *C. placentula*. *Melosira* spp. and *Eunotia* spp. are

still shown, but in decline. *Navicula* spp. keeps its relative abundance consistently throughout the whole core, HN-1. *Pinnularia* spp. does similar with *Navicula* spp., however, it will increase from zone 4 a little bit.

4.1.5. Zone 4: 12,150 cal. yr BP – 10,440 cal. yr BP (Pre-Boreal: the beginning of Holocene)

The predominant species in zone 4 (136-120cm) are *Diadmesmis confervacea*, *Aulacoseira ambigua*, *Epithemia adnata*, and *Planorbulina biporum*. Especially, *D. confervacea* appears for the first time with high relative abundance. Even though it shows a declining trend at the end of this zone but recovers shortly. *Gomphonema parvulum* and *Planorbulina* spp. are common but quite dominant in this zone. *Epithemia* spp. is also prevailing by reaching its maximum relative abundance throughout this core, which is about 20%. *Cocconeis placentula* is also present with high abundance. There is an unusual abrupt increase and decrease in *Stauroneis pinnata* in the beginning of zone 4.

4.1.6. Zone 5: 10,440 cal. yr BP – 7,980 cal. yr BP (Boreal)

The last zone, zone 5 covers sediments between 120 and 90cm. In the section, *Diadmesmis confervacea*, *Eunotia incisa*, *Stauroneis pinnata*, and *Stauroneis construens* is prevailing. *Melosira* spp. and *Pinnularia* spp. account for high relative abundance, too. It shows a pronounced increase in *D. confervacea* in zone 5. *E. incisa* increases after a while in zone 5 begins

and maintains its richness until the end, which is the second dominant appearance for *E. incisa* throughout the core. *Staurosira construens* var. *venter* and *Aulacoseira* spp. are common species. There is two striking decreased species such as *Cocconeis placentula* and *Epithemia* spp. Based on the results of diatom diagram, the interpretation and reconstruction of paleoenvironment of Hanon in detail will be discussed in Chapter 5.1.

4.3. The Ratio of Planktonic to Benthic Diatom Species (P:B ratio)

The graphs describing the changes of benthic and planktonic diatoms have been drawn in Figure 14 and 15 based on the calculation of the equation explained in Chapter 3.5. Before starting looking at the fluctuation of P:B ratio in earnest, the graph in Figure 14 has been drawn to see the individual changes of planktonic and benthic species during the last deglaciation. There are remarkable changes in both diatom types: abrupt decrease in benthic diatoms and an increase in planktonic diatoms approximately at 13,730 and 13,780 cal. yr BP. Those are minimum and maximum points for each one in the graph. The slight age discrepancy between the two points is about 40 to 50 years. This could have happened because of the types of benthic diatom species such as tychoplankton; all the benthic species do not live in the same habitat. Some of them live attached to a rock or sand, whereas others live attached to plant or lakebed. All of these diatoms are called benthic species; however, they do not indicate directly shallow water depth even though they are benthic. For

example, most benthic diatoms which is attached to a plant inhabit shallow water because plants usually inhabit littoral area for plant photosynthesis where light penetrates. On the other hand, another benthic species attached to a rock is able to inhabit much deeper water depth than the one attached to a plant because rocks run into a lakebed straightly caused by runoff of heavy rainfall – this can be related to precipitation. Therefore, it is necessary to search the habitat environments of the benthic species for more accurate interpretation. Overall, both benthic and planktonic species tend to decline slightly from 15,500 to 8,000 cal. yr BP.

Finally, the graph of the ratio change of planktonic to benthic species in Hanon maar paleolake during the last deglaciation has been constructed (Figure 15). Each change in planktonic and benthic species is combined by the equation mentioned in Chapter 3.5. The general trend in Figure 15 is similar to the one of planktonic species in Figure 14. As the name of the graph is “planktonic to benthic,” it shows the ratio change of planktonic species comparing to benthic species (Figure 15). Approximately at 13,780 cal. yr BP, the graph is at the maximum, which means the largest abundance of planktonic species compared with benthic species in Hanon paleolake. The reason why planktonic diatoms thrived in this period could be connected to water depth, which is also related to the strength of the monsoon, sedimentation rate, and so on.

According to P:B ratio analysis, the diversity of planktonic diatom species in Hanon paleolake is much less than the one of benthic species during the last deglaciation. That is, it seems that the water depth of Hanon had been shallow in general from 15,500 to 8,000 cal. yr BP. However, the interpretation should be supplemented by considering sedimentation rate, strength of the monsoon, and other related environmental factors to water

depth to reconstruct more accurate water depth. Last, the P:B ratio graph is also going to be interpreted in detail comparing to Axis 1, 2, 3 components and other proxy data of Hanon from Park et al. (2014b) in Chapter 5.3.

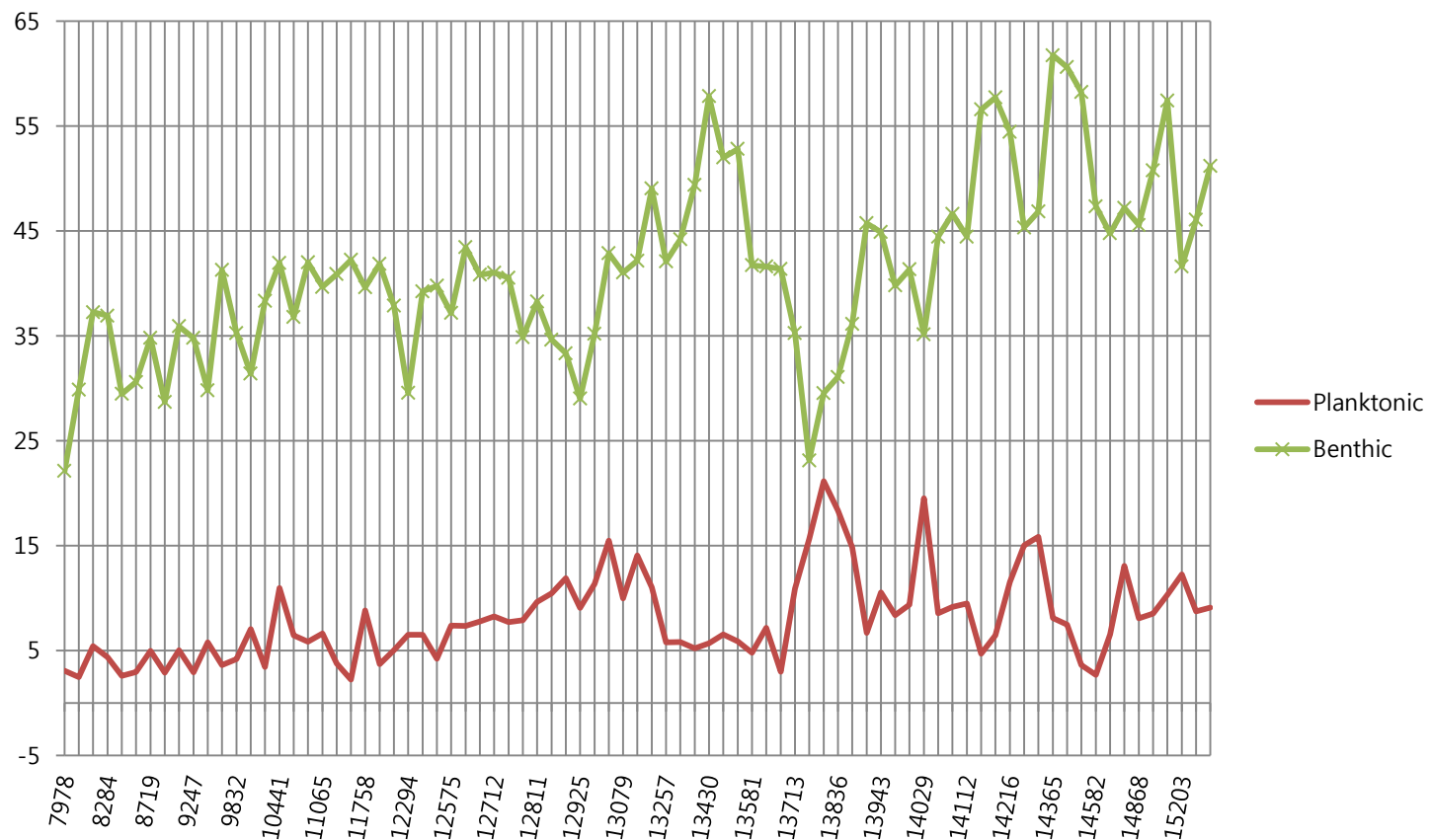


Figure 14. The respective changes of planktonic and benthic species

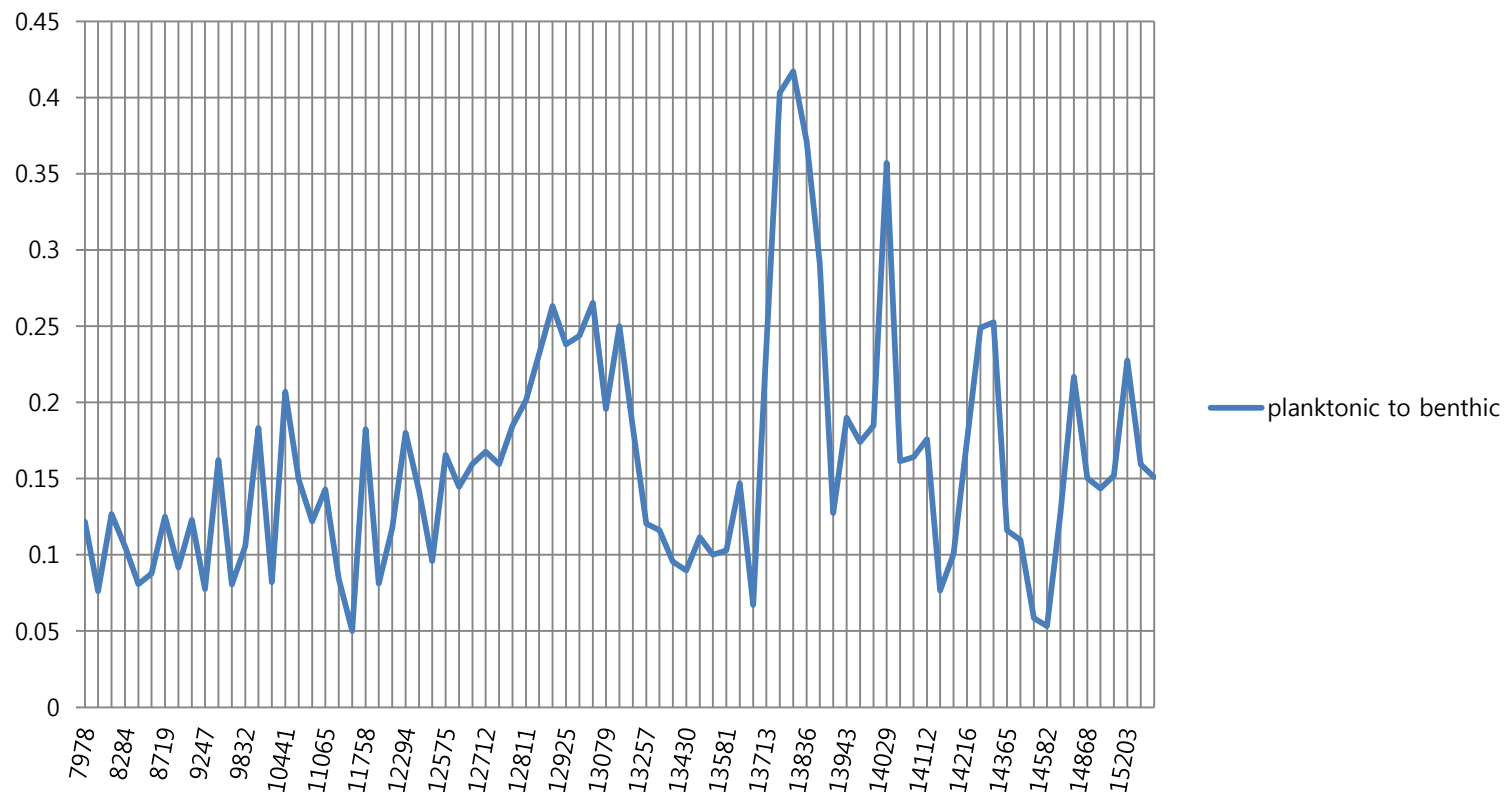


Figure 15. P:B ratio in Hanon maar paleolake during the last deglaciation

Chapter 5. Discussion

The total length of core HN-1 is approximately 10m-long, and the range from 250 to 90cm of HN-1 is selected for this study to observe the environmental change during the last deglaciation, which covers from 15,500 to 8,000 cal. yr BP – approximately 7,500 years among the paleomaar lake history. The analysis has been performed every 2cm of the section. Totally, 47 genera and 221 species have been enumerated throughout the core. The AMS radiocarbon dates are adopted from the research by Park et al. (2014b), which had studied with the same core sediments.

In this chapter, the new version of diatom diagram is going to be interpreted. In Chapter 4, the diatom diagram included “spp.,” but the one in Figure 16 does not contain “spp.” As explained previous chapter, it is difficult to interpret and reconstruct paleoenvironment based on the genus level of diatoms because diatoms in genus level cover quite a wide range of inhabited environment. This is why most diatom analysis has been being performed in species level. Through the interpretation of the diatom diagram, the paleoenvironment in Hanon during the last deglaciation would be reconstructed in Chapter 5.1.1. Based on the reconstructed information, a schematization has been done in Chapter 5.1.2. Also, there will be a few more analyses(verification) using principal components and P:B ratio in Chapter 5.2. Last, comparative analysis with other research in Hanon, especially Park et al. (2014b), is going to be discussed in Chapter 5.3. The diagram delineating all species is in Appendix I, and counting data of major species are in Appendix II.

5.1. Reconstructing the Paleoenvironment of Hanon Maar based on the Diatom Diagram and Schematization

5.1.1. Reconstructing the Paleoenvironment of Hanon Maar through schematization of each zone based on Diatom Diagram

To reconstruct the detailed environmental changes in Hanon, it is essential to interpret the diatom diagram. A new graph is drawn to show the transition of diatom assemblage lucidly according to temporal trend (Figure 16). In Chapter 5.1.1., schematic diagrams are going to be drawn (Chen et al., 2014) and interpreted for a diatom-based reconstruction of the paleoenvironmental changes in Hanon. The reconstructed lacustrine environment based on schematic diagram will be summarized and schematized again for better vision.

The values of diatom concentration are shown in Figure 16. The total amount of diatoms seems to decrease gradually from the bottom to the top of the core according to the transition of absolute number of diatom valves per 1g of dry sample, which varies from 6.95×10^9 to 8.64×10^9 [valves]. The total amount of valves is quite a lot but normal. According to Katsuki et al. (2012), the absolute number of valves from Lagoon Notoro-Ko in northern Japan also had similar amount, which varies from 0.5×10^9 to 2.5×10^9 ; therefore, the absolute number of diatom valves in Hanon are not at abnormal levels. According to diatom concentration from Hanon data, the lake productivity had decreased during the last deglaciation, and it

reached to the maximum at BA. It means that the climate during BA was wet and warm, and the trophic status was good. However, the concentration during Holocene maintained relatively low, and it means the climate was not warm and/or wet. These should be checked later with other results of this study. The diagram of diatom concentration is in Figure 13 and 16.

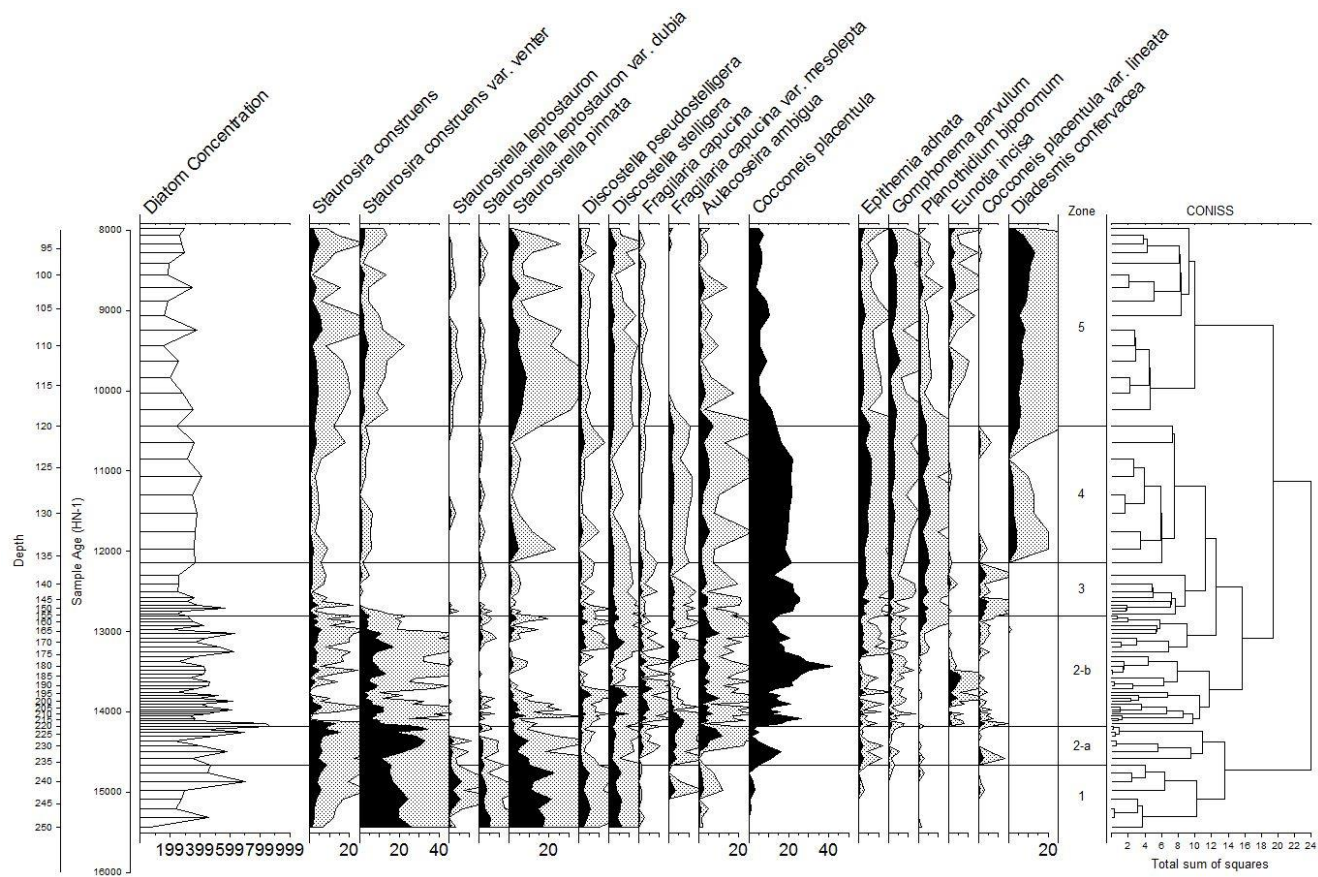


Figure 16. Diatom diagram excluding “spp.” – grey shading means that it is enlarged by five times

Throughout the Chapter 5.1 from now on, there will be the interpretation of diatom diagram with some schematizations for better understanding (Figure 17 – 22). The information is based on lacustrine environment concerning surrounding factors around a lake such as monsoon, vegetation, and so on. The schematic diagrams are created by referring to Chen et al. (2014). Before starting to look at the schematic diagrams, there will be an unfamiliar term – saprobity values. The values specify the levels of dissolved oxygen and Biological oxygen demand(BOD), that is to say water quality class (Kelly et al., 2005) (Table 2). For example, the water quality at β -mesosaprobous is clear which as high level of dissolved oxygen in it while having low level of BOD.

Value	Description	Water quality class	O ₂ saturation (%)	BOD (mg l ⁻¹ O ₂)
1	Oligosaprobous	I, I-II	> 85	< 2
2	β -mesosaprobous	II	70 - 85	2 – 4
3	α -mesosaprobous	III	25 -70	4 -13
4	α -meso/polysaprobous	III-IV	10 - 25	13 – 22
5	Polysaprobous	IV	< 10	> 22

Table 2. Saprobity index – the classes of water quality (Kelly et al., 2005)

Furthermore, here is a table containing habitat environment of major diatom species of HN-1. It is briefly mentioned about each diatom's favorable environmental conditions from the schematic diagrams (Figure 17 – 22), so the readers can refer to Table 3 for further information. From the next paragraph, schematic diagrams will be constructed to reconstruct paleoenvironment of Hanon in detail, and the reconstruction is going to be performed zone by zone.

Species	Ecology	Reference
<i>Staurosira construens</i>	freshwater, β -mesosaprobous, alkaliphilous, meso- to eutrophic	Kobayasi et al. (2006)
<i>Staurosira construens</i> var. <i>venter</i>	freshwater, tolerant of wide environment variables, β -mesosaprobous, alkaliphilous, mesotrophic, opportunistic diatoms	Van Dam et al. (1994), Fluin et al. (2010)
<i>Staurosirella leptostauron</i>	freshwater, epipsammic, oligosaprobous, alkaliphilous, meso- to eutrophic	Kelly et al. (2005)
<i>Staurosirella pinnata</i>	freshwater, tychoplanktonic/epiphytic, alkaliphilous, oligosaprobic, epipsammic, meso- to eutrophic	Round et al. (1990), Ribeiro et al. (2010), Stoermer et al. (1971)
<i>Discostella stelligera</i>	freshwater, planktonic, persist throughout summer thermal stratification, low sinking velocity, inhabit metalimnion, growing all-year-round, oligo- to eutrophic	Wang et al. (2012)
<i>Fragilaria capucina</i>	freshwater, circumneutral, β -mesosaprobous, mesotrophic	Kelly et al. (2005)
<i>Fragilaria capucina</i> var. <i>mesolepta</i>	freshwater, tychoplanktonic/benthic, alkaliphilous, benthic, eutrophic	Kelly et al. (2005), Stoermer et al. (1971)
<i>Aulacoseira ambigua</i>	planktonic, requires higher light and temperature conditions, generally occurs during summer to autumn, oligo- to eutrophic	Rioual et al. (2007), Kossler et al. (2011)
<i>Cocconeis placentula</i>	freshwater to brackish water, circumneutral to alkaliphilous, β -mesosaprobous, attach to rock, pioneer species, fast growing, very widely distributed except oligotrophic environment, meso- to eutrophic, found throughout the year but most abundant in rivers in the summer	Go (2013), Kelly et al. (2005)
<i>Epithemia adnata</i>	freshwater, epiphytic/epilithic, neutral to high pH(alkalibiontic), β -mesosaprobous, meso- to eutrophic, capable of N-fixation	Kelly et al. (2005)
<i>Gomphonema parvulum</i>	freshwater, benthic, α -meso/polysaprobous, circumneutral, eutrophic	Kelly et al. (2005)
<i>Planothidium biporumum</i>	benthic, eutrophic	Kelly et al. (2005), Spaulding (2010)
<i>Eunotia incisa</i>	benthic, reflects acidification of aquatic environment, low in electrolytes, oligotrophic	Fukumoto et al. (2012), Flower et al. (1997)
<i>Cocconeis placentula</i> var. <i>lineata</i>	epiphytic on higher plants, β -mesosaprobous, alkaliphilous, indicates marshy conditions, meso- to eutrophic	Jorgensen (1948), Metcalfe et al. (1991), Bradbury (1989), Barbiero (2000)
<i>Diadesmis confervacea</i>	freshwater, circumneutral, α -mesosaprobous, epilithic in well, epiphytic in river, largely tropical distribution-prefers high water temperature	Torgnan & Santos (2008), Jena et al. (2006), Kelly et al. (2005)

Table 3. Habitat environments of major diatom species in Hanon

During the Oldest Dryas(zone 1), there are two predominant species, *Staurosira construens* var. *venter* and *Staurosirella pinnata* as mentioned in Chapter 4. Both favor meso- to eutrophic and alkaliphilous conditions. They are also β -mesosaprobous and epiphytic (Ribeiro and Senna, 2010; Kelly et al., 2005), and it means that their habitat would be shallow water environment such as littoral region or low precipitation. Therefore, their favorable environment would be built by low precipitation. Based on the reasoning from the dominant diatom species, zone 1 would be experiencing a weak monsoon, low temperature, and low precipitation according to the general limnological process (Chen et al., 2014). The schematic diagram of zone 1 is in Figure 17 in the next page.

Zone 1: 15440 cal yr BP – 14670 cal yr BP (Oldest Dryas)

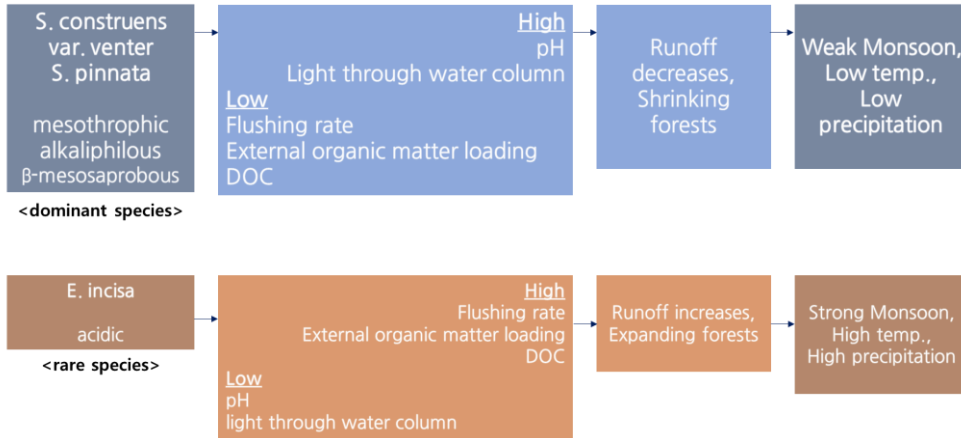


Figure 17. Schematization of diatom assemblage changes – zone 1

Zone 2-a: 14670 cal yr BP – 14180 cal yr BP (Beginning of Bølling-Allerød)

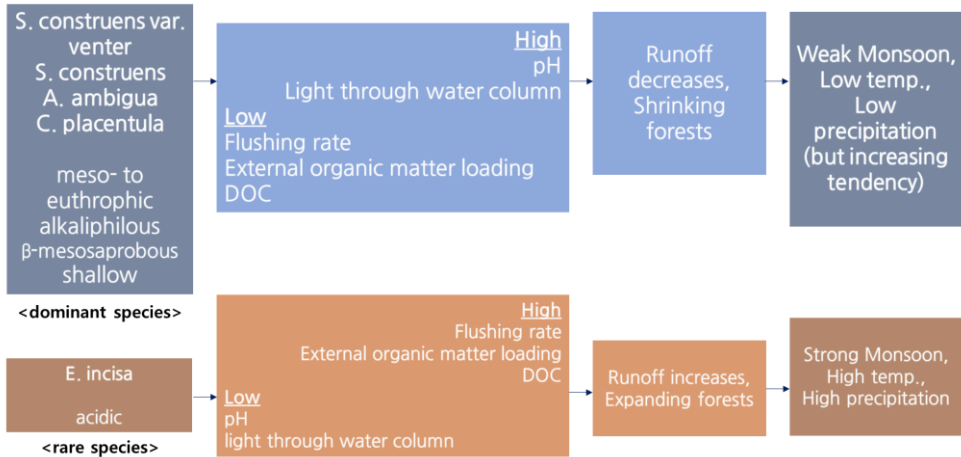


Figure 18. Schematization of diatom assemblage changes – zone 2-a

S. construens var. *venter*, *S. construens*, *Aulacoseira ambigua* and *Cocconeis placentula* are prevailing species at the beginning of Bølling-Allerød(BA) in Figure 18. The two species (*S. construens* and *C. placentula*) inhabit meso- to eutrophic, alkaliphilous environment. Also, they prefer β-mesosaprobous and shallow water depth (Joh et al., 2010; Joh, 2012; Kelly

et al., 2005; Spaulding et al., 2010). Based on these conditions, zone 2-a also had low precipitation, which could be connected to a weak monsoon. Because the BA is a period of increasing temperature and summer monsoon, it does not fit the general known-condition of BA. However, zone 2-a has fewer predominant species indicating low precipitation and more species indicating high precipitation than zone 1 by comparison. It means that the condition of weak monsoon and decline in temperature and precipitation is much weaker than zone 1. That is, their indicative environmental condition tends to be weaker than previous epoch.

C. placentula, *Eunotia incisa*, *S. construens* var. *venter*, and *A. ambigua* are prevalent species in the midst of BA period described in zone 2-b. *C. placentula* is generalist inhabiting in a wide and various environment except oligotrophic condition (Go, 2013), so the species has been ruled out for some parts of interpretation when it is inconsistent with other species. However, the abundance of *C. placentula* in this zone is overwhelmingly high – reaching maximum abundancy of itself, so its habitat condition is surely necessary to be considered, which is that *C. placentula* blooms in summer (Joh, 2012). There are another strong dominant species, *E. incisa*. Its habitat condition is generally known as oligotrophic and shallow water level and reflects the aquatic environment's acidification (Fukumoto et al., 2012). However, *E. incisa* is strongly likely to live in acidic environment; oligotrophic condition is not always right for it, so *E. incisa* indicates acidification of the lake in here. When the limnological condition is low pH generally, its catchment process is usually caused by increased runoff. Therefore, the climate of this period would be strong monsoon with increase in precipitation and temperature followed by the inference in Figure 19.

Zone 2-b: 14180 cal yr BP – 12810 cal yr BP (Bølling-Allerød)

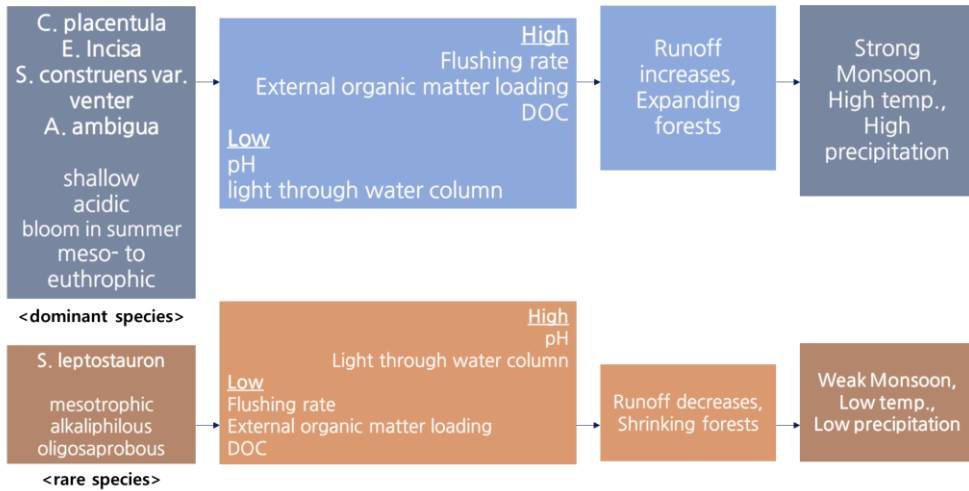


Figure 19. Schematization of diatom assemblage changes – zone 2-b

Zone 3: 12810 cal yr BP – 12150 cal yr BP (Younger Dryas)

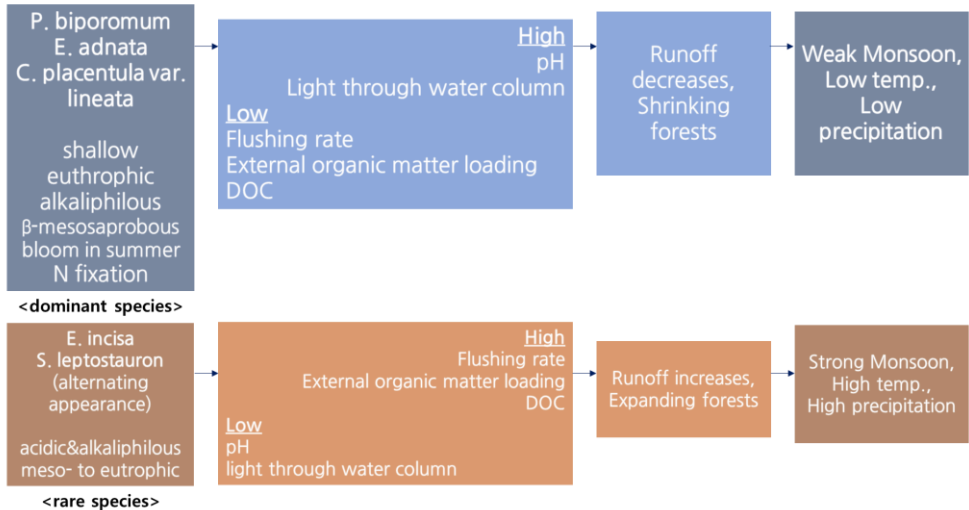


Figure 20. Schematization of diatom assemblage changes – zone 3

According to the prevalence of *Planorbulina biporomum*, *Epithemia adnata* and *C. placentula* var. *lineata*, zone 3 would be Younger Dryas (Figure 20). These species describe that the environment was weak

monsoon with low temperature and precipitation because they prefer shallow water depth, eutrophic and β -mesosaprobous (Spaulding et al., 2010; Barbiero, 2000; Metcalfe et al., 1991). *E. adnata*, capable of N-fixation via cyanobacteria (Kelly et al., 2005), shows uniquely high relative abundancy in this zone. It might be connected to the low maintenance of diatom concentration (Figure 16) because the species is more competitive than any other diatom species due to the ability of N-fixation when it has low runoff of nutrients into a lake, especially nitrogen. Moreover, the fluctuation of Axis 1 seems related to *E. adnata*, too. The Younger Dryas would seem to indicate oligotrophic condition. However, this was not actually the case, according to the graph of Axis 1 (Figure 10 or 25). It is because *E. adnata* would not let the value of Axis 1 going down abruptly. *C. placentula* var. *lineata* also shows high relative abundance in zone 3, and it is connected to the shallow water depth because the species is epiphytic (Barbiero, 2000; Metcalfe et al., 1991; Joh, 2012). There are two rare species in zone 3, which are *E. incisa* and *Staurosirella leptostauron*. Their approving environmental conditions are contradictory; *E. incisa* favors in acidic environment, while *S. leptostauron* favors in alkaliphilous. However, it does not matter because each time of appearance crosses. This may be able to be helpful in interpreting temporary climate change in much smaller time scale.

Zone 4 in Figure 21 indicates Preboreal of early Holocene epoch. During this period, *Diadesmis confervacea*, *A. ambigua*, *P. biporomum* and *E. adnata* clearly indicate eutrophication (Torgan and Santos, 2008; Jena et al., 2006; Kelly et al., 2005; Spaulding et al., 2010; Joh, 2010; Round et al., 1990). However, other conditions such as salinity, temperature and water depth do not match well each other. Other present

species cannot also be merged into specific ecology. The overall relative abundances of diatom assemblages are low. Moreover, it is ambiguous to decide which species is dominant or rare. As mentioned before, the indicated environments by predominant species are inconsistent with each other. It seems that the zone of Preboreal is less likely to be seen by diatom analysis. During this period, the diatom assemblages do not have a visible change along the climate change.

Zone 4: 12150 cal yr BP – 10440 cal yr BP (Pre-Boreal: Beginning of Holocene)

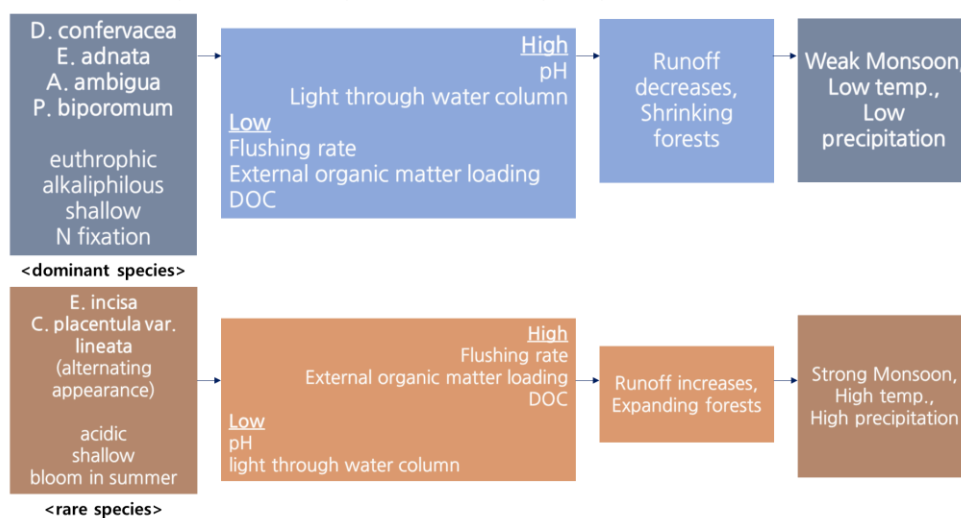


Figure 21. Schematization of diatom assemblage changes – zone 4

Zone 5: 10440 cal yr BP – 7980 cal yr BP (Boreal)

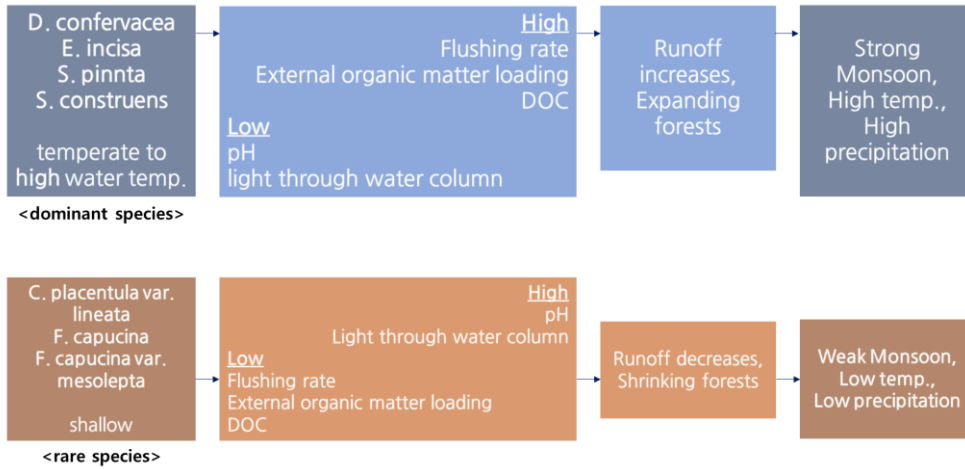


Figure 22. Schematization of diatom assemblage changes – zone 5

The prevalent species in the last epoch in zone 5(Boreal) in Figure 22 are *D. confervacea*, *E. incisa*, *S. pinnata* and *S. construens*. Among of them, *D. confervacea* is the most dominant species undoubtedly. It only cares high temperature condition for the most part; therefore, it is a largely tropical distribution (Kelly et al., 2005; Coste and Ector, 2000; Torgan and Santos, 2008). *D. confervacea* usually indicates high water temperature between 21-30°C (Jena et al., 2006). Coste and Ector (2000) notes that this species is common in power plant discharges in Europe and would be spread much further if global warming persists. Like this, *D. confervacea* depends on temperature. Actually, the dominant species in this zone also does not show specific ecological conditions clearly as similar with zone 4; however, the climate condition during Boreal seems high temperature and strong summer monsoon. It is because the dominantly relatively abundant *D. confervacea* indicates high temperature definitely, and the fact of decline in several species favoring lower water depth such as *C. placentula*,

Fragilaria capucina and *F. capucina* var. *mesolepta* tells us that the lake was deep during this period (Kelly et al., 2005; Stoermer et al., 1971). On account of high temperature indicated by *D. confervacea*, deeper water depth makes the assumption of high precipitation possible around Hanon at that time based on general limnological processes (Jena et al., 2006; Kuwae et al., 2002; Chen et al., 2014).

5.1.2. Summary of the Paleoenvironment of Hanon Maar based on the Schematization

	dominant species	pH	water temp.	nutrient in water	water depth	sensitivity to organic pollution
zone 5 (10,441-7,978 cal. yr BP)	<i>D. confervacea</i> <i>E. incisa</i> <i>S. pinnata</i> <i>S. construens</i>	circumneutral (alkaline → slightly acidic)	High	meso- to eutrophic	shallow	α- mesosaprobous to β- mesosaprobous
zone 4 (11,968-10,441 cal. yr BP)	<i>D. confervacea</i> <i>E. adnata</i> <i>A. ambigua</i> <i>P. biporomum</i>	about circumneutral (between alkaline and slightly acidic)	water temp. ↑	eutrophic	shallow → deep → shallow	α- mesosaprobous → β- mesosaprobous → α- mesosaprobous (<i>D. confervacea</i> → <i>E. adnata</i> → <i>D. confervacea</i>)
zone 3 (12,811-11,968 cal. yr BP)	<i>P. biporomum</i> <i>E. adnata</i> <i>C. placentula</i> var. <i>lineata</i>	circumneutral	cold	eutrophic	shallow	β- mesosaprobous
zone 2-b (14,177-12,811 cal. yr BP)	<i>S. construens</i> var. <i>venter</i> <i>C. placentula</i> <i>E. incisa</i> <i>A. ambigua</i>	acidified temporarily → alkaline	water temp. ↑↑	meso- to eutrophic	shallow	weaker β- mesosaprobous than zone 2-a
zone 2-a (14,671-14,177 cal. yr BP)	<i>S. construens</i> var. <i>venter</i> <i>S. construens</i> <i>A. ambigua</i> <i>C. placentula</i>	alkaline	water temp. ↑	mesotrophic	middle (shallow to deep)	weaker β- mesosaprobous than zone 1
zone 1 (15,443-14,671 cal. yr BP)	<i>S. construens</i> var. <i>venter</i> <i>S. pinnata</i>	alkaline	cold	mesotrophic	middle (shallow to deep)	β- mesosaprobous to oligosaprobous

Table 4. Table of relative phase-dependent reconstruction of the aquatic environmental changes in Hanon maar paleolake

Based on the reconstruction from the schematization from Figure 17 to Figure 22, the reconstructed information of Hanon paleoenvironment is organized in the table above (Table 4). It explains how pH, water temperature, nutrient status, water depth and sensitivity to organic pollution had relatively changed for 7,500 years in the lake. It seems that oligotrophic state of the lake could have been happened, but it is impossible to say it for sure because there is no guaranteed diatom species indicating oligotrophic condition. For this reason, oligotrophic condition is ruled out in this process.

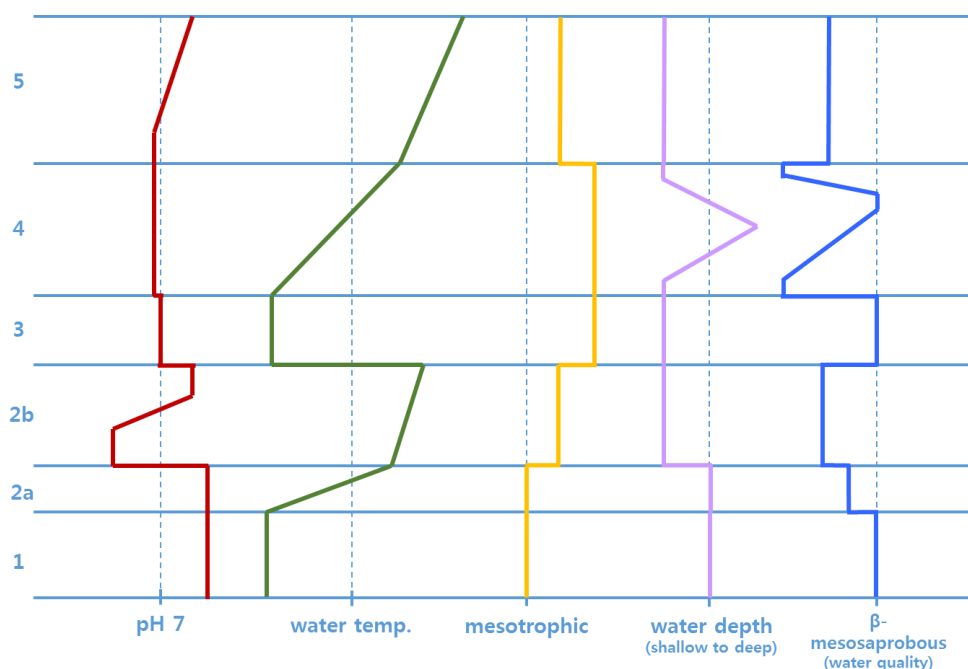


Figure 23. Schematization of relative phase-dependent reconstruction of aquatic environmental changes in Hanon paleo-maar lake based on diatom analysis

Based on the organized information of Hanon in the past (Table 4), the new diagram is drawn as Figure 23. It is a summary to help to grasp

relative changes of environment within Hanon. The table in Table 4 is made for summary of ecological changes within the Lake Hanon over 7,500 years indicating how the lacustrine environment of Hanon maar lake had been changed. As you can see, the pH tended to be high (alkali) when the climate was warm. The water temperature was low whenever a glacial and stadial came. The nutrient status in Hanon was inclined to maintain mesotrophic to eutrophic condition; however, it rose from Younger Dryas and Pre-Boreal periods for some reason. Water depth of Hanon is complicated because it was influenced by two factors such as rainfall and vegetation. For sensitivity to organic pollution, it had maintained fairly clear state in general; however, it became slightly low in oxygen saturation and high in biochemical oxygen demand(BOD) during Pre-Boreal and Boreal. It means the water quality was relatively low in comparison to previous periods.

5.2. Verification of the Reconstructed Paleoenvironment of Hanon Maar Based on Axis 1, 2, 3, and the Values of P:B Ratio

Finally, altogether Axis 1, 2, 3, and the values and P:B ratio will be investigated to verify if the reconstructed paleoenvironment based on each interpretation of the values in Chapter 5.1 was right. Above all, the values of P:B ratio has been tried to compared to Axis 2 to re-examine the reconstructed relative changes of water depth was correct (Figure 24). It is possible that each values of P:B ratio represents water depth, and Axis 2 was interpreted to represent water depth in Hanon paleolake, and thus if

the values correspond with each other, the water depth reconstructed from P:B ratio and Axis 2 would be correct. After then, the water depth is going to be compared to the one reconstructed from diatom diagram for double checking. The values of P:B ratio is enlarged by ten times for easy comparison in Figure 24.

As explained previously, Axis 2 may represent the water depth – the lake water is getting deeper as the Axis 2 component is getting smaller. Also, deep water depth is a favorable environment to planktonic diatom species. Based on the supposition, it seems that the graph in Figure 24 makes sense; the two curves are inversely proportional to each other. During Oldest Dryas, the Axis 2 shows that water depth was shallow,, and the proportion of planktonic species was low as well. During Bølling-Allerød, the water depth became deeper than before, and planktonic species flourished, especially around at 13,780 cal. yr BP. Even though the water depth was not shallower than expected in the beginning of Younger Dryas, it had been becoming increasingly shallower after then. This might indicate wet climate during the early Younger Dryas in Hanon, which was mentioned in Park (2015). Also, planktonic species had been decreased at the same time according to the graph. It is not certain how Hanon paleolake maintained its shallow water depth during the early Holocene; however, it seems that the lacustrine environment of Hanon was dry during the early Holocene for some reason. Furthermore, this inference is in accord with the hypothesis of Park et al. (2014b), which insists that the environment of Hanon during the early Holocene were under the changes of slow weakening in summer monsoon and abrupt decrease in temperature.

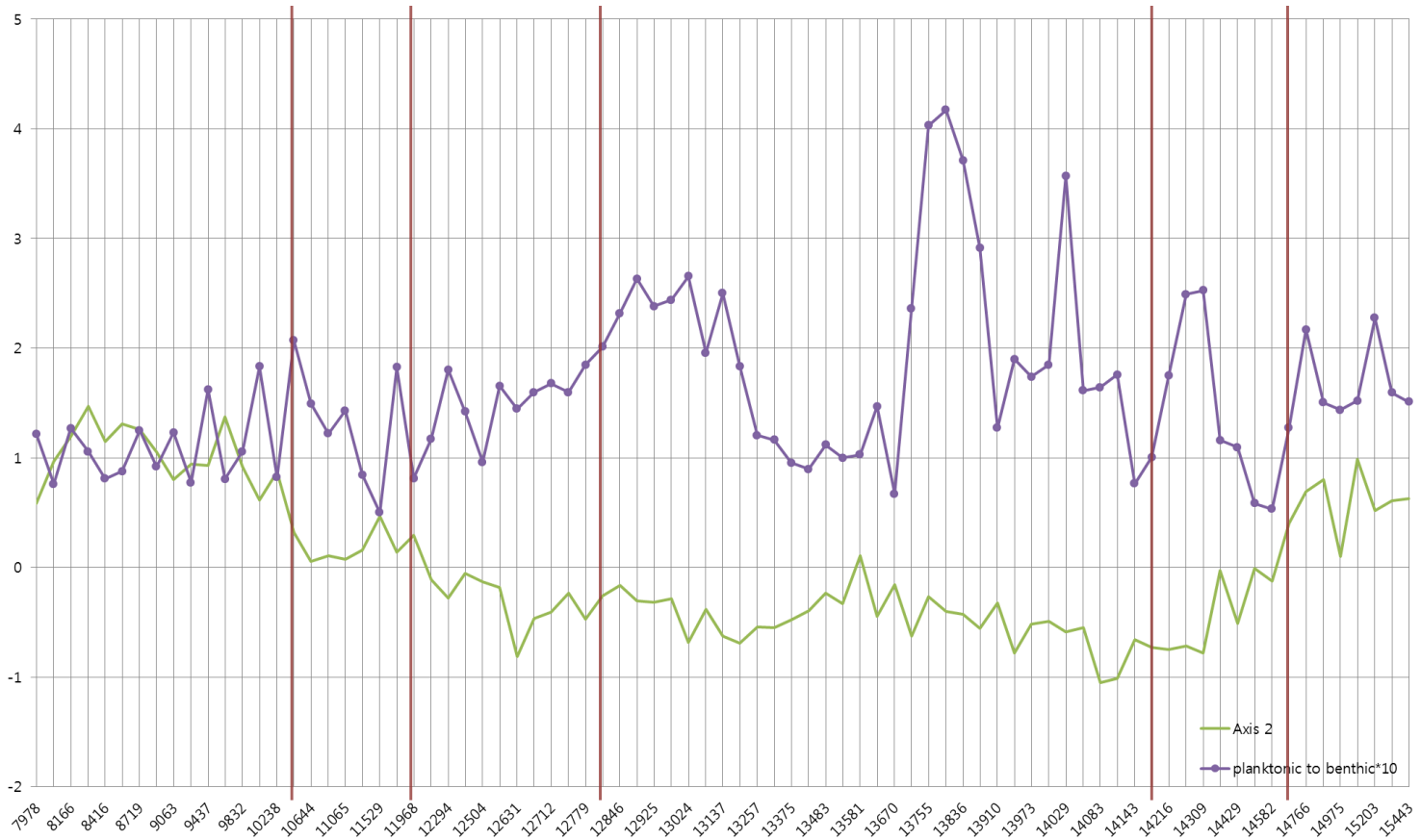


Figure 24. P:B ratio and the component scores of Axis 2 – P:B ratio values are enlarged by ten times

Next, three pairs of graphs which display the components of Axis 1 and 2, 1 and 3, and 2 and 3 respectively are going to be investigated to verify the inference of the reconstructed Hanon paleoenvironment previously (Figure 25 - 27).

First, Axis 1 and 2 are plotted in a graph (Figure 25). Axis 1 represents nutrient status in the lake, while Axis 2 represents water depth as mentioned before. There would be various factors that affect water depth such as sedimentation rate and insolation. However, water depth is usually strongly related to precipitation. Therefore, water depth is interpreted considering as precipitation in here. When it rains, terrigenous nutrients from vegetation and soil are washed away into a lake. These include nutrient limiting factors for diatoms such as P, N, and SiO_2 . As precipitation increases, terrigenous nutrient input into the lake increases, too. By this process, alga such as green algae(i.e. *Botryococcus*) and diatoms in the lake can bloom by the abundant essential nutrients. After then, the lake is acidified because a lot of CO_2 is released due to the respiration of alga. In the process of algal respiration, they consume O_2 and release CO_2 instead. After then, a lot of alga decline due to the lack of O_2 and they will flourish when input of nutrient increases again. This is a circulation of a lake ecosystem. Therefore, nutrient status is usually good when it rains^{1 1}.

Based on this knowledge, the relationship between trophic status(Axis 1) and water depth(Axis 2) is going to be deduced. In Figure 25, the water depth in Hanon seems low, and its nutrient status seems oligotrophic during Oldest Dryas. This environment condition may be correct because Oldest Dryas is cold and dry period. The fluctuation of

^{1 1} However, too much precipitation may not be good because eluviation would happen, so that nutrients would be washed away into the underground water.

water depth and nutrient status is balanced. This graph also shows the wet condition during the early Younger Dryas and dry condition during the early Holocene as well as Figure 24.

Second, Figure 26 shows the relationship between trophic status(Axis 1) and pH(Axis 3). As explained in previous paragraph, a lake is acidified when alga increase due to the respiration of alga, and it leads to eutrophication of the lake. Therefore, two curves in Figure 26 have to be inversely proportional, and it usually matches until BA. From Younger Dryas to the early Holocene, the pH of the lake changes from alkaline to weak acidic while its nutrient status fluctuates between eutrophic and mesotrophic. This may have been associated with the transition of vegetation and dry climate during the early Holocene.

Last, Figure 27 illustrates the relationship between water depth(Axis 2) and pH(Axis 3). As explained in previous paragraph, the two curves must be an inverse proportion, and so are they mostly. However, the curves were proportional during Boreal, and it might be because the lake is likely to be under eutrophication when the water depth is getting lower and lower. This is the matter of water volume and the algal density – relative eutrophication. Each curve was actually described in Figure 25 and 26, so further explanation is going to be skipped.

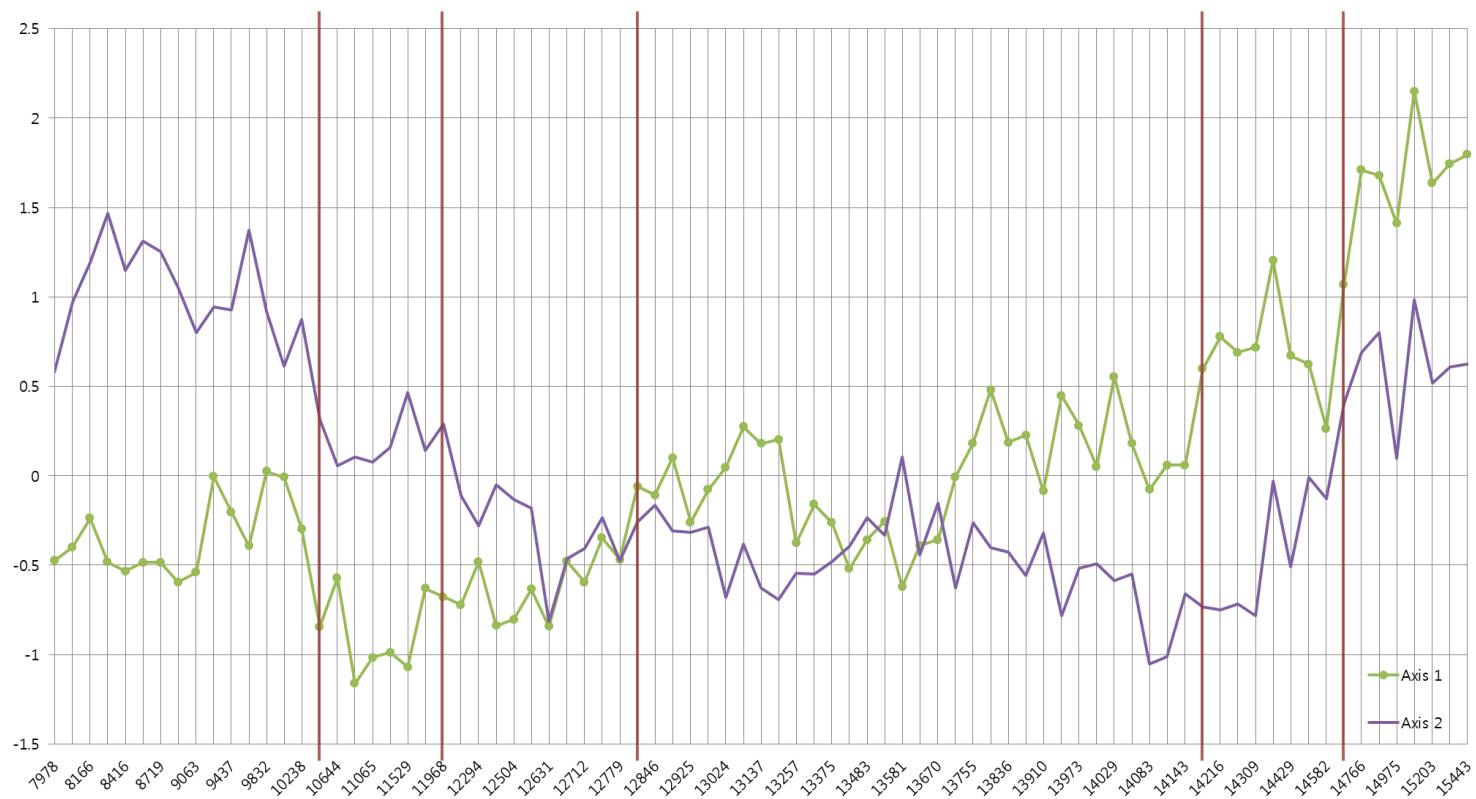


Figure 25. The component scores of Axis 1 and 2

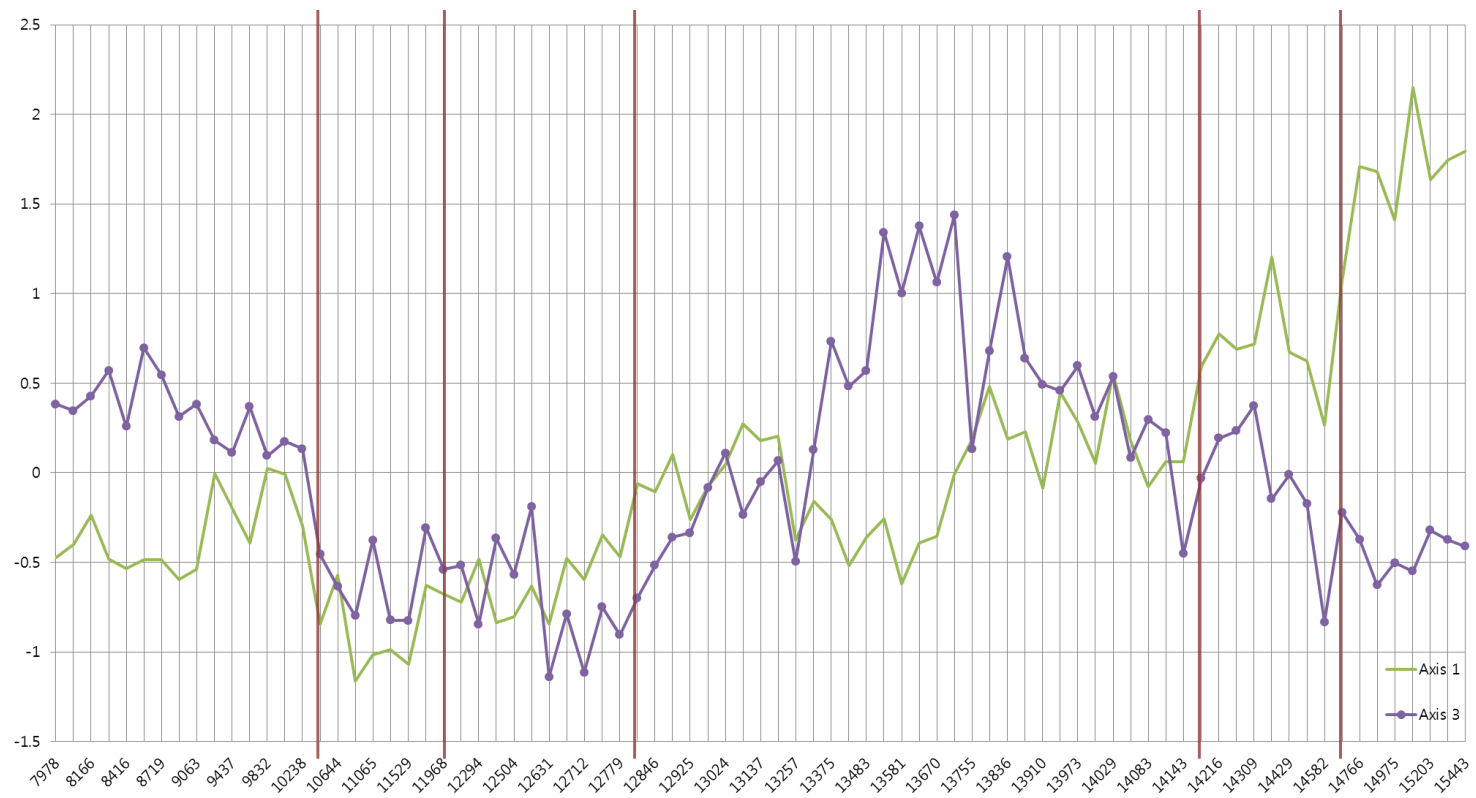


Figure 26. The component scores of Axis 1 and 3

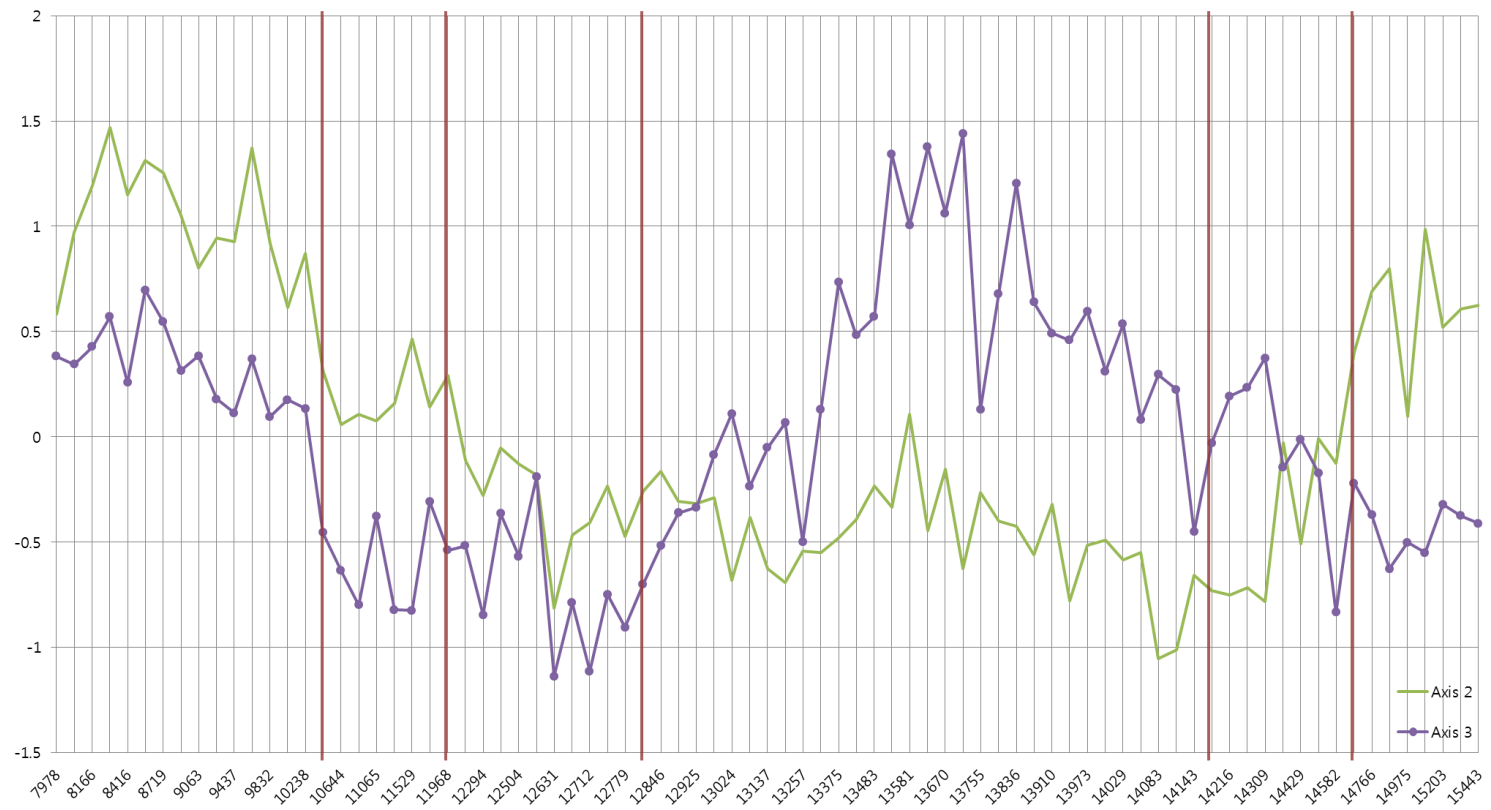


Figure 27. The component scores of Axis 2 and 3

Overall, trophic status(Axis 1), water depth(Axis 2), and pH(Axis 3) have been reconstructed again by principal components. These three environments were reconstructed in Chapter 5.1.2 (Table 4 and Figure 23), and it was reconstructed based on the information of distribution, ecology and habitat of dominant/rare diatom species in each zone from the diatom diagram. The whole tendency corresponds with each other, but some minor points do not. Therefore, it is inevitable to construct revised version of reconstruction of Hanon paleoenvironment, particularly pH, trophic status and water depth (Figure 28). The difference between previous version and the new one may be caused by the lack of information about habitat, distribution and ecology of each diatom species.

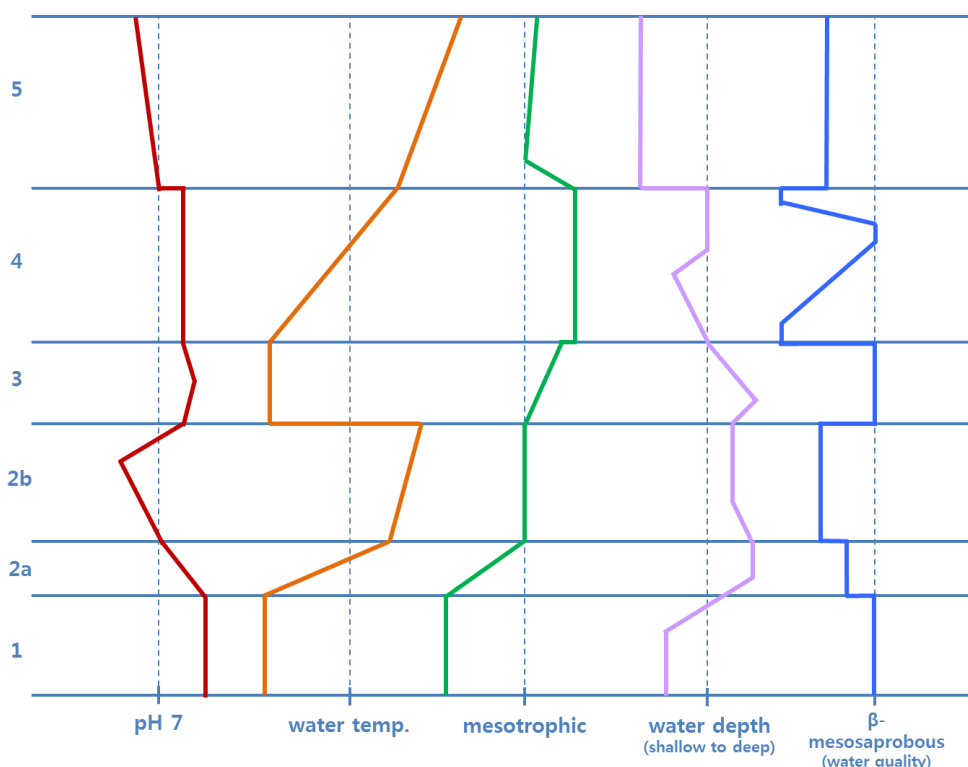


Figure 28. The revised version of the paleoenvironment in Hanon – particularly, pH, trophic status and water depth

5.3. Comparison and Analysis between Diatom Analysis and Other Multi-Proxy Data from Another Research on the Paleoenvironment of Hanon Maar

The reconstruction of the paleoenvironment in Hanon during the last deglaciation using diatom analysis has been elucidated in previous chapters. Also, there have been several researches on reconstructing paleoenvironment around Hanon (Chung, 2007; Park et al., 2014a; Park et al., 2014b) as mentioned in Chapter 2.1. Especially, this study shares the exact same core(HN-1) with Park et al. (2014a; 2014b). This study has also been performed at high resolution and 2cm interval as well as Park et al. (2014b), so it is possible to compare reconstructed paleoenvironment in centennial-scale between these studies, and it is the first time to compare pollen with diatom data in centennial-scale on the Korean Peninsula. After comparing appropriate proxy data as much as possible, the reconstructed paleoenvironment in Hanon will be able to approach much closer to what really happened in the past – the truth.

Above all, the time table of climate shift in Hanon by diatom analysis is analogous to the one of Park et al. (2014b) as expected – not only in millennial-scale but also in centennial-scale (Figure 29). Most periods of climate events are alike except Bølling-Allerød(BA). BA is delineated as a single climate event according to the pollen diagram in Park et al. (2014b)^{1 2}, whereas it is divided into two zones according to the diatom

^{1 2} The intensive studies by Park et al. (2014b) revealed short-term climate variability, actually: Bølling and Allerød oscillations, IBCP, Older Dryas and IACP. They were observed by another multi-proxy data such as X_{ARM} and *Botryococcus*(%) by comparison with Greenland ice core records(NGRIP) and

diagram in this study (Figure 16).

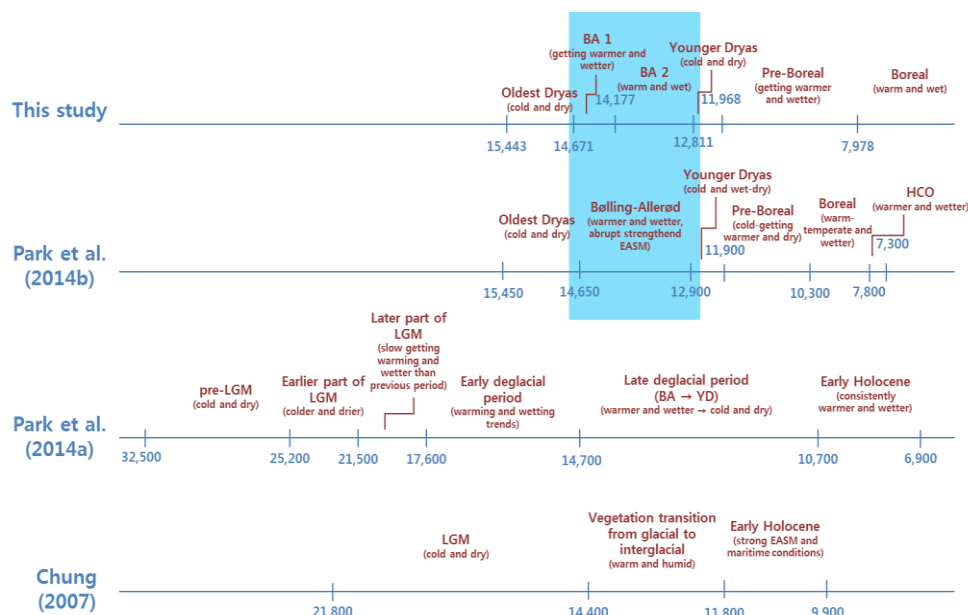


Figure 29. Climate shifts in Hanon maar by adding the one reconstructed by diatom proxy data of this study

Through diatom analysis, it is confirmed that zone 2 is divided into two zones such as 2-a and 2-b according to the zonation as explained before. There are also huge changes in diatom assemblages such as *S. construens*, *S. construens* var. *venter*, *S. pinnta* and *C. placentula* between the two zones; therefore, it could be thought that zone 2-a is Bølling oscillation(14,670-14,180 cal. yr BP) while zone 2-b seems Allerød oscillation(14,180-12,810 cal. yr BP), and the period between Bølling and Allerød oscillation is Older Dryas. However, it is difficult to say there is Bølling oscillation, Older Dryas and Allerød oscillation separately in Hanon paleolake according to the diatom diagram. Even though diatoms are good indicators of

numerous lacustrine records in the North Atlantic.

environmental change, their assemblage changes directly reflect the environmental change within the lake; it is very hard to insist that the BA consists of the three climate shifts respectively. On the other hand, these short-term climate variations are also observed in Park et al. (2014b). The intensive studies by Park et al. (2014b) revealed short-term climate variability, actually: Bølling and Allerød oscillations, IBCP, Older Dryas and IACP. They were observed by another multi-proxy data such as X_{ARM} and *Botryococcus*(%) by comparison with Greenland ice core records(NGRIP) and numerous lacustrine records in the North Atlantic. In conclusion, the time table of this study and Park et al. (2014b) correspond with each other except BA. The result of diatom analysis cannot assure that BA is divided into short-term climate variabilities, while Park et al. (2014b) confirmed that there were short-term climate variations such as Bølling and Allerød oscillations, IBCP, Older Dryas and IACP.

Second, another diagram has been drawn by exhibiting the proxy data together from this study(diatoms) and Park et al. (2014b)(pollen) for comparative analysis (Figure 30). Park et al. (2014b) covers wider range^{1 3} of temporal scopes of the same core(HN-1) than this study, so the diagram in Figure 30 is drawn to embrace both time scales and make it easy to look. The diagrams of Axis 1, 2 and 3 are ten times enlarged to clarify their changes so as to compare other variations precisely.

^{1 3} Park et al. (2014b) covered HN-1 for pollen analysis between the depths of 250 and 50cm (Park et al., 2014b).

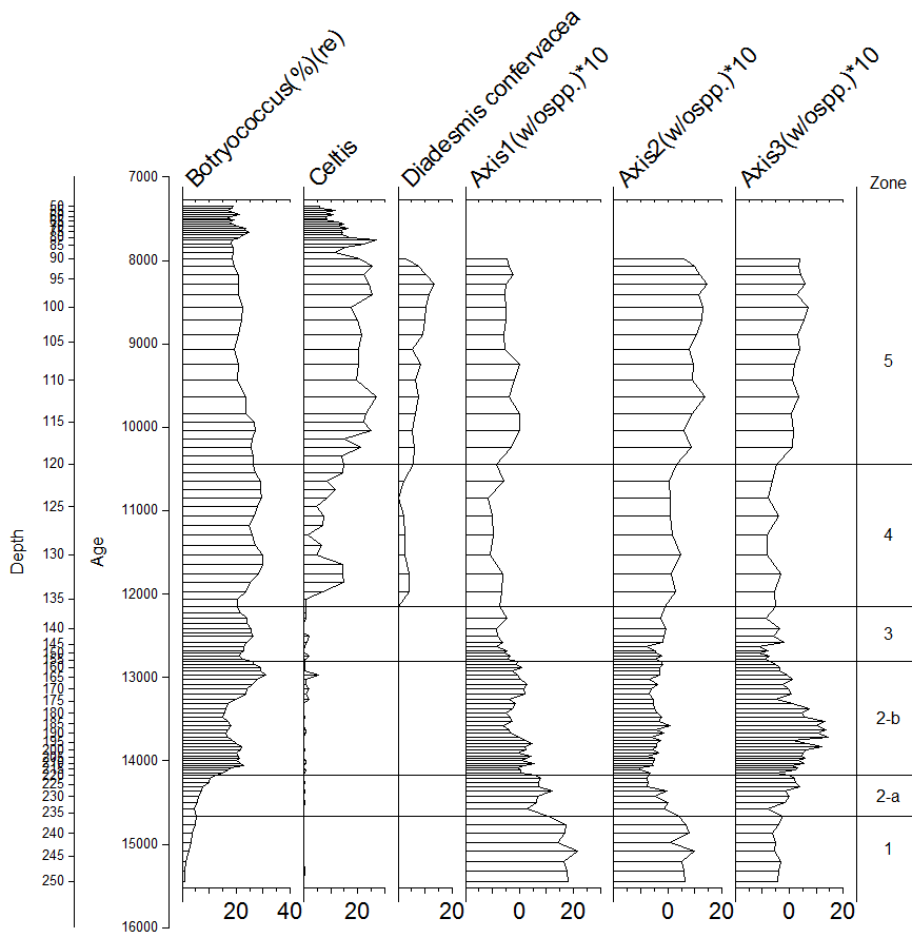


Figure 30. Diagram for comparisons between the changes of *Botryococcus* & *Celtis* (Park et al., 2014b) and *D. confervacea* & PC 1, 2, 3 (this study)

D. confervacea is famous for an indicator of high water temperature (Jena et al., 2006; Torgan and Santos, 2008). Therefore, it would be good to start with *D. confervacea* comparing to an indicator of temperature such as *Botryococcus*^{1 4} and *Celtis*^{1 5}. They increase when

^{1 4} *Botryococcus* is planktonic green algae, which is an indicator of eutrophication and climate warming; increase in *Botryococcus* means increase in temperature and decrease in *Botryococcus* may have been related to the lake eutrophication (Park et al., 2014b). It also suggests agricultural activity (Park, 2005).

temperature of air and water increase, so their fluctuations should be analogous. The overall trend of *D. confervacea* and *Celtis* looks very similar; *Celtis* barely existed until right before the start of Holocene and increased abruptly after Holocene began while *D. confervacea* did not appear until ca. 12,150 cal. yr BP and soared to Boreal, with relatively but considerably great increase in relative abundance. It means that pollen and diatom proxy data correspond to each other while demonstrating a drastic temperature increase both in the air and water at ca. 12,150 cal. yr BP, which can be deduced as the beginning of Holocene. Also, there is an abrupt decline in *D. confervacea* around at 7,980 cal. yr BP, which is the end of the core analyzed in this study. Although it was not analyzed beyond 7,980 cal. yr BP, there is a certain rapid decrease in *D. confervacea*. This decline would be related to a small climate shift such as 8.2ka event or other reasons such as vegetation changes or trophic status changes. Therefore, further research is needed before a conclusion in this part. This rapid decline is also shown in *Botryococcus* and *Celtis*; Park et al. (2014b) explained that the decrease in *Botryococcus* would be caused by eutrophication of the lake, while *Celtis* might have been related to the expansion of the shade-tolerant evergreen trees. 8.2ka event happened in this period, so it is explicable for the declines in *D. confervacea*, *Celtis* and *Botryococcus*; however, it cannot be concluded this time due to the lack of analysis. Furthermore, *D. confervacea* can be considered as an indicator of Holocene. The environment of early Holocene which increases in temperature and

^{1 5} *Celtis/Aphananthe* is an evidence for the high susceptibility to temperature change. Its population is “so fragile that even a small temperature decrease may have drastically culled the tree population.” Also, its pollen certainly indicates the timing of transitions into different climate stages (Park et al., 2014b).

precipitation is delineated in the studies of Park et al. (2014a; 2014b) as well. They explained high frequencies of climate warming indicators such as *Sagittaria*, *Nymphoides* and *Botryococcus* were associated with a large influx of terrigenous organic matter and an increase in water temperature of the lake (Park et al., 2014a). This is in accord with the variation of *D. confervacea* assemblage. As explained in the previous paragraph, it had never appeared before Pre-Boreal, and it had begun to appear since Holocene. Thus, it is possible to say that *D. confervacea* is an indicator of Holocene.

Third, the graph of P:B ratio is going to be compared to several geochemical multi proxy from Park et al. (2014b) while focusing on the maximum point of P:B ratio. The maximum point of P:B ratio is around at 13,780 cal. yr BP. Wang et al. (2012) stated that high P:B ratio characterizes warm period(long ice-free season). That is, the period around at 13,780 cal. yr BP must be warm. This is in accord with other geochemical multi proxy data around at that period. Highly persisted CIA, $\delta^{13}\text{C}$ and TOC indicate warm-wet condition which improves soil and aquatic productivity, which may be connected to strengthened monsoon activity (Park et al., 2014b). Warm-wet condition boosts chemical weathering, and it means more input of nutrient limiting factors into the lake ecosystem such as P(phosphorus), N(nitrogen) and SiO_2 (silica) when chemical weathering increases. The warm-wet condition is also associated with strengthened monsoon. Park et al. (2014b) built the hypothetical climate change curve to reconstruct temperature and summer monsoon in Hanon; it suggested abrupt temperature reduction and continuation of strengthened summer monsoon around at 13,780 cal. yr BP. Continuation of intensified summer monsoon brought higher precipitation while the lake water could not evaporate well

due to the sudden decreased temperature. Those effects may have resulted in deeper water depth in the lake than the previous state, and thus deepened water depth in addition to increased inflow of nutrient into the lake may have been more favorable to planktonic diatom species than ever such as *Discostella* spp. and *Aulacoseira* spp.

As a result, comparing reconstructions of paleoenvironment in Hanon, especially Park et al. (2014b) (pollen and geochemical analysis), to this study (diatom analysis) testifies that each studies are correlated and whether the interpretations are correct. The results from diatom, pollen and geochemical analyses give different aspects for reconstructing the paleoenvironment and paleoclimate in Hanon maar. The studies by Park et al. (2014a; 2014b) mainly focused on change of vegetation and paleoenvironment near Hanon maar lake, while this study predominantly focused on the change of paleoecology and paleoenvironment within Hanon. The environmental change near and within Hanon is closely related to each other; therefore, each proxy data is necessary to reconstruct the environment in Hanon. Performing one of the proxy data would show just half of the environmental changes in the place. It should be performed all of them to demonstrate accurate environmental change reconstruction.

Chapter 6. Conclusions

Hanon maar on Jeju Island is located in a geographically significant place that can fill in the missing link of the paleoenvironment between China and Japan, whereupon the paleoenvironment study of Hanon maar will play a key role in the reconstruction of the paleoenvironment in East Asia. However, only the morphology and terrestrial environment of Hanon paleolake has been studied, so it was necessary to investigate Hanon maar paleoenvironment using another type of proxy data in different aspects. Hanon maar had been a paleolake until 500 years ago, so diatom analysis is a proper methodology for the reconstruction of Hanon maar paleoenvironment; it provides information about lacustrine environmental changes. This study covers the last deglaciation (15,500 – 8,000 cal. yr BP) in the sediment core(HN-1) extracted from Hanon maar. The last deglaciation is important because there are many abrupt climate shifts during the period, which is an interesting research topic these days related to future climate change triggered by global warming. In this regard, it is necessary to study the last deglaciation using various proxy data. Therefore, this study aimed to reconstruct Hanon maar paleoenvironment during the last deglaciation using diatom analysis and provide another proxy data for reconstruction of paleoenvironment on the Korean Peninsula.

Diatoms are a good indicator of environmental change; diatom assemblages respond sensitively to climate/environmental change due to their short life cycle. In this study, it was possible to reconstruct water depth, trophic status, water temperature, pH and water quality according to

the change of diatom assemblage. It was the first time to apply diatom analysis into the paleoclimate studies in Hanon. Furthermore, it was the first time to perform diatom analysis in the reconstruction of freshwater environment on the Korean Peninsula as well in spite of its popularity in other regions; therefore, this study itself is meaningful.

After identifying diatoms by microscope analysis, diatom diagrams were constructed. The zones in the diagram were determined based on constrained incremental sum of squares cluster analysis, and climate events during the last deglaciation have been reconstructed: Oldest Dryas for 15,440 – 14,670 cal. yr BP, the beginning of Bølling-Allerød for 14,670 – 14,180 cal. yr BP, ongoing Bølling-Allerød for 14,180 cal. yr BP – 12,810 cal. yr BP, Younger Dryas for 12,810 – 12,150 cal. yr BP, Preboreal for 12,150 – 10,440 cal. yr BP, and Boreal for 10,440 – 7,980 cal. yr BP. The time table of the climate shifts in Hanon paleolake in this study was generally corresponded with other paleoclimate studies in Hanon paleolake (Chung, 2007; Park et al., 2014a; Park et al., 2014b).

The results of the diatom diagram were schematized to reconstruct the lacustrine environment based on changes of diatom assemblages and limnological processes. The reconstructed aquatic environment has also been drawn in the graph which outlined relative phase-dependent environment change in the Hanon paleolake. After that, the reconstructed environment based on the diatom diagram has been verified by the results of PCA and P:B ratio. The components of Axis 1, 2 and 3 and the value of P:B ratio were created into several graphs, and they were compared to each other. Based on the meaning of each value such as trophic status, water depth and pH, the verification made the previously reconstructed aquatic environment revised. For example, Hanon paleolake had been alkalified

during the Boreal period according to the interpretation only by diatom diagram; however, it had been acidified actually according to the PCA. Also, the degree of water depth could be adjusted based on the P:B ratio and PCA; diatom diagram only indicated the relative change of water depth (Figure 23), while the results of P:B ratio and Axis 2 provided more quantitative changes of water depth than the one of the diatom diagram (Figure 24). Overall, Hanon maar paleoenvironment during the last deglaciation has changed as follows: cold and dry for the Oldest Dryas, increasing in temperatures and moisture for the Bølling-Allerød, cold and wet-dry for the Younger Dryas, an increase in temperatures and temporarily drier for the Preboreal, and warm and dry/wet for the Boreal.

This study using diatom analysis reconstructed the paleoenvironment of Hanon maar during the last deglaciation and provided the new proxy data – diatoms – of the paleoenvironment during the last deglaciation on the Korean Peninsula and over greater East Asia. To collect proxy data is important to reconstruct the paleoclimate because of the limitations of proxy data. There are always suitable ways to reconstruct paleoenvironment for each region. Hanon maar was a lake about until 500 years ago, and thus the reconstruction of the lacustrine environment is important. Therefore, this study applying diatom analysis provides the new significant proxy data. However, studying and applying single proxy data may cause an error for paleoenvironmental reconstruction. Using appropriate proxy data together will make it possible to reconstruct more accurate paleoenvironment.

Bibliography

- Allen, C.S., Pike, J., Pudsey, C.J., Leventer, A., 2005. Submillennial variations in ocean conditions during deglaciation based on diatom assemblages from the southwest Atlantic. *Paleoceanography* 20, PA2012, 1-16.
- Anonymous, 2010. Climate Change in Jeju Island. National Institute of Meteorological Research.
- Bak, Y.-S., Lee, J.-D., Yun, H., Yoon, H.-I., 2001. Paleoenvironmental significance of diatom assemblages from Core GC 98-08, Bransfield Strait, Antarctica. *Journal of the Paleontology Society of Korea* 17(2), 99-111.
- Bak, Y.-S., Lee, J.-D., Yoon, H.-I., Yun, H., Kim, H.-J., 2002. Quaternary Diatom Assemblages from Sediment Core GC 98-06 in the Southern Drake Passage, Antarctica. *Journal of Korean Earth Science Society* 23(5), 442-453.
- Bak, Y.-S., Lee, S.-J., Chun, J.-H., Lee, J.-D., 2010. Paleoclimatic Changes from Quaternary Sediments in the Ulleung Basin, Korea: Evidence from the Diatom Record. *Journal of the Paleontology Society of Korea* 26(2), 183-192.
- Barbiero, R.P., 2000. A multi-lake comparison of epilithic diatom communities on natural and artificial substrates. *Hydrobiologia* 438, 157-170.
- Bennett, K.D., 1996. Determination of the number of zones in a biostratigraphical sequence. *New Phytologist* 132, 155-170.
- Boden, P., 1991. Reproducibility in the random settling method for quantitative diatom analysis. *Micropaleontology* 37(3), 313-319.
- Chen, X., Li, Y., Metcalfe, S., Xiao, X., Yang, X., Zhang, E., 2014. Diatom response to Asian monsoon variability during the Late Glacial to Holocene in a small treeline lake, SW China. *The Holocene* 24(10),

1369-1377.

- Choi, K.H., Yoon, K.S., Kim, J.W., 2006. Reconstruction of the Volcanic Lake in Hanon Volcano Using the Spatial Statistical Techniques. *The Korean Geographical Society* 41(4), 391-403. (in Korean)
- Chung, C.-H., 2007. Vegetation response to climate change on Jeju Island, South Korea, during the last deglaciation based on pollen record. *Geosciences Journal* 11(2), 147-155.
- Conway, J., Kosemen, C.M., Naish, D., 2012. All Yesterdays – Unique and Speculative Views of Dinosaurs and Other Prehistoric Animals. Irregular Books.
- Domestic Climate Data, Korea Meteorological Administration (n.d.). From http://www.kma.go.kr/weather/climate/average_30years.jsp. Accessed on 18 June, 2015.
- Flower, R.J., Juggins, S., Battarbee, R.W., 1997. Matching diatoms assemblages in lake sediment cores and modern surface sediment samples: the implications for lake conservation and restoration with special reference to acidified systems. *Hydrobiologia* 344, 27-40.
- Fluim, J., Tibby, J., Gell, P., 2010. The palaeolimnological record from Lake Culleraine, lower Murray River, (south-east Australia): implications for understanding riverine histories. *Journal of Paleolimnology* 43, 309–322.
- Fukumoto, Y., Kashima, K., Orkhonselenge, A., Ganzorig, U., 2012. Holocene environmental changes in northern Mongolia inferred from diatom and pollen records of peat sediment. *Quaternary International* 254, 83-91.
- Go, A., 2013. Sedimentary environment of Hwajinpo using diatom analysis. Master Degree Dissertation. Kyung-Hee University.
- Go, A, Tanaka, Y., Kashima, K., 2013. Sedimentary environment of Hwajinpo using diatom analysis. *Journal of the Korean Geomorphological Association* 20(2), 15-25.

- Grimm, E.C., 1987. CONISS: A Fortran 77 Program for Stratigraphically Constrained Cluster Analysis by the Method of Incremental Sum of Squares. *Computers & Geosciences* 13(1), 13-35.
- Grimm, E.C., 1992. *Tilia and Tilia-graph: pollen spreadsheet and graphic programs*. 8th International Palynological Congress, Aix-en-Provence (France), September 6-12, 56.
- Hasle, G.R., Syvertsen, E.E., 1997. Marine Diatoms. In: Tomas, C.R. (Ed.), *Identifying Marine Phytoplankton*. Academic Press, Florida, pp.5-385.
- Hillebrand, H., Durselen, C-D., Kirschtel, D., Pollinger, U., Zohary, T., 1999. Biovolume Calculation for Pelagic and Benthic Microalgae. *Journal of Phycology* 35, 403-424.
- Janžekovič, F., Novak, T., 2012. PCA – A Powerful Method for Analyze Ecological Niches. pp. 127-142. In: Sanguansat, P. (Ed.), *Principal Component Analysis – Multidisciplinary Applications*. InTech Books. Available at <http://www.intechopen.com/books/principal-component-analysis-multidisciplinary-applications/pca-a-powerful-method-to-analyze-the-ecological-niche->. Accessed on 6 April 2015.
- Jena, M., Ratha, S.K., Adhikary, S.P., 2006. Diatoms (Bacillariophyceae) from Orissa State and Neighbouring Regions, India. *Algae* 21(4), 377-392.
- Joh, G., 2010. Algal Flora of Korea: Freshwater Diatoms I, Chrysophyta: Bacillariophyceae: Centrales, Vol.3, No. 1. National Institute of Biological Resources, Ministry of Environment.
- Joh, G., Lee, J.H., Lee, K., Yoon, S.-K., 2010. Algal Flora of Korea: Freshwater Diatoms II, Chrysophyta: Bacillariophyceae: Pennales: Araphidineae: Diatomaceae, Vol.3, No. 2. National Institute of Biological Resources, Ministry of Environment.
- Joh, G., 2011. Algal Flora of Korea: Freshwater Diatoms III, Chrysophyta: Bacillariophyceae: Pennales: Raphidineae: Eunotiaceae, Vol.3, No. 3.

- National Institute of Biological Resources, Ministry of Environment.
- Joh, G., 2012. Algal Flora of Korea: Freshwater Diatoms V, Chrysophyta: Bacillariophyceae: Pennales: Raphidineae: Achnanthaceae, Vol.3, No. 7. National Institute of Biological Resources, Ministry of Environment.
- Joh, G., 2012. Algal Flora of Korea: Freshwater Diatoms VII, Chrysophyta: Bacillariophyceae: Pennales: Raphidineae: Naviculaceae: *Biremis*, *Caloneis* I, *Pinnularia* I, Vol.3, No. 9. National Institute of Biological Resources, Ministry of Environment.
- Katsuki, K., Takahashi, K., Okada, M., 2003. Diatom Assemblage and Productivity Changes during the Last 340,000 Years in Subarctic Pacific. *Journal of Oceanography* 59, 695-707.
- Katsuki, K., Takahashi, K., 2005. Diatoms as paleoenvironmental proxies for seasonal productivity, sea-ice and surface circulation in the Bering Sea during the late Quaternary. *Deep-Sea Research II* 52, 2110-2130.
- Katsuki, K., Seto, K., Saito, M., Noguchi, T., Sonoda, T., Kim, J.-Y., 2012. Paleoecological and Paleoenvironmental Changes in Lagoon Notoro-Ko (Japan) during the Last 200 Years Based on Diatom Assemblages and Sediment Chemistry. *Geomorphology* 33(2), 197-217.
- Kelly, M.G., Bennion, H., Cox, E.J., Goldsmith, B., Jamieson, J., Juggins, S., Mann, D.G., Telford, R.J., 2005. Common freshwater diatoms of Britain and Ireland: an interactive key. Environment Agency, Bristol. <http://craticula.ncl.ac.uk/EADiatomKey/html/index.html>. Accessed on 20 April, 2015.
- Kim, J., Hwang, S., 2008. The result and task of diatom analysis for reconstructing paleoenvironment. *地理學論究* 27, 91-117. (in Korean)
- Kingston, J.C., 2003. Araphid and Monoraphid Diatoms. In: Wehr, J.D.,

- Sheath, R.G. (Eds.), *Freshwater Algae of North America: Ecology and Classification*. Academic Press, San Diego, pp. 595-636.
- Ko, H.-S., Jhun, M., Jeong, H.C., 2015. A Comparison Study for Ordination Methods in Ecology. *The Korean Journal of Applied Statistics* 28(1), 49-60.
- Kociolek, J.P., Spaulding, S.A. 2003. Symmetrical Naviculoid Diatoms. In: Wehr, J.D., Sheath, R.G. (Eds.), *Freshwater Algae of North America: Ecology and Classification*. Academic Press, San Diego, pp. 637-653.
- Kociolek, J.P., Spaulding, S.A. 2003. Eunotioid and Asymmetrical Naviculoid Diatoms. In: Wehr, J.D., Sheath, R.G. (Eds.), *Freshwater Algae of North America: Ecology and Classification*. Academic Press, San Diego, pp. 655-668.
- Kociolek, J.P., 2012. Diatoms of the Southern California Bight. http://dbmuseblade.colorado.edu/DiatomTwo/dscb_site/index.php. Accessed on 20 April, 2015.
- Kossler, A., Tarasov, P., Schlolaut, G., Nakagawa, T., Marshall, M., Brauer, A., Staff, R., Ramsey, C.B., Bryant, C., Lamb, H., Demske, D., Gotanda, K., Haraguchi, T., Yokoyama, Y., Yonenobu, H., Tada, R., 2011, Onset and termination of the late-glacial climate reversal in the high-resolution diatom and sedimentary records from the annually laminated SGO6 core from Lake Suigetsu, Japan. *Palaeogeograph, Palaeoclimatology, Palaeoecology* 306, 103-115.
- Krammer, K., Lange-Bertalot, H., 1986. Bacillariophyceae: 1. Teil: Naviculaceae. In: Ettl, H., Gerloff, J., Heynig, H., Mollenhauer, D. (Eds.), *Süßwasser flora von Mitteleuropa*, Band 2/1. Gustav Fischer Verlag, Stuttgart, New York. 876 pp.
- Krammer, K., Lange-Bertalot, H., 1988. Bacillariophyceae: 2. Teil: Bacillariaceae, Epithemiaceae, Surirellaceae. In: Ettl, H., Gerloff, J., Heynig, H., Mollenhauer, D. (Eds.), *Süßwasser flora von Mitteleuropa*, Band 2/2. Gustav Fischer Verlag, Stuttgart, New York.

596 pp.

- Krammer, K., 1982. Valve Morphology in the Genus *Cymbella* C.A. Agardh. In: Helmcke, J.-G., Krammer, K. (Eds.), *Micromorphology of Diatom Valves*, Vol. XI. Gantner. 299 pp.
- Krammer, K., Lange-Bertalot, H., 1985. Naviculaceae. In: Cramer, J. (Ed.), *Bibliotheca Diatomologica*, Band 9. Gebrüder Borntraeger, Berlin, Stuttgart. 230 pp.
- Kuwae, M., Yoshikawa, S., Inouchi, Y., 2002. A diatom record for the past 400 ka from Lake Biwa in Japan correlates with global paleoclimatic trends. *Palaeogeograph, Palaeoclimatology, Palaeoecology* 183, 261-274.
- Lange-Bertalot, H., Krammer, K., 1987. Bacillariaceae, Epithemiaceae, Surirellaceae. In: Cramer, J. (Ed.), *Bibliotheca Diatomologica*, Band 15. Gebrüder Borntraeger, Berlin, Stuttgart. 288 pp.
- Lange-Bertalot, H., Krammer, K., 1989. Achnanthes: eine Monographie der Gattung. In: Cramer, J. (Ed.), *Bibliotheca Diatomologica*, Band 18. Gebrüder Borntraeger, Berlin, Stuttgart. 393 pp.
- Lee, S., Ahn, Y., 2005. Fundamental Study of Hanon wetland in Seoquepo city, Jeju Island. *Korea society of Environment and Ecology* 2, 122-125.
- Lee, S.H., Lee, Y.I., Yoon, H.I., Yoo, K.-C., 2008. East Asian monsoon variation and climate changes in Jeju Island, Korea, during the latest Pleistocene to early Holocene. *Quaternary Research* 70, 265-274.
- Lee, J.H., 2011. Algal Flora of Korea: Freshwater Diatoms IV, Chrysophyta: Bacillariophyceae: Pennales: Raphidineae: Naviculaceae: *Cymbella*, *Cymbopleura*, *Encyonema*, *Encyonopsis*, *Reimeria*, *Gomphonema*, Vol.3, No. 4. National Institute of Biological Resources, Ministry of Environment.
- Lee, J.H., 2012. Algal Flora of Korea: Freshwater Diatoms VI, Chrysophyta:

- Bacillariophyceae: Pennales: Raphidineae: Naviculaceae: *Navicula*, Vol.3, No. 8. National Institute of Biological Resources, Ministry of Environment.
- Lee, J.H., 2012. Algal Flora of Korea: Freshwater Diatoms VIII, Chrysophyta: Bacillariophyceae: Pennales: Raphidineae: Naviculaceae: 20 genera including *Navicula*, Vol.3, No. 10. National Institute of Biological Resources, Ministry of Environment.
- Lowe, R.L., 2003. Keeled and Canalled Raphid Diatoms. In: Wehr, J.D., Sheath, R.G. (Eds.), *Freshwater Algae of North America: Ecology and Classification*. Academic Press, San Diego, pp. 669-684.
- Mackay, A.W., Jones, V.J., Battarbee, R.W., 2005. Approaches to Holocene Climate Reconstruction Using Diatoms. In: Mackay A., Battarbee, R., Birks, J., Oldfield, F. (Eds.), *Global Change in the Holocene*. Hodder Arnold, New York, pp. 294-309.
- Metcalfe, S.E., Street-Perrott, F.A., Perrott, R.A., Harkness, D.D., 1991. Palaeolimnology of the Upper Lerma Basin, Central Mexico: a record of climate change and anthropogenic disturbance since 11600 yr BP. *Journal of Paleolimnology* 5, 197-218.
- Meyers, P.A., Takemura, K., Horie, S., 1993. Reinterpretation of Late Quaternary Sediment Chronology of Lake Biwa, Japan, from Correlation with Marine Glacial-Interglacial Cycles. *Quaternary Research* 39, 154-162.
- Moos, M.T., Laird, K.R., Cumming, B.F., 2009. Climate-related eutrophication of a small boreal lake in northwestern Ontario: a palaeolimnological perspective. *The Holocene* 19(3), 359-367.
- Bowers, K., Suh, Y.B., Kang, S.Y., Ko, C.S., Kim, D.S., Kim, E.S., Kim, C.S., Kim, H.K., Ryu, C.K., Park, K.W., Yang, Y.C., Lee, S.C., Cho, D.S., Hwang, K.S., 2014. Progress in Hanon Maar Crater Restoration Research. *National Promotion Committee for Restoring Hanon Crater* 1-38.

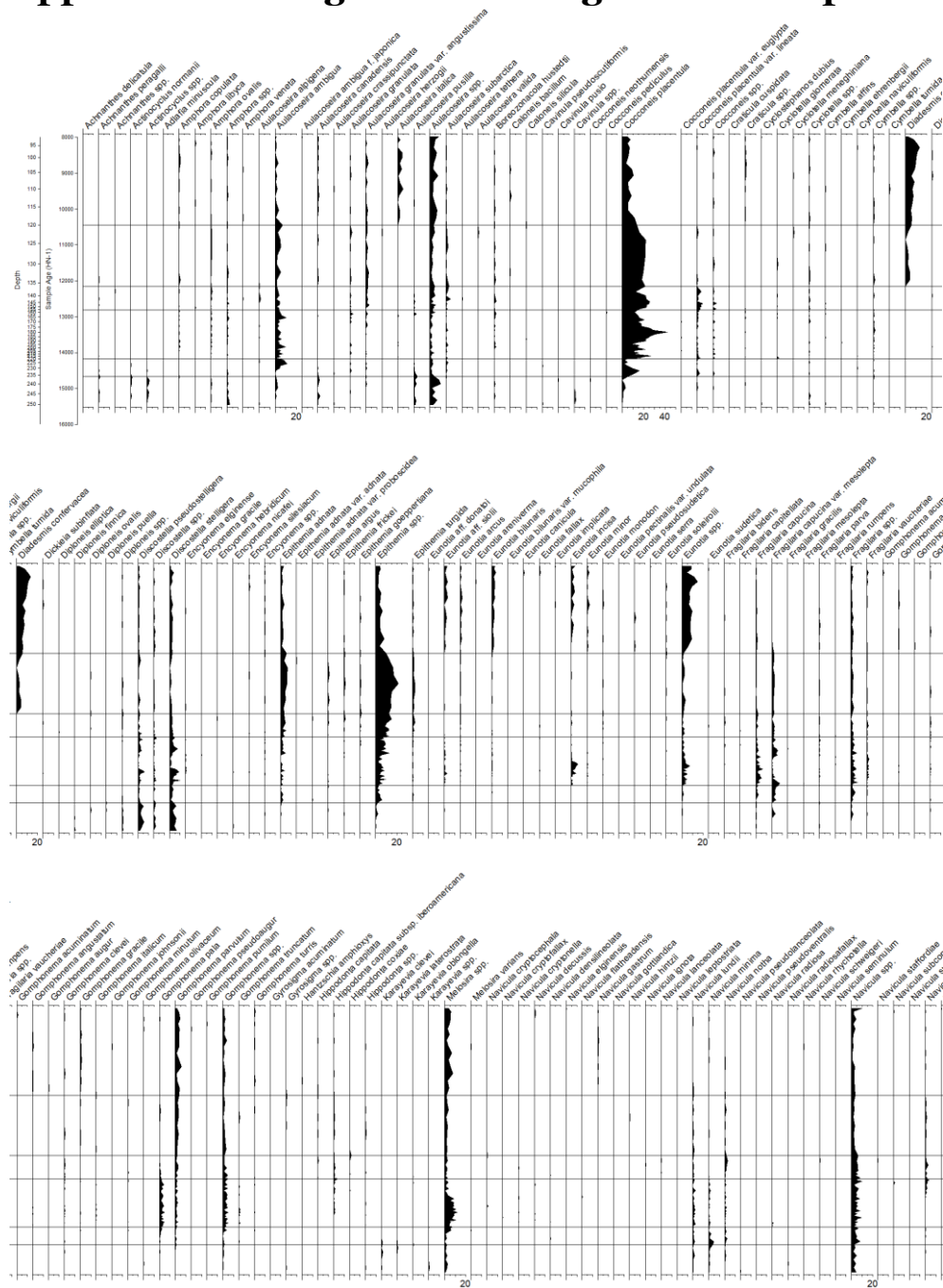
- Ortiz-Lerin, R., Cambra, J., 2007. Distribution and taxonomic notes of *Eunotia* Ehrenberg 1837 (Bacillariophyceae) in rivers and streams of Northern Spain. *Limnetica* 26(2), 415-434.
- Park, J., 2005. Holocene Climate Change and Human Environmental Impacts in Guanajuato, Mexico. Ph.D. Dissertation. University of California, Berkeley.
- Park, J., 2015. Centennial- to Millennial-scale Climate Change Since the Last Glacial: the review of related studies from the North Atlantic, East Asia, and Korea. *Journal of Climate Research* 10(1), 25-41. (in Korean)
- Park, J., Lim, H.S., Lim, J., Yu, K.B., Choi, J., 2014a. Orbital- and millennial-scale climate and vegetation changes between 32.5 and 6.9k cal a BP from Hanon Maar paleolake on Jeju Island, South Korea. *Journal of Quaternary Science* 29(6), 570-580.
- Park, J., Lim, H.S., Lim, J., Park, Y.-H., 2014b. High-resolution multi-proxy evidence for millennial- and centennial- scale climate oscillations during the last deglaciation in Jeju Island, South Korea. *Quaternary Science Reviews* 105, 112-125.
- Reimer P.J., Baillie, M.G., Bard, E., et al., 2009. IntCal09 and Marine09 radiocarbon age calibration curves, 0-50,000 years cal BP. *Radiocarbon* 51, 11-50.
- Ribeiro, F.C.P., Senna, C.D.S.F.D., 2010. The Use of Diatoms for Paleohydrological and Paleoenvironmental Reconstructions of Itupanema Beach, Para State, Amazon Region, during the Last Millennium. *Revista Brasileira de Paleontologia* 13(1), 21-32.
- Roberts, N., 1998. The Holocene – An Environmental History. Blackwell Publishers Ltd., Malden.
- Round, F.E., Crawford, R. M., Mann, D. G., 1990. The Diatoms: Biology & Morphology of the Genera. Cambridge University Press, New York.
- Scherer, R.P., 1994. A new method for the determination of absolute

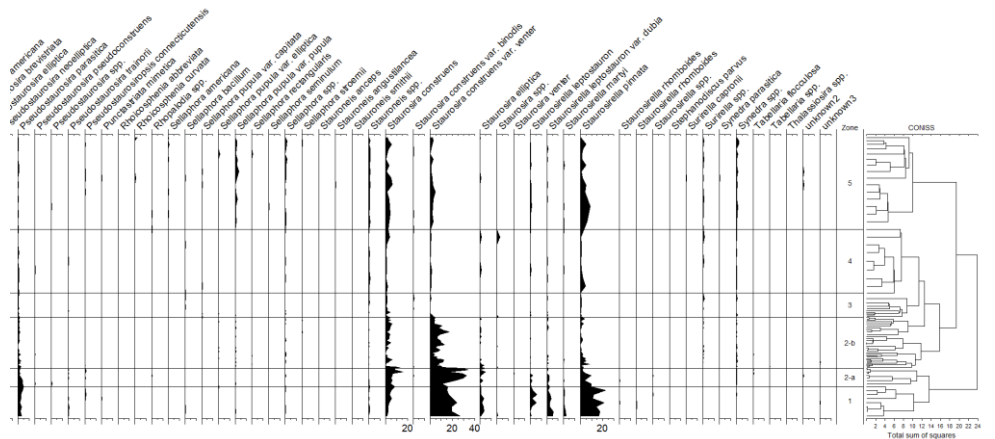
- abundance of diatoms and other silt-sized sedimentary particles. *Journal of Paleolimnology* 12, 171-179.
- Shim, J.H., 2003. Plankton Ecology. Seoul National University Press.
- Sigman, D.M., Hain, M.P., 2012. The Biological Productivity of the Ocean. Nature Education Knowledge 3(10):21.
- Šmilauer, P., Lepš, J., 2014. Multivariate Analysis of Ecological Data using Canoco 5. Cambridge University Press, New York.
- Spaulding, S.A., Lubinski, D.J. and Potapova, M., 2010. Diatoms of the United States. <http://westerndiatoms.colorado.edu>. Accessed on 20 April, 2015.
- Stoermer, E.F., Taylor, S.M., Callender, E., 1971. Paleoecological interpretation of the Holocene Diatom Succession in Devils Lake, North Dakota. *Transactions of the American Microscopical Society* 90(2), 195-206.
- Stoermer, E.F., Julius, M.L., Kociolek, J.P., Spaulding, S.A., 2003. Centric Diatoms. In: Wehr, J.D., Sheath, R.G. (Eds.), *Freshwater Algae of North America: Ecology and Classification*. Academic Press, San Diego, pp. 559-594.
- Sun, J., Liu, D., 2003. Geometric models for calculating cell biovolume and surface area for phytoplankton. *Journal of Plankton Research* 25(11), 1331-1346.
- Torgan, L.C., Santos, C.B.D., 2008. *Diadesmis confervacea* (Diadesmiaceae-Bacillariophyta): morfologia externa, distribuicao e aspectos ecologicos. *IHERINGIA, Sér. Bot., Porto Alegre* 63(1), 171-176.
- ter Braak, C.J.F., Šmilauer, P., 2012. *Canoco Reference Manual and User's Guide: Software for Ordination (Version 5.0)*. Ithaca: Microcomputer Power.
- Väliranta, M., Weckström, J., 2007. Applying principal components analysis (PCA) for separating wingless birth fruits – a

- palaeoecological case study from northern Norway. *Annales Botanici Fennici* 44, 213-218.
- Wang, L., Rioual, P., Panizzo, V.N., Lu, H., Gu, Z., Chu, G., Yang, D., Han, J., Liu, J., Mackay, A.W., 2012. A 1000-year record of environmental change in NE China indicated by diatom assemblages from maar lake Erlongwan. *Quaternary Research* 78, 24-34.
- Wang, L., Mackay, A.W., Leng, M.J., Rioual, P., Panizzo, V.N., Lu, H., Gu, Z., Chu, G., Han, J., Kendrick, C.P., 2013. Influence of the ratio of planktonic to benthic diatoms on lacustrine organic matter $\delta^{13}\text{C}$ from Erlongwan maar lake, northeast China. *Organic Geochemistry* 54, 62-68.
- Xiao, J., Inouchi, Y., Kumai, H., Yoshikawa, S., Kondo, Y., Liu, T., An, Z., 1997. Biogenic Silica Record in Lake Biwa of Central Japan over the Past 145,000 Years. *Quaternary Research* 47, 277-283.
- Yoon, S.-H., Lee, B.-G., Sohn, Y.K., 2006a. Geomorphic and Geological Characteristics and Eruption process of the Hanon Volcano, Jeju Island. *Journal of the Geological Society of Korea* 42(1), 19-30. (in Korean)
- Yoon, S.-H., Lee, S.H., Yoon, H.I., 2006b. Proceedings of the 4th International Symposium of IGCP-476, Busan, Korea.
- Yoon, S.-H., Yoon, H.-I., Lee, S.-H., 2006c. Sedimentary Characteristics of Hanon Crater-Lake Deposit and Implications for Paleo-Environmental Changes. *Korean Journal of Plant and Environment* 2(1), 19-28. (in Korean)

APPENDIX

Appendix I. A diagram including all diatom species





Appendix II. A count sheet of 17 major diatom species^{1 6}

Depth	<i>Aulacoseira</i> <i>ambigua</i>	<i>Cocconeis</i> <i>placentula</i>	<i>Cocconeis</i> <i>placentula</i> var. <i>lineata</i>	<i>Diadlesmis</i> <i>confervacea</i>	<i>Discostella</i> <i>pseudostelligera</i>	<i>Discostella</i> <i>stelligera</i>	<i>Epithemia</i> <i>adnata</i>	<i>Eunotia</i> <i>incisa</i>	<i>Fragilaria</i> <i>capucina</i>
90	3	15	1	8	3	3	9	11	0
92	1	25	0	25	3	4	6	3	1
94	3	17	0	35	2	13	3	4	2
96	3	23	1	46	6	6	5	10	0
98	0	20	0	35	0	8	6	3	2
100	3	18	0	35	5	2	4	10	2
102	9	12	0	32	3	4	4	11	1
104	1	31	0	31	4	5	7	2	2
106	4	31	0	16	3	8	10	8	1
108	2	19	0	29	3	5	5	3	3
110	6	18	0	20	3	9	5	0	1
112	1	29	0	25	3	8	6	7	1
114	4	16	0	20	2	7	7	5	2
116	12	19	0	18	4	8	8	2	4

^{1 6} These species are selected because their relative abundance is greater than 5% frequency in at least one sample.

118	2	36	0	19	2	7	3	0	3
120	24	45	0	19	4	8	19	0	2
122	8	50	4	7	8	4	10	0	2
124	17	75	0	0	2	1	22	0	2
126	18	74	0	7	2	3	22	1	1
128	7	74	0	9	1	5	21	0	1
130	5	64	0	8	1	1	14	0	0
132	19	69	0	14	7	5	17	0	2
134	5	59	3	13	0	7	9	0	2
136	5	73	0	0	5	7	11	1	6
138	9	38	12	0	4	7	11	0	4
140	13	75	2	0	1	8	16	3	2
142	3	74	4	0	5	6	9	0	6
144	14	87	1	0	3	8	7	0	1
146	14	83	17	0	1	9	17	0	2
148	14	80	12	0	4	9	9	0	2
150	5	77	13	0	11	12	8	0	2
152	10	75	9	0	5	11	8	1	2
154	12	48	9	0	5	7	12	0	2
156	11	49	6	0	6	15	7	0	1
158	15	43	5	0	5	15	4	0	3

160	16	38	1	0	14	10	3	0	4
162	17	44	4	0	5	8	6	0	1
164	23	51	3	1	4	12	7	0	3
166	34	53	4	0	7	11	8	1	6
168	10	72	3	0	9	16	7	0	3
170	13	45	2	0	7	23	8	0	5
172	9	64	0	0	13	18	6	0	9
174	12	61	4	0	0	8	17	1	1
176	7	89	1	0	5	8	1	1	3
178	11	94	0	0	2	4	0	2	13
180	18	148	0	0	0	2	1	3	2
182	17	109	0	0	0	6	1	2	5
184	13	94	0	0	3	5	2	19	11
186	9	77	2	0	1	5	6	21	0
188	20	79	1	0	2	4	4	19	14
190	8	74	0	0	1	1	3	14	9
192	14	48	1	0	5	19	2	11	23
194	11	29	3	0	16	25	12	4	8
196	23	58	1	0	22	33	1	10	5
198	34	47	0	0	8	20	0	15	8
200	21	54	3	0	8	24	4	4	14

202	4	67	2	0	4	13	8	5	12
204	19	44	1	0	6	13	5	0	17
206	15	40	5	0	6	11	2	0	20
208	16	57	0	0	6	12	8	0	10
210	23	34	4	0	10	32	0	5	9
212	12	63	3	0	6	12	3	2	6
214	12	90	5	0	7	12	2	2	13
216	17	72	2	0	6	12	3	5	6
218	2	54	10	0	4	9	6	5	0
220	13	15	4	0	4	6	2	0	8
222	29	9	1	0	2	8	1	0	3
224	37	18	0	0	6	13	2	0	2
226	36	6	1	0	4	10	1	0	4
228	17	16	0	0	4	8	3	0	3
230	15	30	0	0	2	8	8	0	7
232	2	58	4	0	2	9	3	0	5
234	0	39	9	0	5	4	8	0	0
236	2	18	0	0	7	14	3	0	1
238	5	0	0	0	18	21	0	0	1
240	7	8	1	0	11	11	1	0	0
242	8	10	2	0	8	12	2	0	1

244	0	2	0	0	14	22	0	0	1
246	3	3	0	0	18	17	0	0	0
248	1	1	0	0	15	16	0	0	2
250	1	0	0	0	6	20	0	0	0

Depth	Fragilaria capucina var. mesolepta	Gomphonema parvulum	Planothidium biporum	Staurosira construens	Staurosira construens var. venter	Staurosirella leptostauron	Staurosirella leptostauron var. dubia	Staurosirella pinnata
90	1	5	2	5	7	0	0	1
92	0	10	0	9	9	0	0	9
94	1	14	4	18	7	1	1	17
96	0	15	3	9	3	1	3	8
98	0	8	5	5	1	1	1	4
100	0	14	2	1	9	2	2	5
102	0	12	8	10	3	2	0	17
104	0	13	2	4	3	0	0	4
106	0	11	3	15	6	0	0	6
108	0	5	3	21	8	3	2	18
110	0	11	3	5	14	2	1	13
112	0	19	4	11	9	3	2	21

114	0	4	4	12	8	4	1	27
116	0	6	2	14	6	2	1	25
118	2	13	5	11	9	1	1	20
120	7	12	13	8	2	1	0	10
122	6	7	12	11	3	0	1	1
124	4	11	19	4	2	0	1	4
126	8	11	7	2	2	0	0	3
128	8	6	16	3	0	0	2	1
130	6	10	19	3	4	2	0	3
132	6	8	7	2	4	0	2	8
134	5	6	14	6	4	0	0	15
136	7	5	19	4	1	0	1	0
138	1	3	9	5	3	0	2	3
140	6	9	10	5	0	0	1	4
142	9	9	16	1	1	0	0	3
144	7	8	8	6	0	0	0	1
146	8	2	7	4	0	0	0	2
148	5	4	10	15	0	1	2	2
150	9	7	17	3	2	0	1	0
152	6	5	11	2	7	3	4	4
154	6	1	10	6	9	0	1	2

156	6	3	12	15	16	0	3	9
158	6	6	14	6	12	0	4	13
160	11	5	13	15	14	0	3	5
162	8	4	7	7	13	0	1	1
164	2	4	5	21	13	0	1	10
166	6	6	2	15	36	0	4	3
168	5	0	2	14	28	0	6	4
170	13	6	2	12	34	0	2	0
172	20	6	4	6	62	0	1	0
174	13	0	3	14	31	0	0	1
176	18	5	0	11	22	0	0	1
178	6	6	1	11	21	1	0	6
180	2	5	0	4	32	0	0	6
182	0	9	1	17	36	0	0	3
184	2	4	0	9	47	0	1	0
186	0	5	0	2	18	0	0	0
188	2	3	0	10	18	0	0	1
190	1	2	0	3	30	0	0	3
192	4	5	0	1	26	0	0	2
194	3	4	1	0	7	0	1	5
196	3	4	1	1	16	0	0	9

198	3	6	1	7	8	0	5	5
200	5	6	0	4	23	1	3	8
202	4	4	0	10	17	0	1	14
204	11	1	0	22	43	0	4	14
206	1	3	0	15	46	0	0	20
208	9	4	0	10	43	0	0	9
210	12	9	0	1	25	1	5	12
212	17	2	0	1	30	0	0	29
214	20	3	0	0	17	0	2	4
216	28	0	0	4	39	0	0	5
218	21	5	0	41	30	0	0	9
220	23	5	2	31	104	0	4	8
222	15	2	0	27	116	0	4	6
224	12	2	0	58	64	0	0	11
226	9	1	0	21	90	0	0	15
228	10	1	0	21	117	8	7	35
230	12	0	1	17	101	0	6	21
232	6	4	0	22	80	7	7	13
234	13	1	2	15	36	2	2	33
236	1	2	0	30	56	3	9	35
238	0	1	2	17	51	8	3	76

240	4	0	0	14	60	22	10	44
242	11	0	0	19	67	5	13	37
244	0	0	0	12	85	19	8	74
246	0	0	0	8	61	4	8	45
248	0	0	0	9	72	0	20	65
250	0	0	1	4	79	2	16	50

Appendix III. The component scores of Axis 1, 2, 3 and 4 by depth

depth	age	Axis 1	Axis 2	Axis 3	Axis 4
90	7978	-0.6565	0.9065	0.6502	-0.1221
92	8064	-0.5515	1.5136	0.5866	-0.5563
94	8166	-0.3285	1.8622	0.7282	-0.5475
96	8284	-0.6683	2.2896	0.9687	-0.1001
98	8416	-0.7385	1.7917	0.4382	-0.2692
100	8561	-0.6721	2.0441	1.185	0.002
102	8719	-0.6712	1.9557	0.928	-0.3852
104	8886	-0.8247	1.6421	0.534	-0.1204
106	9063	-0.7469	1.2481	0.6523	-0.3607
108	9247	-0.0041	1.4714	0.3053	-0.9596
110	9437	-0.2794	1.4444	0.1908	-0.0897
112	9633	-0.5424	2.1383	0.6258	-0.1836
114	9832	0.0344	1.431	0.1614	-0.4188
116	10034	-0.0124	0.9567	0.2974	-0.3597
118	10238	-0.4114	1.3606	0.2269	-0.4134
120	10441	-1.1705	0.492	-0.7755	-0.1616
122	10644	-0.7911	0.0887	-1.0808	0.1607
124	10850	-1.6092	0.1652	-1.3581	-0.0523
126	11065	-1.4082	0.1187	-0.6406	-0.266
128	11294	-1.3666	0.2476	-1.3989	-0.0424
130	11529	-1.4816	0.726	-1.4022	-0.2215
132	11758	-0.8722	0.2207	-0.5225	0.2418
134	11968	-0.936	0.4521	-0.9164	-0.1082
136	12148	-0.9986	-0.1765	-0.8799	0.6547
138	12294	-0.6657	-0.4326	-1.4378	0.6839

140	12411	-1.1599	-0.0799	-0.6218	0.1286
142	12504	-1.1131	-0.2025	-0.9658	0.746
144	12575	-0.8776	-0.2822	-0.3238	0.0621
146	12631	-1.1675	-1.2696	-1.9367	0.4365
148	12675	-0.6636	-0.7245	-1.3417	0.143
150	12712	-0.8239	-0.6352	-1.8954	1.5581
152	12746	-0.4815	-0.3627	-1.274	0.922
154	12779	-0.6471	-0.7381	-1.5399	0.3934
156	12811	-0.0828	-0.4034	-1.1894	0.3391
158	12846	-0.1492	-0.2579	-0.8801	0.7641
160	12883	0.1389	-0.4779	-0.6133	0.5183
162	12925	-0.359	-0.4922	-0.5695	-0.0283
164	12972	-0.1069	-0.4479	-0.1437	-0.4308
166	13024	0.0644	-1.0628	0.1871	-0.1949
168	13079	0.38	-0.5947	-0.3988	0.4849
170	13137	0.2501	-0.9749	-0.0879	0.5467
172	13197	0.2818	-1.0795	0.1113	0.6332
174	13257	-0.522	-0.8481	-0.8465	-1.0352
176	13317	-0.2213	-0.8555	0.2207	-0.5068
178	13375	-0.3623	-0.7471	1.2472	-0.3357
180	13430	-0.7179	-0.6112	0.8216	-0.4985
182	13483	-0.4966	-0.3621	0.9707	-0.8812
184	13533	-0.355	-0.5199	2.2812	-0.0116
186	13581	-0.8598	0.1673	1.7073	0.2701
188	13626	-0.5421	-0.6926	2.3413	0.0327
190	13670	-0.4943	-0.2403	1.8073	-0.0972
192	13713	-0.0096	-0.9767	2.4459	1.4755
194	13755	0.253	-0.411	0.2232	2.5691
196	13796	0.6651	-0.6246	1.1545	2.9666

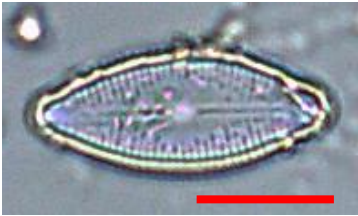
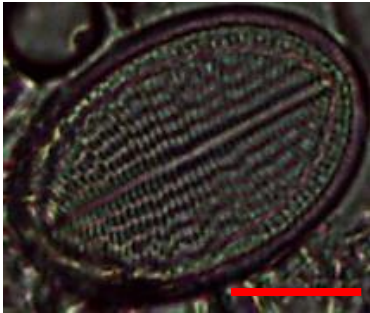
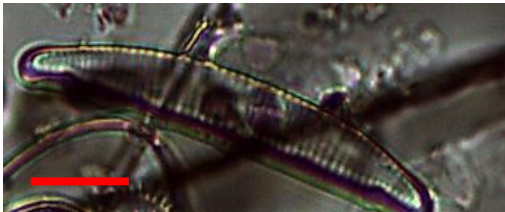
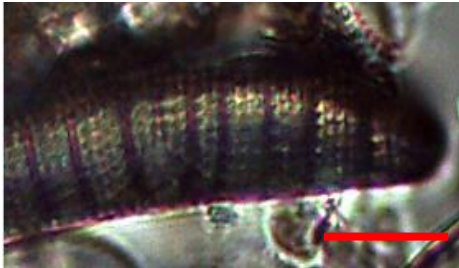
198	13836	0.258	-0.6634	2.0484	1.2853
200	13874	0.3145	-0.8704	1.0885	1.4857
202	13910	-0.1182	-0.5012	0.8371	0.6093
204	13943	0.6202	-1.2169	0.7805	-0.4052
206	13973	0.387	-0.8027	1.0152	0.1363
208	14001	0.0709	-0.7672	0.5302	-0.0893
210	14029	0.7671	-0.9113	0.9097	2.0445
212	14055	0.2492	-0.8546	0.1401	0.3028
214	14083	-0.1081	-1.6401	0.5032	0.8061
216	14112	0.0834	-1.5767	0.3813	-0.2381
218	14143	0.0823	-1.0249	-0.7684	-2.0421
220	14177	0.8264	-1.1406	-0.054	-2.32
222	14216	1.0749	-1.1696	0.3293	-2.5836
224	14260	0.9552	-1.1179	0.3957	-2.8501
226	14309	0.994	-1.218	0.6355	-1.806
228	14365	1.6678	-0.0455	-0.2478	-1.7099
230	14429	0.9297	-0.792	-0.0194	-1.5501
232	14501	0.8644	-0.0125	-0.2929	-1.1358
234	14582	0.3658	-0.1975	-1.4174	-0.7666
236	14671	1.4783	0.6285	-0.3766	-0.7809
238	14766	2.3662	1.0759	-0.6333	1.1693
240	14868	2.3251	1.2455	-1.0682	-0.0011
242	14975	1.9528	0.1525	-0.8538	-0.6075
244	15087	2.9776	1.5368	-0.9352	0.9006
246	15203	2.2659	0.811	-0.5471	1.42
248	15322	2.4156	0.9483	-0.6383	0.979
250	15443	2.4864	0.9744	-0.6999	0.7724

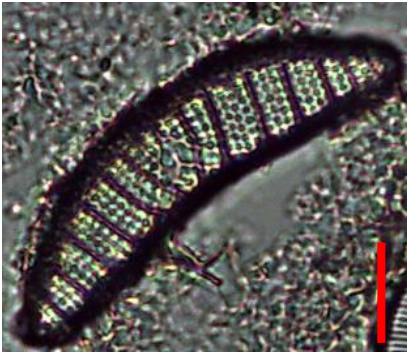
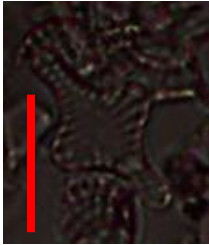
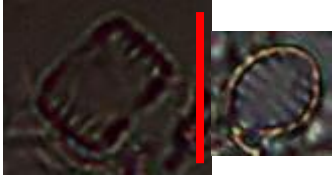
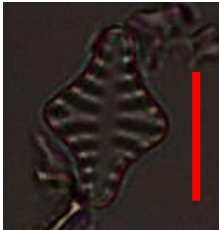

Appendix IV. The component scores of major species^{1 7} at Axis 1, 2, 3 and 4 from PCA

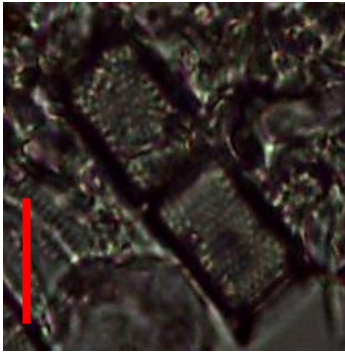



	Resp.1	Resp.2	Resp.3	Resp.4
<i>Aulacoseira ambigua</i>	-0.011	-0.6095	0.2158	-0.1108
<i>Cocconeis placentula</i>	-0.6171	-0.4939	0.0211	0.1362
<i>Cocconeis placentula</i> var. <i>lineata</i>	-0.1819	-0.4048	-0.5039	0.1388
<i>Diadlesmis confervacea</i>	-0.3174	0.794	0.1952	-0.148
<i>Discostella pseudostelligera</i>	0.5874	-0.0385	-0.115	0.6016
<i>Discostella stelligera</i>	0.558	-0.2047	0.0602	0.5853
<i>Epithemia adnata</i>	-0.654	0.0189	-0.4924	0.0159
<i>Eunotia incisa</i>	-0.2106	0.1368	0.7277	0.1537
<i>Fragilaria capucina</i>	0.0223	-0.5065	0.5623	0.2205
<i>Fragilaria capucina</i> var. <i>mesolepta</i>	0.0411	-0.6766	-0.2147	-0.2656
<i>Gomphonema parvulum</i>	-0.6043	0.5355	0.166	0.0131
<i>Planothidium biporum</i>	-0.5694	0.0818	-0.6173	0.1649
<i>Staurosira construens</i>	0.3826	-0.1049	-0.033	-0.7213
<i>Staurosira construens</i> var. <i>venter</i>	0.7914	-0.2211	0.0519	-0.3978
<i>Staurosirella leptostauron</i>	0.5784	0.3877	-0.2013	0.0133
<i>Staurosirella leptostauron</i> var. <i>dubia</i>	0.7447	0.1689	-0.2296	0.0972
<i>Staurosirella pinnata</i>	0.7952	0.4015	-0.1827	0.0533

^{1 7} These species are selected because their relative abundance is greater than 5% frequency in at least one sample.

Appendix V. Images of diatom species in Hanon maar paleolake

Species Names	Images
<i>Diadesmis confervacea</i>	 A micrograph showing a single, elongated, oval-shaped diatom with a distinct, finely textured surface. A red scale bar is visible in the bottom right corner.
<i>Cocconeis placentula</i>	 A micrograph showing a single, elongated, oval-shaped diatom with a distinct, finely textured surface. A red scale bar is visible in the bottom right corner.
<i>Eunotia incisa</i>	 A micrograph showing a single, elongated, oval-shaped diatom with a distinct, finely textured surface. A red scale bar is visible in the bottom left corner.
<i>Epithemia adnata</i>	 A micrograph showing a single, elongated, oval-shaped diatom with a distinct, finely textured surface. A red scale bar is visible in the bottom right corner.

<p><i>Epithemia tugida</i></p>	
<p><i>Staurosira construens</i></p>	
<p><i>Staurosira construens</i> var. <i>venter</i></p>	
<p><i>Staurosirella pinnata</i></p>	
<p><i>Discostella stelligera</i></p>	

<p><i>Aulacoseira ambigua</i></p>	
<p><i>Gomphonema pala</i></p>	
<p><i>Gomphonema acuminatum</i></p>	
<p><i>Pinnularia gibba</i></p>	

국 문 초 록

규조분석을 통한 마지막 해빙기 동안의 제주도 하논 마르형 호수 고환경 복원

지구 온난화 문제로 미래기후변화 예측은 중요한 문제가 되었다. 미래기후변화를 예측함에 있어 고기후 및 고환경의 복원은 핵심적인 것이라고 할 수 있는데, 기후는 일정한 주기로 반복적인 경향을 보이기 때문이다. 특히, 마지막 해빙기는 미래기후변화 예측에 중요한 시기인데, 이 시기의 기후 변화는 매우 다양한 모습을 보이며, 이러한 변화는 가까운 미래의 기후변화와 유사할 가능성이 있기 때문이다.

제주도 하논은 동아시아 계절풍과 쿠로시오 해류의 영향을 동시에 받는 지역이기 때문에 동아시아 고기후 및 고환경 복원에 있어 중요한 곳이다. 하논 지역에 대한 기존 연구들은 주로 지형분석 및 화분분석을 통해 육상환경을 복원해왔다. 그러나 이 지역이 원래 호수지역이었다는 점을 고려하여 본 연구에서는 호소환경을 포함하여 보다 자세한 고환경 및 고기후 복원에 유용한 규조분석을 사용하였다.

규조는 호수의 염도, 수심, 산성화, 영양상태, 수온 등과 같은 다양한 환경 정보를 제공하는 환경변화 지시종으로, 규조분석은 퇴적물 속에 남아있는 규조 미화석을 분석하여 조사하는 방법론이다. 그 중에서도, 본 연구에서는 규조분석을 통해 얻어진 정보를 바탕으로 마지막 해빙기 동안의 하논 고호수의 수심, 영양상태, 부수성, 수온, 산성화 정도를 자세히 복원하였다.

10m코어 중, 마지막 해빙기에 해당하는 시기인(약 15,500 - 8,000cal. yr BP) 90cm에서 250cm의 구간을 연구했다. 현미경 분석으로 규조를 동정하여 규조 다이어그램을 그렸으며, constrained incremental sum of squares cluster analysis를 통해 구분된 규조 구간

(zone)으로 마지막 해빙기 동안의 하논 기후사건 시기를 정했다. 그 결과 Oldest Drays는 15,440 - 14,670 cal. yr BP, Bølling-Allerød 초반부는 14,670 - 14,180 cal. yr BP로 나타났다. 이어서 Bølling-Allerød는 14,180 cal. yr BP - 12,810 cal. yr BP, Younger Dryas는 12,810 - 12,150 cal. yr BP, Preboreal은 12,150 - 10,440 cal. yr BP, and Boreal은 10,440 - 7,980 cal. yr BP로 확인되었다. 이러한 기후 시기 구분은 하논의 고기후를 연구한 선행연구와 일치하는 것으로 나타났다.

이어서 규조 군집변화와 호소학적 과정(limnological process)를 고려하여 규조 다이어그램 결과를 도식화함으로써 하논 고호수의 영양 상태, 수심, 부수성, 수온, 산성화 정도를 복원하였다. 복원된 호소환경을 구간별로 살펴봄으로써 상대적인 환경변화를 복원하였고, 이를 주성분분석과 P:B 비율을 통해 검토하였다. 복원결과 마지막 해빙기 동안의 하논 고환경 변화는 다음과 같았다. Oldest Drays에는 춥고 건조했다가 Bølling-Allerød가 시작되면서 점점 따뜻해지고 습윤해졌다. 이후 Younger Dryas때는 습윤했다 건조해지는 추운 날씨가 계속되었고, Preboreal때에는 점점 따뜻해지고 일시적으로 건조해졌으며, Boreal에 들어서 따뜻해지고 건조 또는 습윤해졌다.

규조분석을 통해 한국 담수지역의 고기후 및 고환경을 처음으로 복원했다는 의미를 갖는다. 또한, 전체적인 기후 경향뿐 아니라 하논 고호수의 영양 상태, 수심, 부수성, 수온, 산성화 정도 등도 밝혀냈다. 마지막으로, 본 연구의 결과는 한반도 마지막 해빙기 동안의 고환경 및 고기후 복원에 유용한 새로운 방법론과 자료를 제시하였다는 의의를 갖는다.

주 요 어 : 규조분석, 제주도, 하논 마르형 고호수, 고환경 복원, 고기후, 마지막 해빙기

학 번 : 2013-20114